Steady state properties of underwater towed systems.

Wingham, P. J.

Award date:
1983

Awarding institution:
University of Bath

STEADY STATE PROPERTIES

OF

UNDERWATER TOWED SYSTEMS

submitted by P.J. Wingham, M.Sc.

for the degree of Doctor of Philosophy

of the University of Bath

1983

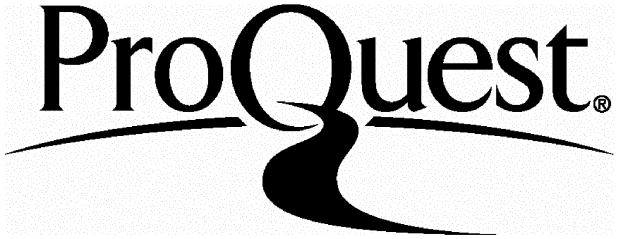

This thesis contains two separate papers having the common aim of providing methods for assessing the steady state performance characteristics of underwater towed systems utilising bare and faired cables.

The first paper was published in February 1983 by Pergamon Press, (Ocean Engineering Vol. 10, No. 1).

COMPARATIVE STEADY STATE DEEP TOWING PERFORMANCE OF BARE AND FAIRED CABLE SYSTEMS

SUMMARY

The measured drag characteristics of a variety of cable fairings are reviewed and compared with those of bare cables. The effect of cable inclination angle has been studied and an empirical rule developed for dealing with faired cables, the hydrodynamic properties of which are shown to depend significantly on the section shape of the fairing.

Non-dimensional cable functions are tabulated for both bare and faired cable profiles and applied to show how the addition of fairings can improve the towing performance of a given system.

Simple formulae are developed for calculating faired cable system properties and for assessing the effect of fish drag.

LIST OF CONTENTS

TABLE 1 Fairing section drag data

Figure 1 Fairing sections and drag coefficients.

Figure 2 Velocity distributions over aeronautical and wrap-round fairing sections

Figure 3 The variation of drag coefficient with Reynolds Number

Figure 4 Hydrodynamic effects of cable inclination angle

Figure 5 Magnitude and direction of water force on inclined fairing

Figure 6 Hydrodynamic force per unit length. Models used for bare and faired cable calculations

Figure 7 Non-dimensionalising of cable profiles

Figure 8 Variation of depression angle with w/r_o and fish weight/cable weight for bare and faired cables

Figure 9 Variation of cable top angle with fish weight/cable weight and w/r_o

Figure 10 Cable top tension ratio of bare and faired cables

Figure 11 Examples of towing performance

Figure 12 Effect of fish drag on cable profile at constant scope and w/r_o.

TABLE 2 Non-dimensional characteristics of bare and faired cables

NOTATION

A	a constant in equation (16)
A_F	maximum cross sectional area of fish body
c	length of chord of aerofoil or streamlined section
C	chord length of cable profile (fig. 7)
d	diameter of cable
D	drag force acting on fish = $C_D . \frac{1}{2}\rho v^2 . A_F$
g	gap between cable and rear unit of clip-on fairing
r	drag force per unit length of faired or unfaired cable
r_o	drag force per unit length of faired or unfaired cable when set at 90 deg to the flow direction
r_t, r_n	components of r tangential and normal to a cable element
r_p, r_f	pressure drag and friction drag of inclined fairing element
s	non-dimensional arc length of cable. $s = S/(W/w)$
S	arc length (scope) measured along the cable
t	maximum thickness of fairing or fairing section
t	cable tension ratio $t = T/T_o$
T	cable tension
T_o	cable tension at lower end where ϕ = 90 deg
v	towing speed
v_L	local velocity over fairing section
w	weight in water per metre of faired or unfaired cable
W	weight in water of fish
x	chordwise distance from leading edge of fairing section (fig. 2)
x	non-dimensional trail of fish. $x = X/(W/w)$
X	trail of fish (behind ship)
y	non-dimensional depth of fish. $y = Y/(W/w)$
Y	depth of fish

γ depression angle (fig. 7)

ϕ local inclination angle of cable to the horizontal

ψ critical angle of cable

ρ density of sea water (taken as 1030 kg/m^3 for calculations)

C_D drag coefficient of fish

C_{r_o} section drag coefficient = $r_o/(\frac{1}{2}\rho v^2 t)$ or $r_o/(\frac{1}{2}\rho v^2 d)$

1. INTRODUCTION

The use of fairings to reduce cable drag and eliminate strumming is common. Such fairings can vary from crude devices ('hairy' fairings) for suppressing wake vortices to sophisticated wrap-round units that transform the circular cable section into a streamlined profile.

Their favourable effect is primarily due to the resulting reduction of the drag coefficient, from values of order 1.5 to 0.25 or less. In addition, however, they change the hydrodynamic characteristics of the cable so that different rules are required for calculating the cable loading and the cable-fish configuration.

The steady state hydrodynamic properties of bare cables are well known and well validated (refs. 1, 2, 3) and the calculation of towing depth and cable configuration presents few problems other than the uncertainties that arise from strumming.

The hydrodynamic properties of faired cables are less well understood, and current literature, eg. refs. 4 and 5 indicate much uncertainty about the effects of cable inclination upon the loading functions. In addition their basic drag coefficients cannot be easily be estimated because fairing section profiles differ so much from aerofoil shapes. Wrap-round fairing sections have bluff nose profiles that provoke boundary layer separation (ref. 8) and clip-on fairings have gaps between cable and fairing. These both cause adverse effects which are not amenable to theoretical treatment.

This paper is an attempt to reduce some of these hydrodynamic uncertainties and provide the designers of towed underwater systems with methods for assessing towing performance with or without cable fairings for cases where depressors are not employed. Experimental evidence has been collected from several sources to show how fairing drag coefficients may vary, and an empirical law has been developed to account for faired cable inclination angle effects, based upon consideration of the expected physical flow conditions over inclined streamlined profiles.

Tables of non-dimensional cable functions are presented for both bare and faired cables, and used to compare the relationships between depth, speed, scope and tension, over a range of fish to cable weight ratios.

Additional analysis provides, in the case of faired cables, a rapid method for calculating cable shape properties; and, for both bare and faired cables, a method to allow for the effect of the fish drag force.

2. HYDRODYNAMIC PROPERTIES OF BARE AND FAIRED CABLES

Many examples of cable loading functions suitable for bare and faired cables have been published (see Refs. 1, 2, 4, 5). These have been examined and compared with data derived from experimental sources in order to see how well they match the expected physical flow properties appropriate to either circular or streamlined profiles. The broad hydrodynamic distinction is that friction forces are insignificant in the former case but predominant in the latter.

There are two requirements; to estimate the drag coefficient of the profile when set normal to the flow direction and to quantify the effect of cable inclination on the magnitude and direction of the resulting drag force. These two aspects are treated separately.

2.1 Normal-flow drag of bare cables

The drag force per metre is given by

$$r_o = C_{r_o} \cdot \tfrac{1}{2}\rho v^2 d \qquad (1)$$

where C_{r_o} is the section drag coefficient for flow at 90 deg to the cable axis, and d the cable diameter.

Smooth circular cylinders have $C_{r_o} = 1.2$ for Reynolds Numbers between 10^3 and the critical value 3×10^5 (ref. 3), the latter corresponding to a 10 mm diameter cable being towed at 27 kt. In practice however, due to strumming, C_{r_o} values between 1.4 and 1.7 are more realistic (ref.6). It is not yet possible to predict them more precisely.

2.2 Normal-flow drag of faired cables

Fig. 1 illustrates a selection of section shapes used as fairings and Table 1 provides measured values of their drag coefficients C_{r_o}. The latter are based upon the thickness so that the drag force per unit length is given by

$$r_o = C_{r_o} \cdot \tfrac{1}{2}\rho v^2 t \qquad (2)$$

where t is the section maximum thickness.

The sections are divided into 3 classes; aeronautical, wrap-round and clip-on, and have been drawn with the same chord length to facilitate

comparison. The aeronautical sections are characterised by having their maximum thickness located at or aft of 30 percent chord. As a consequence their drag coefficients are very low because the chordwise distribution of local surface velocity is relatively flat so that the boundary layer never separates. Such sections are not easily adapted to enclose a circular cable located near the leading edge, and their use as wrap-round fairings is thus limited. Ref. 7 illustrates their use as an integrated fairing system employing a non-circular strength member.

The wrap-round sections have in common very much bluffer nose profiles. These create peaky velocity distributions which cause the boundary layer to separate over the maximum ordinate region, leading to much increased boundary layer and wake thicknesses and hence larger drag coefficients. Ref. 8 provides evidence of this. Chordwise velocity distributions over an aeronautical and wrap-round section are compared in fig. 2, the data being derived from Refs. 7 and 8 respectively. The increase in drag coefficient is significant, being in most cases 3 to 4 times that of the NACA sections. Some of the increase is due to the base drag created when the trailing edge is thick, fairing AN/SQS-504 being an extreme example.

These drag coefficients may still be unrepresentative of the values to be expected in the sea-going state when small gaps will exist between adjacent fairing elements. Flexnose B illustrates this effect (ref. 9).

Clip-on fairings are seen to have even greater drag coefficients, due to the gap between cable and fairing, unless care is taken to match the fairing frontal thickness to the cable diameter. When this is done their C_{r_o} values may approach those of the better wrap-round sections but the addition of the clips required to secure the fairings can add a significant drag increment. The example given, of Bath cusped B, is pessimistic because in this case the clips were numerous and bulky.

2.2.1 The estimation of C_{r_o}

Estimating the drag coefficient of streamlined sections is difficult because so many factors influence it. The main source of drag is skin friction but an additional 30% (very roughly) is form drag, being the contribution of the pressure forces acting over the profile. The two components are related because the development of the boundary layer governing the friction depends upon the pressure distribution.

The magnitude of C_{r_o} is influenced by

a) the profile shape, in particular the thickness/chord ratio and the chordwise position of the maximum thickness.

b) the Reynolds Number, based on the chord length.

c) the proportion of the chord over which a laminar boundary layer is maintained, which depends upon (a) and (b) and the degree of roughness of the profile.

Existing prediction methods such as refs. 3 and 10 only relate to aeronautical type sections which usually have their maximum thickness located at or aft of 30% chord. No satisfactory methods are available for the bluff nosed sections common to cable fairings. The data provided in fig. 1 and Table 1 will hopefully provide some guidelines.

2.2.2 The variation of C_{r_o} with Reynolds Number

Collected data in ref. 3 on streamlined strut and aerofoil sections having t/c ratios of order 20 to 25% indicate that C_{r_o} will decrease until the Reynolds number exceeds 10^6 and remain fairly constant for values beyond. Some sample variations fig.(3) show this trend to be borne out in practice, although the bluffer sections exhibit changes which are less consistent and which emphasise the need for experimental drag determination at the correct Reynolds Numbers.

2.3 The effect of cable inclination on drag

2.3.1 Bare cables

The hydrodynamic force, being almost solely due to pressure forces, must act at right angles to the cable length and will be proportional to the component of the dynamic pressure in that direction. Thus if r is the drag per unit length at an inclination angle ϕ the relationship shown in fig. 4(a) will hold. As ϕ tends to zero and the pressure force disappears one may expect a small friction force due to the tangential flow. In practice (ref. 3) this only amounts to 2 or 3 per cent of r_o and is often ignored (refs. 2 and 6).

The added effect of strumming when the cable is inclined is still a matter for further research.

2.3.2 Faired cables

The situation with faired cables is quite different because the major part of the drag force is skin friction. If the faired section had zero thickness the drag force would be solely friction and would act along the flow direction at all angles of inclination. The drag per unit length would, to a first order, remain constant because the wetted area would not change. The presence of thickness, however, makes fundamental changes. The fairing sections illustrated have thickness/chord ratios of order 20 percent which create a pressure drag about 30 percent of the total drag when the section is set normal to a flow (ref. 11). However, when such a section is inclined to the flow the drag-producing mechanism becomes complicated.

Fig. 4(b) illustrates features of the prevailing flow over a section with moderate inclination. The apparently slight curvature of the streamlines just outside the boundary layer (ref. 12), caused by the isobars being parallel to the leading edge, induces a marked spanwise component in the boundary layer very close to the surface, as evinced by the surface oil streak (ref. 13). This causes the friction force on average to lie in the general direction indicated by the vector r_f in fig. 4(c). The smaller pressure force, r_p, must act at right angles to the leading edge. The resulting drag force r will be the vector sum of the two components

acting at some angle θ to the flow direction. Since the friction and pressure forces are interdependent it is not easy to predict how the vector r will vary with inclination angle ϕ.

A theoretical calculation of the drag variation with ϕ is only possible in the case of low drag aeronautical sections where boundary layer separation does not occur (see ref. 7). For most wrap-round sections there is no theoretical guide.

Fig. 5 shows how θ and r/r_o vary with ϕ, both in theory and practice for the low drag NACA and AEW sections, and in practice for the Flexnose A and AN/SQS-504 wrap-round sections, the latter having very high drag (fig. 1, Table 1). The data is very scattered but an overall trend is discernible which may be represented by a simple rule. The resultant drag force direction is seen to lie within ±10 deg of the flow direction, and the magnitude of the drag force expressed as r/r_o is seen to vary approximately as sin ϕ. The two theoretical curves support these findings.

There remains uncertainty about the value of r/r_o when ϕ falls below 30 deg. Ref. 19 provides measurements at ϕ = 0 deg for some wrap-round sections, but the scatter when other results are considered suggest values between 0.2 and 0.3. It is proposed that the broken line for $0 < \phi < 30$ deg in fig. 5 would be applicable to many wrap-round sections.

2.3.5 Summary of cable drag characteristics

Where bare cables are concerned the effects of cable inclination are well known and well validated, but the value of C_{r_o} will lie between 1.2 and 1.7, depending upon strumming behaviour which is difficult to predict.

With faired cables it is not possible to estimate with certainty the value of C_{r_o} unless the maximum thickness of the section is at or aft of 30% chord, when refs. 3 and 10 are applicable. Otherwise it is necessary to measure C_{r_o}. The effect of cable inclination should also be

determined experimentally, but as a working rule, for prediction purposes only, the drag force may be assumed to act horizontally and to shrink in proportion to sin ϕ for 30 deg < ϕ < 90 deg, and to reduce further to about 30 percent at ϕ = 0 deg. The value 0.273 of r/r_o at ϕ = 0 for the faired cable has been chosen to permit a smooth blend into the sine curve at ϕ = 30 deg. Its precise value is not very significant.

When these ideas are used to determine the components of the drag force normal and tangential to the cable, the functions shown in fig. 6 emerge.

It may be remarked that the normal component ratio r_n/r_o is unchanged by a switch from the bare to the faired model. The corollary of this is that the use of fairings adds a tangential force to the cable that would otherwise be absent.

3. NON-DIMENSIONAL CABLE FUNCTIONS

It is usual (refs. 1, 2 et al) to present cable configurations in non-dimensional form, giving, at successive values of w/r_o, the tension ratio and cable angle as functions of co-ordinates expressed as proportions of a characteristic length T_o/r_o, where T_o is the tension at the origin and r_o the normal drag force per unit length of the cable. This has the disadvantage that both w/r_o and T_o/r_o vary with towing speed. When the characteristic length is made T_o/w, which is independent of speed, the cable properties can be presented so that the effects of changing speed may be judged separately from the effects of changing fish weight or scope.

The following analysis develops this approach.

Writing the normal and tangential components of the local cable drag force as

$$r_n = r_o . f_n(\phi) \tag{3}$$

$$r_t = r_o . f_t(\phi) \tag{4}$$

where $f_n(\phi)$, $f_t(\phi)$ are given in fig. 6 for both bare and faired hydrodynamic models, the standard cable equations become

$$T d\phi = (w\cos\phi - r_o . f_n(\phi)) dS \tag{5}$$

$$dT = (w\sin\phi + r_o . f_t(\phi)) dS \tag{6}$$

where T is the local tension and S the arc length along the cable measured from the origin where the cable inclination is 90 deg, (see fig. 7(a)). Dividing through by T_o/w, the characteristic length, gives

$$\frac{T}{T_o} d\phi = (\cos\phi - \frac{f_n(\phi)}{w/r_o}) \frac{dS}{T_o/w} \tag{7}$$

$$\frac{dT}{T_o} = \left(\sin\phi + \frac{f_t(\phi)}{w/r_o}\right) \frac{dS}{T_o/w} \tag{8}$$

Writing the tension ratio T/T_o as t, and $S/(T_o/w)$ as s gives

$$td\phi = \left(\cos\phi - \frac{f_n(\phi)}{w/r_o}\right) ds \tag{9}$$

$$dt = \left(\sin\phi + \frac{f_t(\phi)}{w/r_o}\right) ds \tag{10}$$

where s is the non-dimensional arc length up the cable.

Because the fish drag is ignored $T_o = W$ at the origin, where $\phi = 90$ deg, and $t = 1$.

$$\text{Thus } s = \frac{S}{W/w} = \frac{\text{cable weight}}{\text{fish weight}} \tag{11}$$

Equations (9) and (10) need only to be integrated once, at each w/r_o, to provide cable profiles expressed as in fig. 7(b) and applicable to an extensive range of fish to cable weight ratios. The integration was carried out using 1500 steps with a second approximation applied to each step. The steps near the origin were smaller to allow for the increased curvature.

The results of the numerical integration are given in Table 2 for both bare and faired cable models. At successive values of w/r_o the table gives, against increasing values of the argument s, values of x, y the non-dimensional depth and trail, gamma the depression angle, phi the cable inclination to the horizontal, and t the tension ratio. The last column C/S is the ratio of chord length to scope at each point.

Values of the critical angle psi have also been computed. Putting $d\phi = 0$ in equation (9) yields psi as the solution of

$$\cos\psi = f_n(\psi)/(w/r_o)$$

4. STEADY STATE BARE AND FAIRED CABLE CONFIGURATIONS

4.1 Depth and trail

Because the chord length C is so nearly equal to the scope S the depth and trail are closely given by $S\sin\gamma$ and $S\cos\gamma$ respectively, γ being the depression angle. The latter is therefore a good measure of the achieved towing depth.

Fig. 8 illustrates by a carpet plot the variation of γ with w/r_o and W/wS the ratio of fish weight to cable weight, for both bare and faired cable models. Lines of constant W/wS showing the effect of changing towing speed and the lines of constant w/r_o show the effect of changing scope for a given fish weight W. Increasing scope implies movement from right to left on these lines, giving the expected reduction of depression angle.

The values of γ at $W/wS = 0$ represent the unloaded cable in its critical condition. It will be noticed that where $\gamma > 30$ deg this value is the same for bare and faired because r_n/r_o is also unchanged (fig. 6).

An interesting feature revealed by fig. 8 is the fact that for $w/r_o > 0.5$ the depression angle is the same whichever drag law, bare or faired, is used. This reflects the fact that, as the cable profile becomes straighter, differences in the tangential drag force components have less effect on the shape of the profile, (although corresponding top tensions may differ considerably).

It will be seen that the variation of γ with W/wS, in most cells of the mesh, is straight enough to permit linear interpolation with little error, and Table 2 provides values of the argument at closer intervals than shown in fig. 8 in those areas where the lines are more curved. It will be found that the cable functions are best plotted against $1/s$ if interpolation is required. It is easiest to work at the given values of w/r_o even though the resulting towing speeds may not be integral.

Fig. 8 is a useful aid for the preliminary design phase of a deep towed fish because it allows one to make a rapid assessment of the independent effects of tow speed, fish weight and cable weight upon the achieved depth.

The relatively small change of depression angle due to the drag of the fish is evaluated in Section 7.

4.2 Cable top angle

Fig. 9 illustrates the cable inclination at the top (ship) end and its variation with fish weight/cable weight for values of w/r_o up to 0.6. At greater values the top angle is seen to depend little upon the hydrodynamic model used. This graph will show whether or not the cable inclination of a given system will fall below 30 deg., the threshold of the faired cable "sine law" (fig. 5).

The ϕ values at $W/wS = 0$ are, of course, the critical angles.

4.3 Tension ratio

Referring to equation (10), and noting that for the bare cable $f_t(\phi) = 0$, it is seen that

$$dt = \sin\phi \frac{dS}{W/w} \tag{12}$$

$$\text{ie } dt = \frac{dY}{W/w} = dy \tag{13}$$

Thus, since $t = 1$ at $y = 0$,

$$t = 1 + y \tag{14}$$

which is confirmed by Table 2.

For bare cables one can therefore derive the tension ratio at any point by adding 1 to the non-dimensional depth.

For the faired cable, in contrast, the significant tangential component of the hydrodynamic force gives greater increases of tension up the cable (and provides the 'stacking' loads that can be a contributory factor to causing tow-off (ref. 8)). This is shown by fig. 10 which compares the variation of faired cable tension ratio at selected values of w/r_o with the unique line applicable to bare cables.

It will be seen from the examples to follow that the additional tension produced by adding a fairing is offset by the associated increase in w/r_o, and by the reduced scope required to achieve a given depth.

5. COMPARATIVE TOWING PERFORMANCE

Four examples of towed fish configurations are given in fig. 11 to illustrate the main performance differences between bare and faired cables. They relate to a fish assumed to weigh 1025 N in water, towed by a 16 mm diameter cable weighing 4.1 N/m and having a normal-flow drag coefficient of 1.5. When fitted with a neutrally buoyant wrap-round fairing, of drag coefficient 0.20, the frontal thickness is increased to 20 mm.

These values have been chosen to provide convenient values of w/r_o to facilitate the application of Table 2. The value of W/w is 250, which becomes the factor required to convert the non-dimensional lengths s, x, y into real values S, X, Y.

Examples A and C show the effect of adding the fairing to 100 m scope towed at 5 kt. It is seen that the depth is more than doubled but at the expense of a 57 percent increase in top tension. Table 2 shows that even if the fish weight were increased eightfold (giving s = 0.05 instead of 0.4) the greater depth would not be achieved with the bare cable.

Example B represents the same scope, unfaired and towed at only 2 kt, to demonstrate how slight is the difference due to the two hydrodynamic drag laws at this value of w/r_o.

Finally, case D shows that without the fairing a scope of 315 m is necessary to achieve, at 5 kt, the depth attained by 100 m scope of faired cable, with the same fish weight.

These examples illustrate the benefits to be gained from the use of a fairing, e.g. greater tow speeds at the same depth or greater depth at the same fish weight, in addition to the suppression of strumming. Even a crude fairing such as the 'neoprene' example (fig. 1) will give a significant improvement, due to its reducing the cable drag coefficient by about 70 percent.

However, these gains have to be weighed against some of the disadvantages, particularly the additional complexity of the handling requirements needed to reef and stow the faired cable.

The dynamic response of the fish to ship heaving motion will also be increased. Ref. 14 shows that, to a first order, the ratio of fish perturbation amplitude to ship heave amplitude varies as the sine of the cable top angle. In the two examples A and D the cable top angles are 50 deg and 13 deg respectively, their sines being in the ratio 3.4 to 1. This could be significant if very steady fish motion is required.

A further point for consideration is the possible occurrence of tow-off (kiting), due to imperfect fairing behaviour (refs. 8, 9, 15).

5.1 The use of partial fairing

Fairing only the lower part of the submerged cable can offer improved towing performance without incurring handling difficulties on deck, although strumming may not be completely eliminated.

When a given length of bare cable is fully faired the gain in fish depth is considerable. There is a favourable exchange between the percentage of this gain which is achieved and the percentage of the cable which is faired (from the fish upwards). The exchange rate varies according to the values of bare-cable w/r_o, s, and the ratio of the two drag coefficients. On average one achieves about 50 percent of the fully-faired depth gain when one third of the scope is faired and 75 percent when half the cable is faired.

These results are based upon calculations using the two hydrodynamic models with the assumption that the addition of the fairing quarters the cable drag coefficient.

6. ANALYTICAL EXPRESSIONS FOR FAIRED CABLE PROPERTIES

The empirical hydrodynamic drag law proposed for faired cables allows one to represent the cable-fish configuration by a simple model that provides effective formulae for determining depression angle, cable inclination and tension ratio. As well as giving quick answers for assessing faired cable systems they provide a useful check on results obtained by numerical integration. Furthermore they allow one to calculate the effect of fish drag, which has so far been ignored.

The assumption (fig. 5) that $\theta = 0$ and $r = r_o \sin\phi$ implies that the drag force on any element of cable acts horizontally with a magnitude proportional to the length of its projection on the vertical. Thus at depth Y the total cable drag is $r_o Y$ acting horizontally at the half-depth point. If the cable weight wS is assumed also to act through the same point and the latter is located midway along the chord line (fig. 12a) the addition of the fish weight W completes a 'straight-cable' mechanical model to replace the curved system.

The following quantities can then be determined.

6.1 Depression angle

Taking moments about the top point yields the equilibrium value of γ in the form

$$WC\cos\gamma + \tfrac{1}{2}wSC\cos\gamma = \tfrac{1}{2}r_o C^2 \sin^2\gamma \qquad (15)$$

where C is the chord length.

The scope S may, with little error, be substituted for C because they never differ by more than 4 percent (Table 2). Since by definition (fig. 7b)

$$wS/W = s$$

equation (15) becomes, in non-dimensional form

$$\sin^2\gamma = (w/r_o)(1. + 2/s)\cos\gamma \qquad (16)$$

giving $\cos\gamma = \frac{1}{2}\{(A^2 + 4)^{\frac{1}{2}} - A\}$ (17)

where $A = (w/r_o)(1 + 2/s)$ (18)

Equation (17) yields γ values within 5 percent of the computed values in Table 2 when $w/r_o > 0.10$, and within 10 percent when $w/r_o = 0.05$.

6.2 Inclination angle

In order to achieve equilibrium the cable-top inclination angle will be given by

$$\tan\phi = \frac{(1 + s)w/r_o}{s.\sin\gamma} \qquad (19)$$

When γ is derived from equation (17) this formula gives ϕ within 1 deg. of Table 2 values for $w/r_o > 0.10$, and within 2½ deg. at $w/r_o > 0.05$.

6.3 Tension ratio

It may also be shown from the balance of vertical forces that

$$t = (1 + s)/\sin\phi \qquad (20)$$

This equation, with ϕ derived from equation (19), gives t within 5 percent of Table 2 values for $w/r_o > 0.10$. At $w/r_o = 0.05$ the error is unacceptable unless $s < 1.0$.

When $w/r_o < 0.05$ none of the equations (17), (19) and (20) can be successfully utilised because the cable profile is too curved for this simple model to be applicable. Such a low value, however, is unlikely in faired cable operations.

7. THE EFFECT OF FISH DRAG

The magnitude of the drag force acting on a typical towed fish, operating without depressors, is usually such a small proportion of the fish weight that its effect upon the cable profile may be ignored, particularly in preliminary design work. At high towing speeds, however, or with large fishes it is desirable to determine the drag effect.

The fish drag force is given by

$$D = C_D \tfrac{1}{2}\rho v^2 A_F \qquad (21)$$

where C_D is the fish drag coefficient based upon its maximum cross-sectional area A_F.

A streamlined fish with stabilising fins will have C_D of the order of 0.15. The addition of an unfaired tow-staff can double this value (ref. 9). An upper limit may be taken as 0.47 (ref. 3) corresponding to a sphere at its critical Reynolds Number which would occur at approximately 2 knots with a diameter of ½ metre.

If the depth and trail of a given fish are determined with its drag ignored the addition of the (small) drag force, at the same speed, will move the fish along an almost circular path whose centre is the cable top; i.e. the chord length is practically unaltered and the depression angle is reduced slightly. This has been demonstrated in ref. 18. The cable inclination angle at the bottom also changes, from 90 deg. to arc-tan (W/D), as illustrated in fig. 12(a), where the change of depression angle has been grossly exaggerated.

Table 2 may be used to reveal the cable profile when drag is present. Fig. 12(b) illustrates the non-dimensional curve corresponding to fig. 12(a), the points O, a, b and c showing how the real and the non-dimensional co-ordinates are related for the cases with and without fish drag.

Writing x, y, s as the non-dimensional values of X, Y, S and using suffixes a, b, c to denote their values at the points a, b, c the depression angle appropriate to bc may be determined as follows.

In fig. 12(b) the point b is defined by $\phi = \phi_b = \arctan(W/D)$. Thus x_b, y_b, s_b and t_b may be interpolated from Table 2.

The tension, To, at the origin is equal to W for Oa and $\sqrt{D^2 + W^2}\ /t_b$ for bc. Noting that $D/W = \cot\phi_b$ the characteristic lengths, T_o/w, are respectively W/w and $W/(wt_b\sin\phi_b)$.

The non-dimensional point a is therefore given by $s_a = S/(W/w)$, from which x_a, y_a may be found. The point c may be derived from the equality of the real scopes, giving the equations

$$S = s_a \frac{W}{w} = (s_c - s_b) \cdot \frac{W}{wt_b \sin\phi_b} \tag{22}$$

so that

$$s_c = s_b + s_a \cdot t_b \sin\phi_b \tag{23}$$

from which x_c, y_c may be obtained using Table 2.

Thus, using x_b, y_b, the depression angle of the fish with drag is calculated from

$$\tan\gamma = (y_c - y_b)/(x_c - x_b) \tag{24}$$

This process is laborious but the 'straight-cable' model provides a quicker alternative method for correcting the depression angle to allow for fish drag provided the change is small, i.e. < 10 deg.

If, as for the derivation of equation (15), moments about the top point are taken but with the fish drag force D included, the final form of the equation becomes

$$\sin^2\gamma = w/r_o(1 + 2/s)\cos\gamma - 2(w/r_o)(\sin\gamma/s)(D/W) \tag{25}$$

when from comparison with equation (16) it may be shown that if $\delta\gamma$ is the change of depression angle caused by the addition of D

$$\delta\gamma = \frac{-(2/s)(w/r_o)(D/W)}{2\cos\gamma + w/r_o(1 + 2/s)} = \frac{-(2/s)(w/r_o)(D/W)}{2\cos\gamma + A} \tag{26}$$

This equation shows that, to a first order, the change in depression angle is proportional to the fish drag/weight. Most valuable is the fact that, because tangential forces do not enter into its derivation the equation can also be applied to bare cable systems, as the following examples show.

7.1 Examples of fish drag effects

The numerical results in fig. 11 were calculated assuming zero fish drag. It is instructive to determine the depression angle change that would be caused by an assumed fish drag.

When expressed in terms of the towed system constants the fish drag to weight ratio becomes

$$\frac{D}{W} = \frac{C_D A_F}{C r_o t} \cdot \frac{w}{W} \Big/ \frac{w}{r_o} \qquad (27)$$

for a faired cable, and with d in place of t for a bare cable.

Assuming that C_D = 0.3 and A_F = 0.2 m^2 the value of D/W becomes 0.2 for cases A, C & D. In case B D/W = 0.033 which may be ignored.

In case A the change in γ given by the non-dimensional analysis is -6.48 deg. and equation (26) gives -6.45 deg.

In case C the corresponding changes are -1.12 deg. and -1.35 deg. respectively, and in case D - 0.47 deg. and -0.44 deg.

The results reveal the validity of equation (26) and show that, in general, the greater the zero-drag depression angle the greater its change due to drag.

8. CONCLUSIONS

The use of cable fairings is seen to improve significantly the towing performance of body-cable systems but at the expense of both an increase in cable top tension and in the fish response to ship heave.

The variation of faired cable normal-flow drag coefficients can be wide, and general theoretical methods are not yet available for their estimation or for predicting how the drag coefficient will vary with cable inclination. However, it has been possible to produce a feasible working rule for use when experimental data is not available. This has shown that, for $w/r_o > 0.5$, the fish depression angle (though not the tension) may be calculated using the more familiar bare cable functions.

The proposed rule to account for the hydrodynamic drag properties of faired cable leads to some simple formulae for calculating faired cable properties which are accurate enough for preliminary design work and sea trial performance predictions. A quick method for determining the effect of fish drag has been shown to apply whether or not the cable is faired.

It is evident that more work is needed to provide a better understanding of the effects of strumming on bare cable drag, and better methods for dealing with the hydrodynamic properties of faired cables.

9. ACKNOWLEDGEMENT

This work is part of a research programme financed by the Science and Engineering Research Council, the Department of Industry and the University of Bath. This support is gratefully acknowledged.

The author is much indebted to many colleagues for help and advice, in particular to Dr. J. F. Henderson, Mr. D. A. Chapman and Mr. M. J. P. Heaton.

10. REFERENCES

1) Michael C. Eames — Steady-State Theory of Towing Cables. Royal Institution of Naval Architects, 1967, 10 Upper Belgrave Street, London SW1.

2) S. Neumark — Equilibrium Configurations of Flying Cables of Captive Balloons, and Cable Derivatives for Stability Calculations. R and M No. 3333, June 1961, Aeronautical Research Council.

3) S. F. Hoerner — Fluid-Dynamic Drag. Published by the author, 1965. PO Box 342, Brick Town, New Jersey 08723, USA.

4) G. B. Springston Jr. — Generalised Hydrodynamic Loading Functions for Bare and Faired Cables in Two-Dimensional Steady State Cable Configurations, Report 2424. June 1967, Hydromechanics Laboratory, Naval Ship Research and Development Centre, Washington D.C.

5) M. J. Casarella & M. Parsons — Cable Systems Under Hydrodynamic Loading. Marine Technology Soc. Journal, June 1980.

6) D. S. Weaver — Unmanned Submersible Umbilical Drag and Analysis - A Review with Recommendations for Future Research. TRC 1203, December 1979, BHRA Cranfield, England.

7) D. E. Calkins — Faired Towline Hydrodynamics. J. Hydronautics, Vol. 4 No. 3, July 1970.

8) J. F. Henderson — Some Towing Problems with Faired Cables. Ocean Engineering, Vol. 5 No. 2, April 1978.

9) P. J. Wingham & N. R. Keshavan — Predicting the Equilibrium Depth of a Body Towed by a Faired Cable. Ocean Engineering, Vol. 5, No. 1, February 1978.

10) - — EDSU Data Sheets. Vol. A2a. Wings 02.04.03. July 1978.

11) F. M. White — Fluid Mechanics. McGraw-Hill 1979.

12) B. Thwaites — Incompressible Aerodynamics. Oxford University Press 1960.

13) C. D. Holmes & A. C. Brown — Measurement of the Normal and Tangential Components of the Drag of a Swept Fairing Section. School of Engineering Report No. 527, University of Bath, 1981.

14) D. A. Chapman — Effects of Ship Motion on a Neutrally Stable Towed Fish. School of Engineering Report No. 551, University of Bath, May 1981.

15) Neville E. Hale — Performance Investigation of Improved 'Flexnose' and 'Rigstream' Cable Fairings with an Emphasis on Anti-Kiting. Report No. 4-116-F1. December 1979. Fathom Oceanology Limited, Port Credit, Ontario, Canada.

16) C. R. Hiett & S. G. G. Dalton — Force and Restoring Moment Measurements on Fairings for Underwater Towing Cables. School of Engineering Report No. 335, University of Bath, June 1976.

17) - — Variable Depth Asdic. Resistance and Lift of Modified Cable Fairing when Inclined to Direction to Flow. Admiralty Exptl. Works Report No. 31/59, August 1959.

18) P. J. Wingham — The Use of Variable Body Forces to Control the Depth of Towed Submersibles. Ocean Engineering, Vol. 4, No. 2. May 1977.

19) D. Day & M. Michailidis — Report LTR-SH-167. Division of Mechanical Engineering, Defence Research Establishment Atlantic, Dartmouth, N.S. Canada, 1974.

TABLE 1

FAIRING SECTION DRAG DATA

TYPE	NAME	CONDITION	REYNOLDS NUMBER x 10^{-6}	C_{R_O}
Aeronautical	NACA 0020	-	1.0	0.050
"	NACA 63A022	nat. transition	1.0	0.043
"	"	fully turbulent	1.0	0.060
Wrap-round	AEW	nat. transition	0.26	0.075
"	Flexnose A	" "	0.26	0.120
"	" B	" "	0.20	0.162
"	" "	at sea	0.30	0.219
"	AN/SQS-504	nat. transition	0.26	0.250
"	Rigstream	" "	0.05	0.155
"	"	" "	0.35	0.130
Clip-on	Neoprene	with clips	0.10	0.44
"	Bath triangle	no clips, zero gap	0.30	0.39
"	" "	" " g/d = 0.3	0.30	0.35
"	" rounded	" " g/d = 0.20	0.30	0.30
"	" cusped B	" " zero gap	0.30	0.175
"	" " B	with clips. g/d = 0.24	0.30	0.40

FIG. 1 (a)

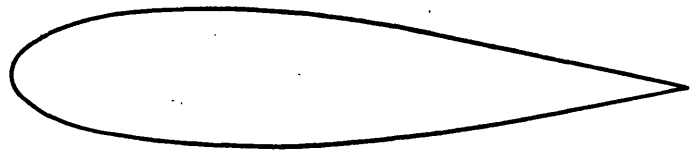

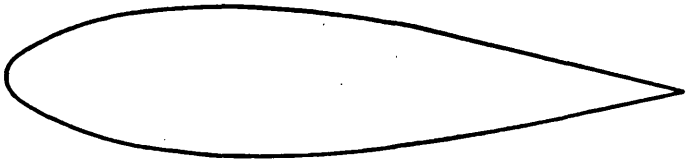

AERONAUTICAL

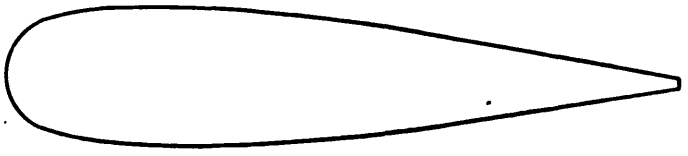

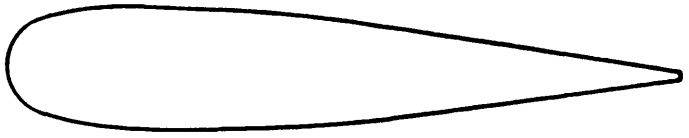

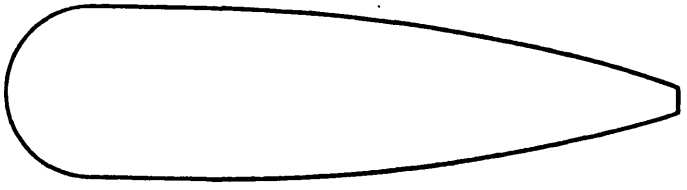

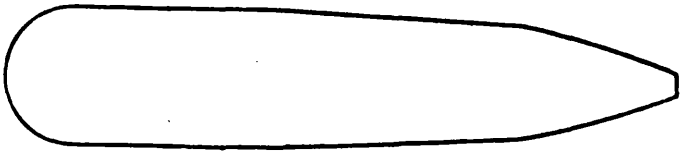

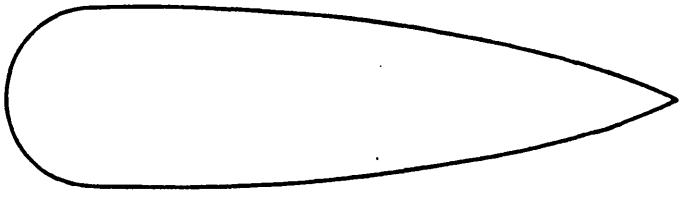

WRAP - ROUND

	C_{R_0}	Ref. No.
NACA 0020	0·050	7
NACA 63A022	0·043	7
AEW	0·075	7, 17
FLEXNOSE A	0·120	19
FLEXNOSE B	0·162	9
AN/SQS -504	0·250	19
RIGSTREAM	0·155	15
	SEE TABLE 1	

FIG.1(a) FAIRING SECTIONS AND DRAG COEFFICIENTS

FIG. 1(b)

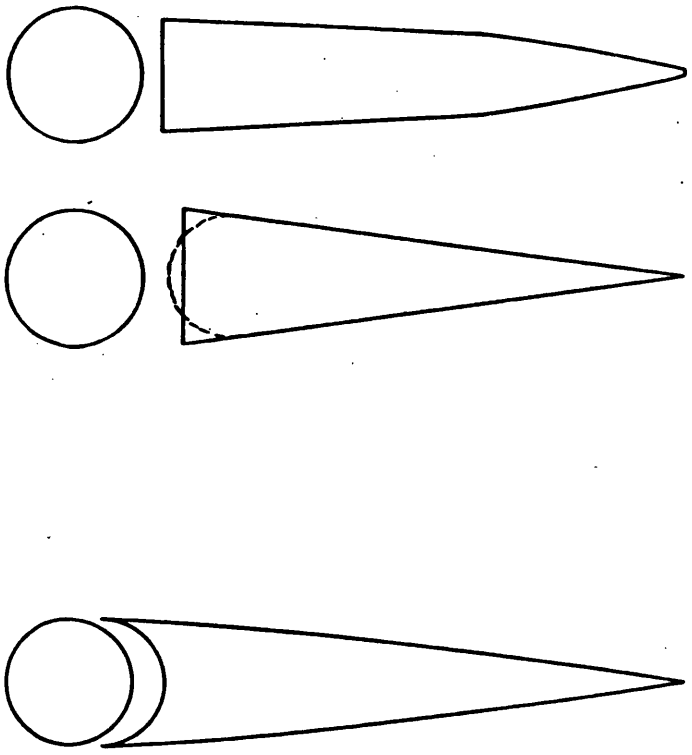

	C_{R_0}	Ref. No.
NEOPRENE	0·44	-
BATH TRIANGLE AND ROUNDED	0·3 to 0·4	16
BATH CUSPED B	SEE TABLE 1	-

CLIP - ON

FIG. 1(b) FAIRING SECTIONS AND DRAG COEFFICIENTS

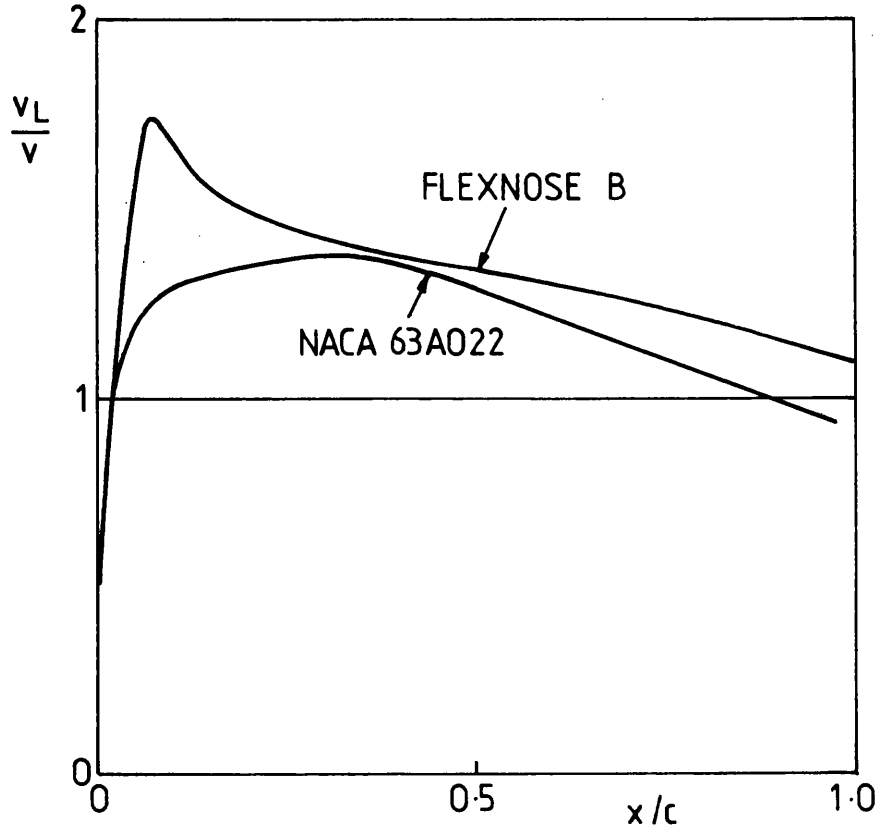

FIG. 2. VELOCITY DISTRIBUTIONS OVER AERONAUTICAL AND WRAP-ROUND FAIRING SECTIONS

FIG. 3.

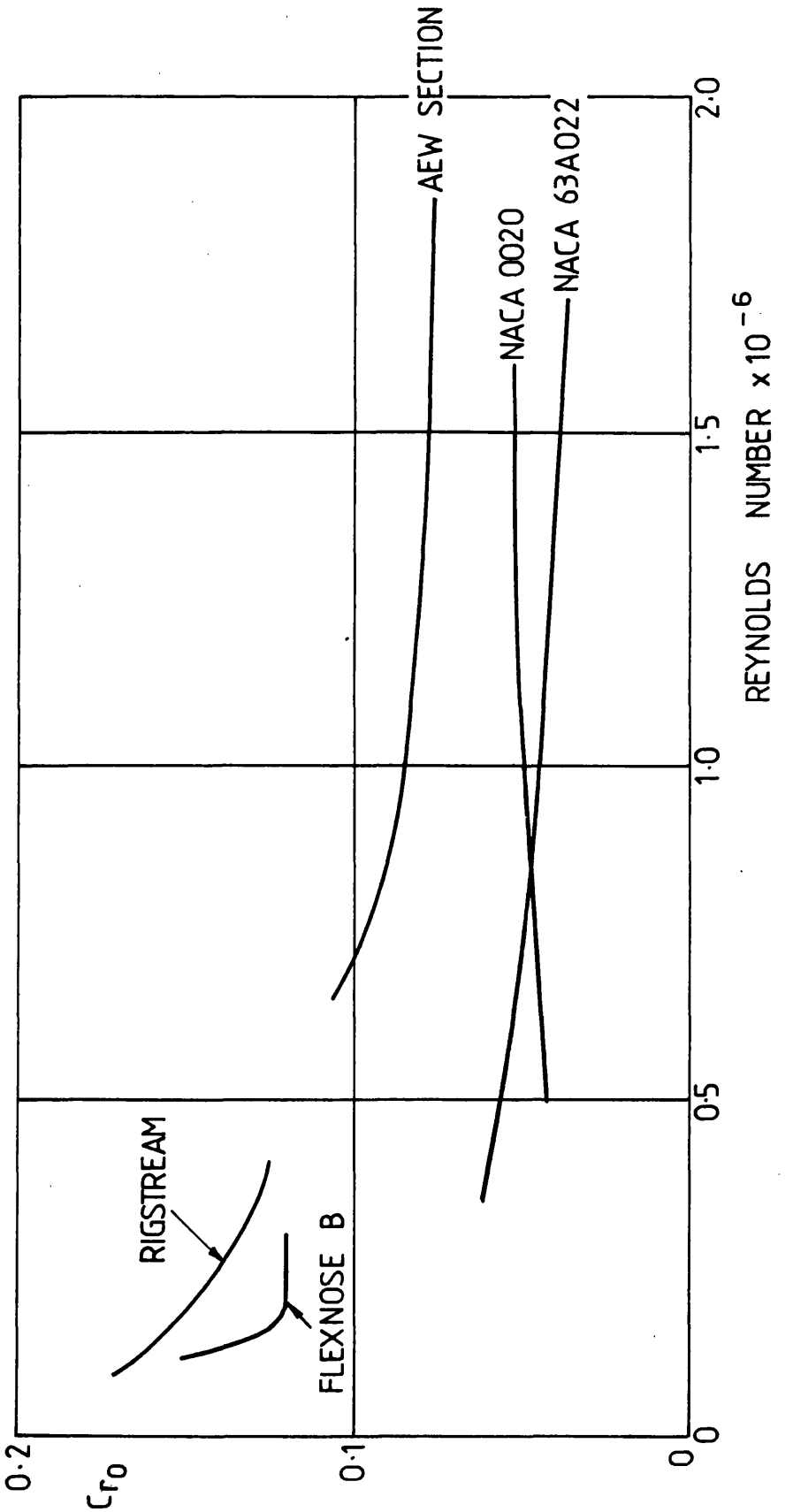

FIG.3. THE VARIATION OF DRAG COEFFICIENT WITH REYNOLDS NUMBER

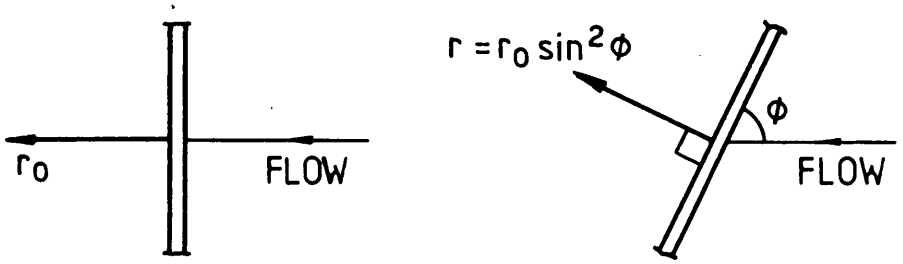

(a) HYDRODYNAMIC FORCE ON INCLINED CYLINDER, FRICTON FORCES NEGLIGIBLE

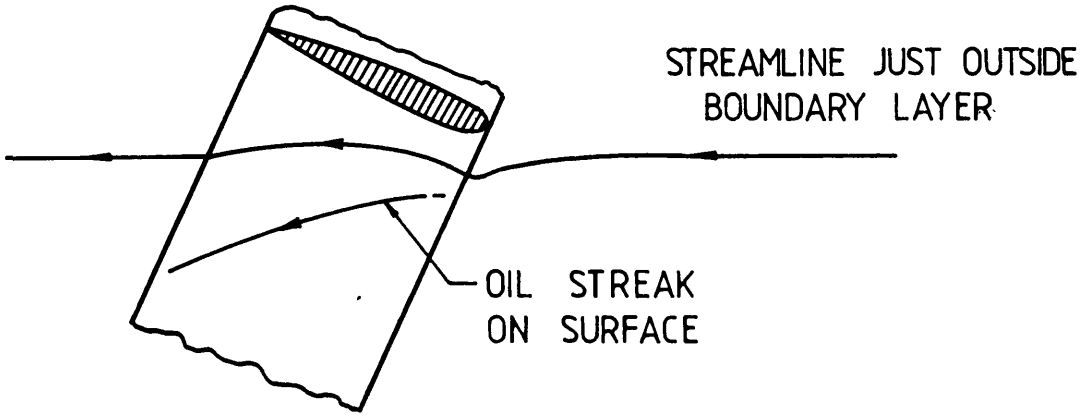

(b) FLOW OVER INCLINED FAIRED SECTION

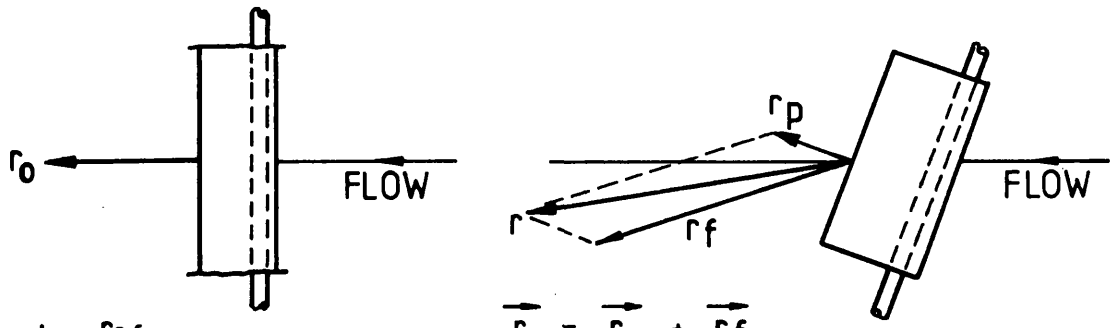

$r_o = r_{op} + r_{of}$
pressure 30% friction 70%

$\vec{r} = \vec{r_p} + \vec{r_f}$

(c) HYDRODYNAMIC FORCES ON INCLINED FAIRING

FIG. 4. HYDRODYNAMIC EFFECTS OF CABLE INCLINATION ANGLE

FIG. 5.

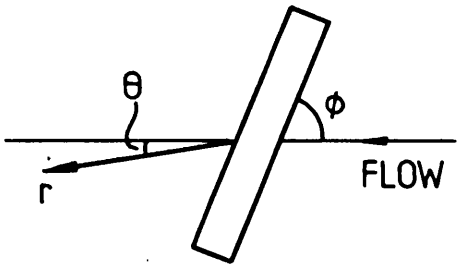

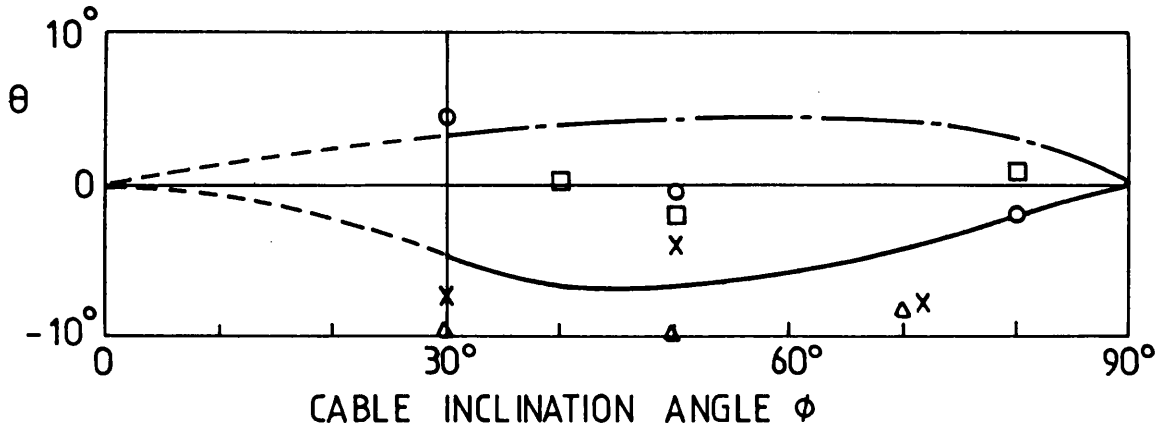

AEW Theory
AEW Observed
NACA 63A022 Theory
NACA 63A022 Observed
} ref. 7
FLEXNOSE A
AN SQS -504
} ref. 19

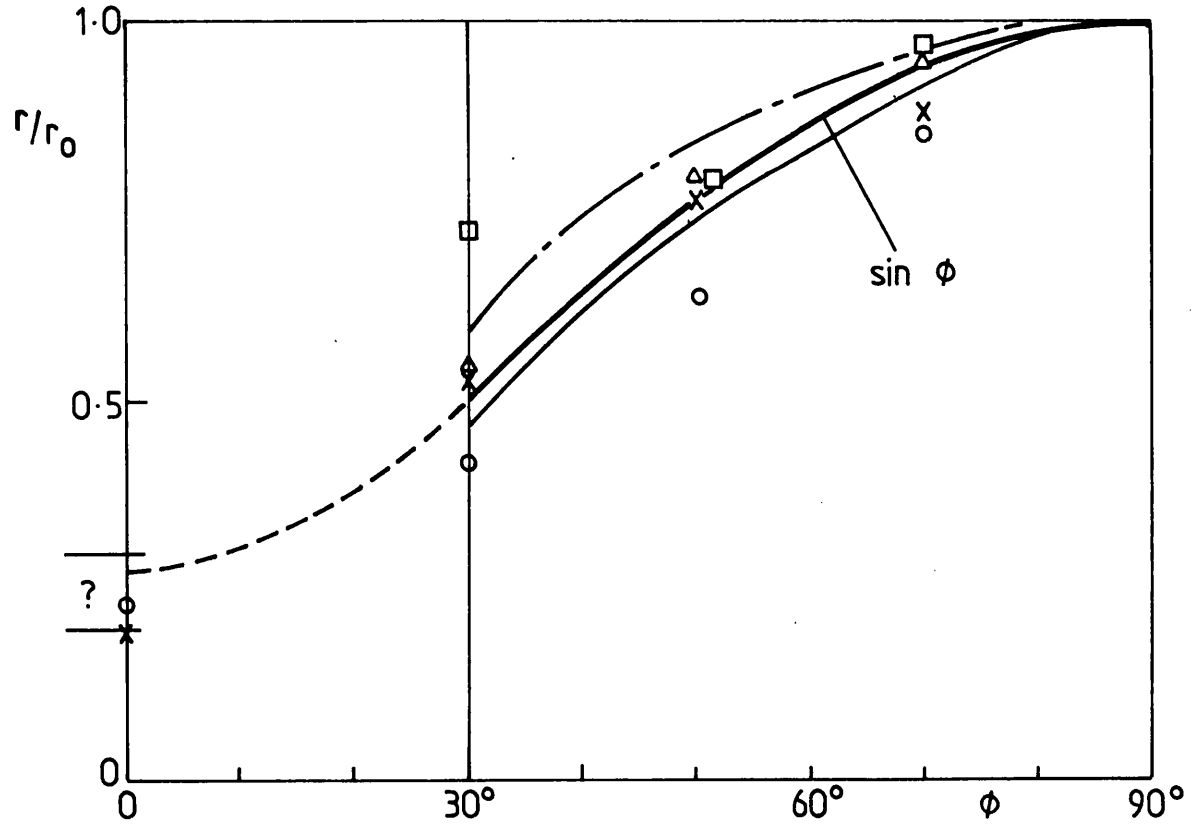

FIG. 5. MAGNITUDE AND DIRECTION OF WATER FORCE ON INCLINED FAIRING

FIG. 6

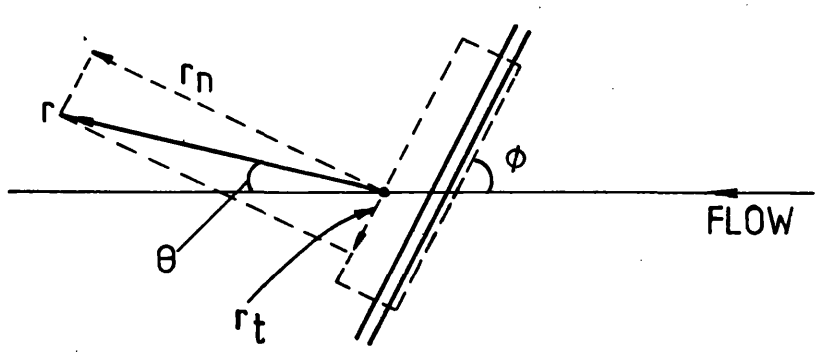

CONDITION	θ	r/r_o	r_n/r_o	r_t/r_o
BARE	$90-\phi$	$\sin^2\phi$	$\sin^2\phi$	0
FAIRED $\phi > 30°$	0	$\sin\phi$	$\sin^2\phi$	$\sin\phi\cos\phi$
FAIRED $\phi < 30°$	0	$0\cdot273 + 0\cdot827\phi^2$	$\frac{r}{r_o}\sin\phi$	$\frac{r}{r_o}\cos\phi$

FIG. 6. HYDRODYNAMIC FORCE PER UNIT LENGTH. MODELS USED FOR BARE AND FAIRED CABLE CALCULATIONS

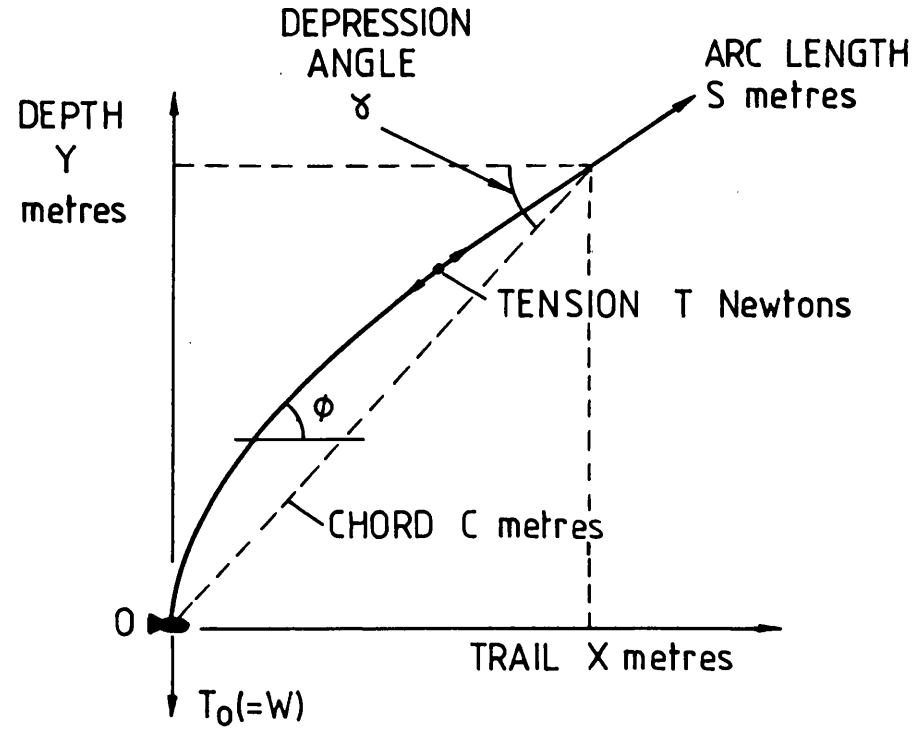

(a) DIMENSIONAL CABLE PROFILE AT GIVEN TOW SPEED

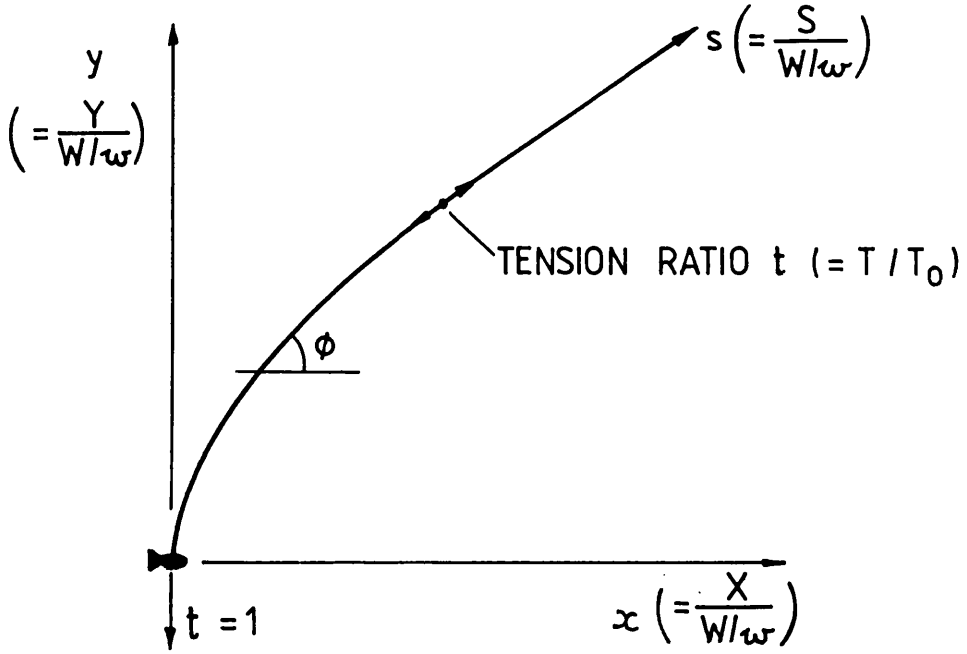

(b) NON-DIMENSIONAL CABLE PROFILE AT GIVEN w/T_0

FIG. 7. NON-DIMENSIONALISING OF CABLE PROFILES

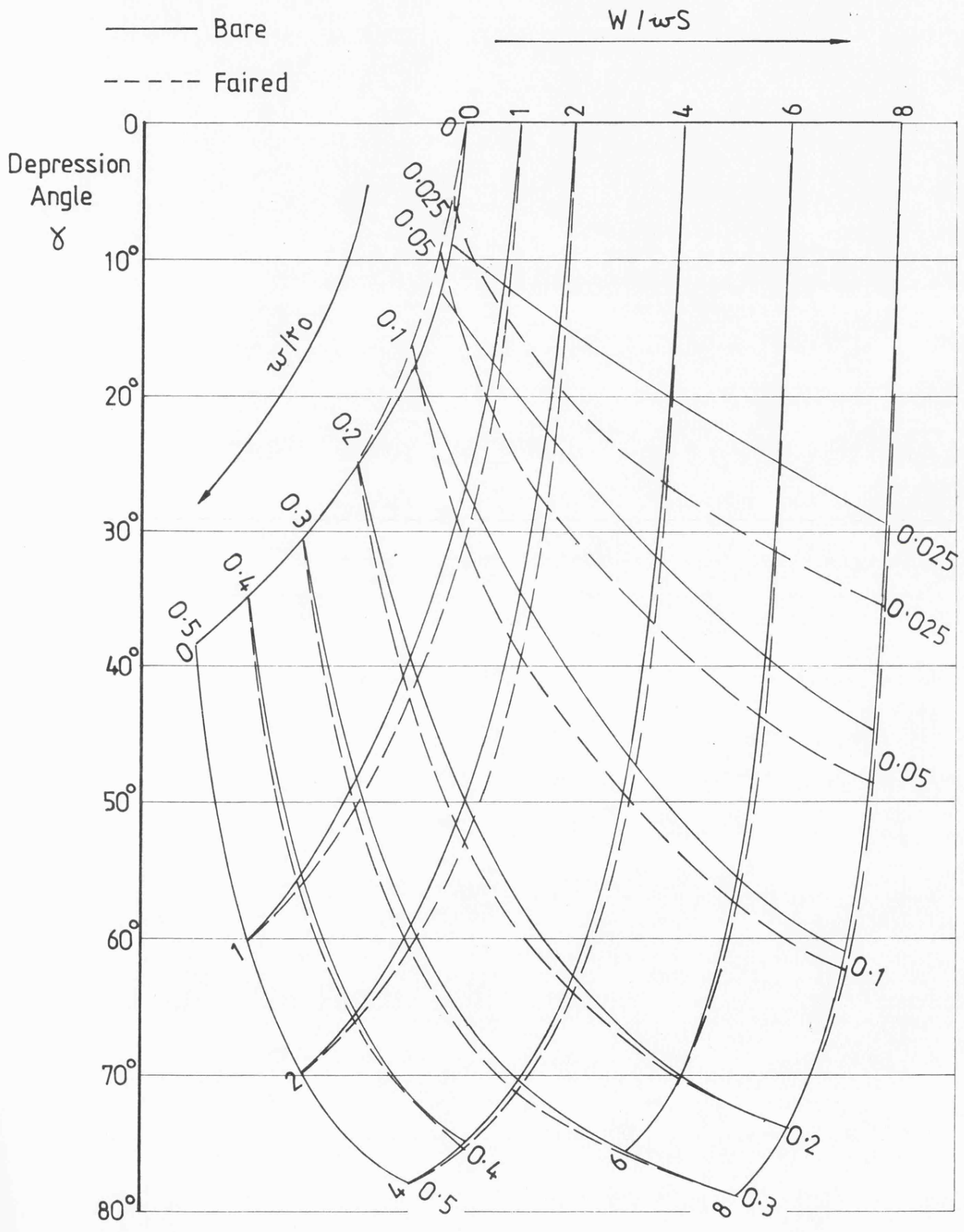

FIG. 8. VARIATION OF DEPRESSION ANGLE WITH ω/τ_0 AND FISH WEIGHT / CABLE WEIGHT FOR BARE AND FAIRED CABLES

FIG. 9

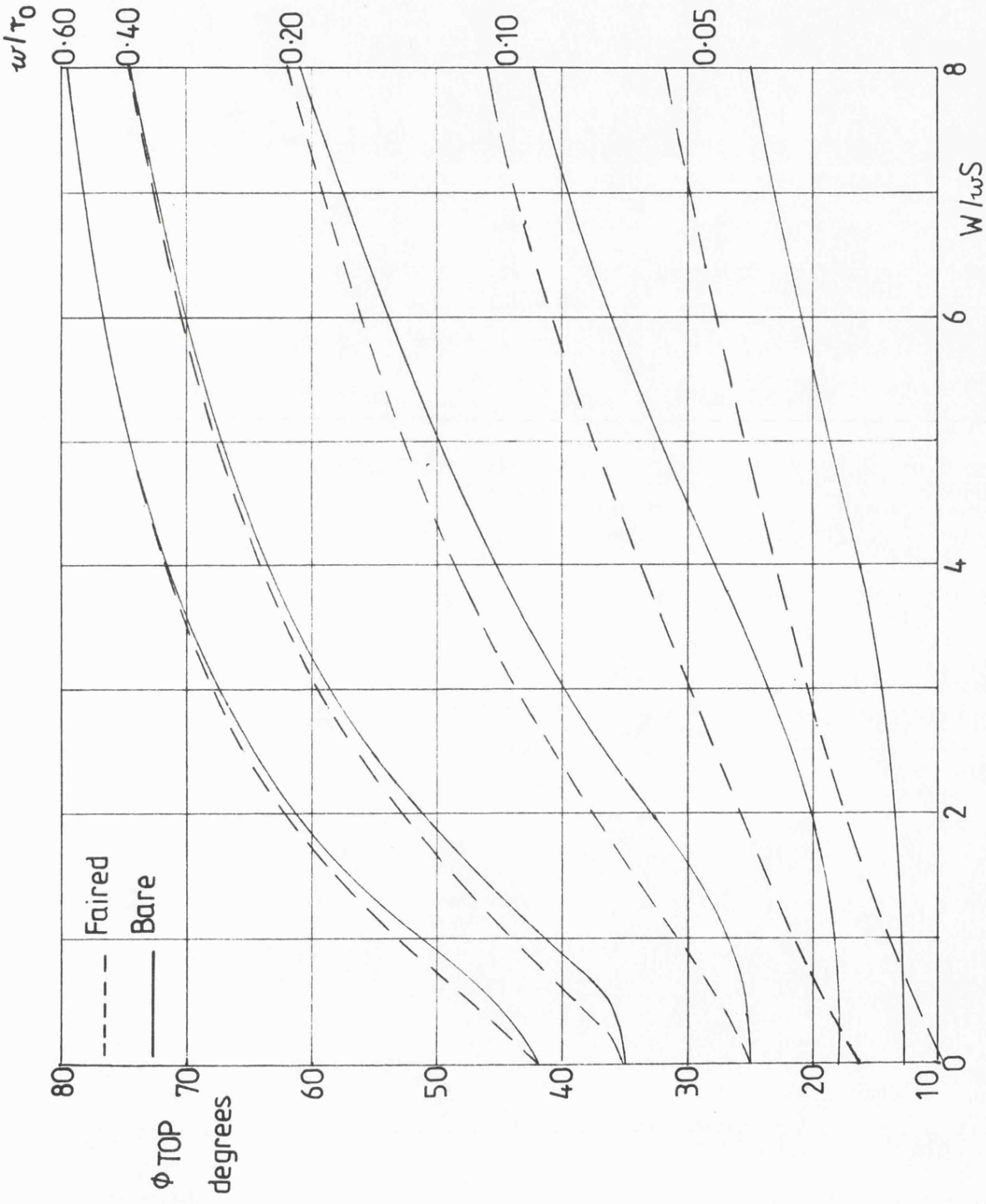

FIG. 9. VARIATION OF CABLE TOP ANGLE WITH FISH WEIGHT / CABLE WEIGHT AND w/τ_0

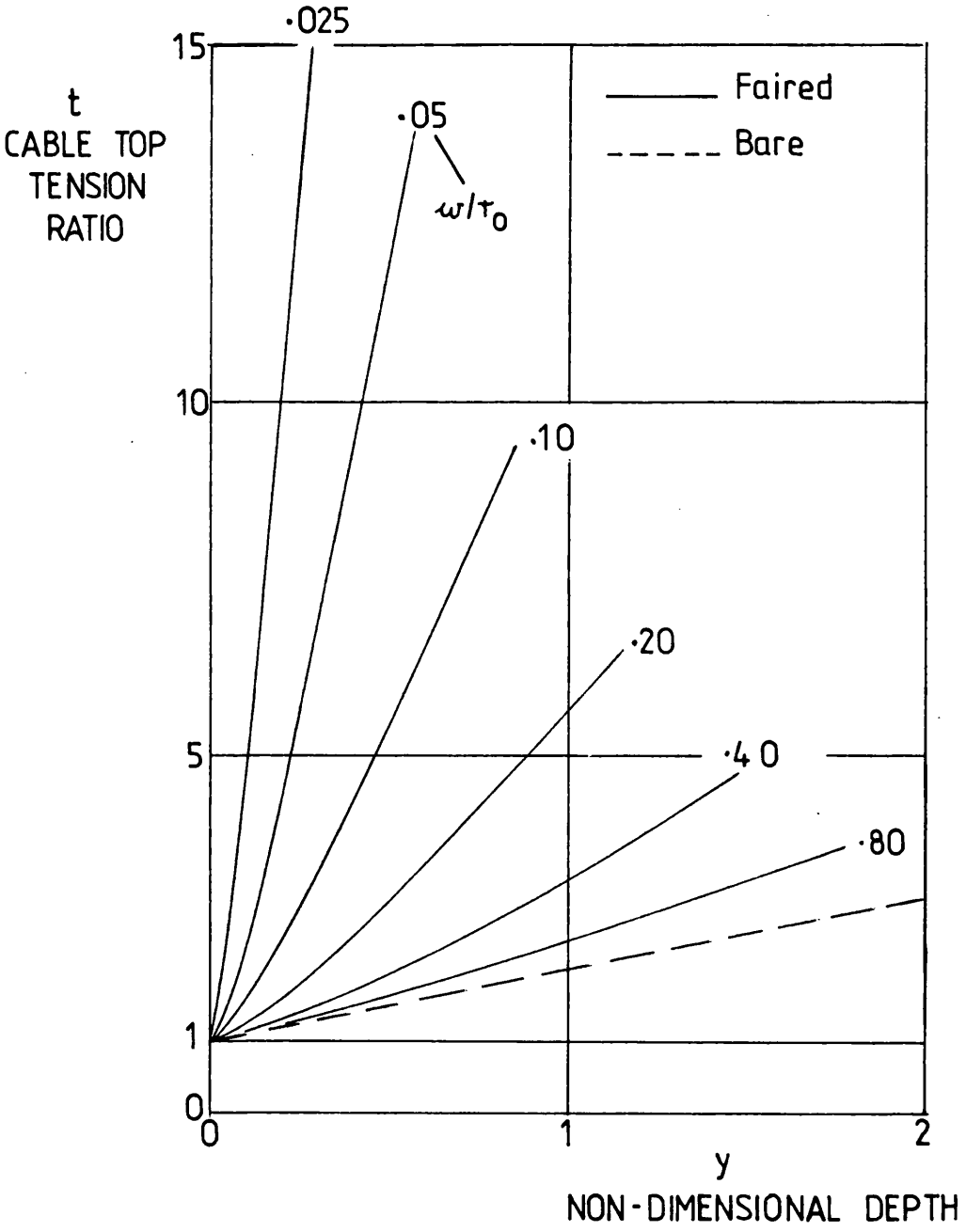

FIG. 10. CABLE TOP TENSION RATIO OF BARE AND FAIRED CABLES

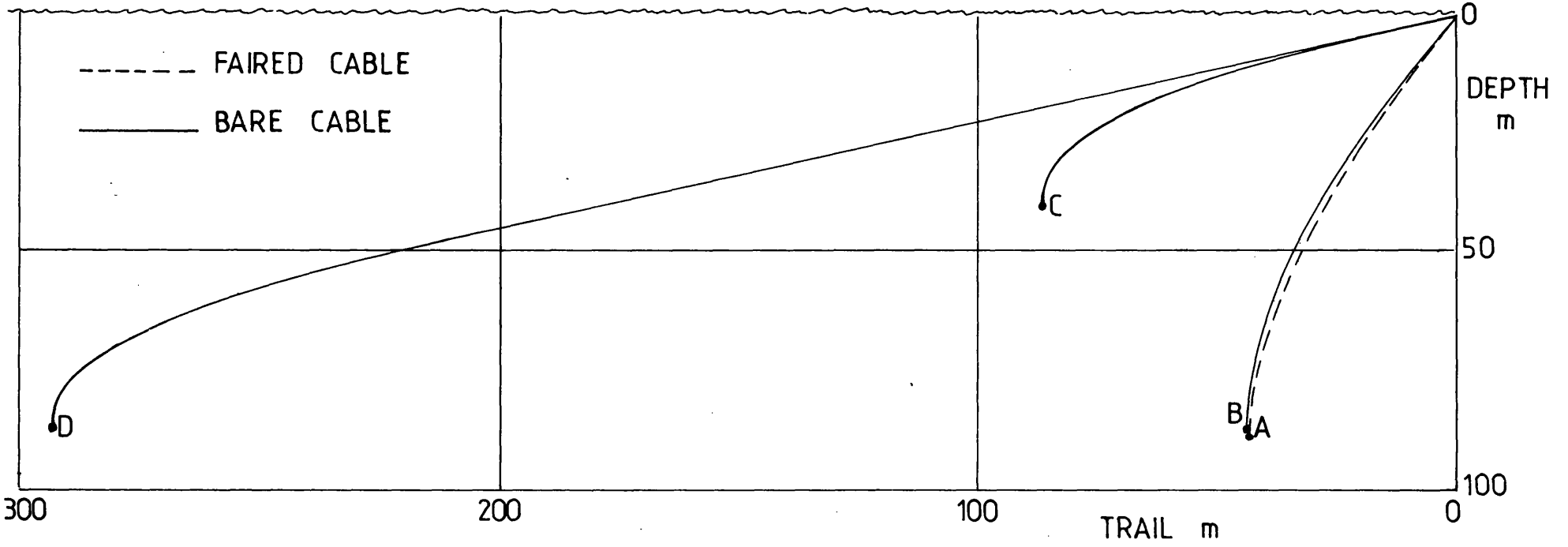

	W N	w N/m	d mm	t mm	C_{r_0}	v kt	r_0 N/m	w/r_0	SCOPE m	DEPTH m	TRAIL m	TOP ANGLE deg	TOP TENSION N
A	1025	4·10	—	20	0·20	5	13·65	0·30	100	88·6	41·9	49·8	1878
B	1025	4·10	16	—	1·50	2·04	13·65	0·30	100	87·3	44·0	47·1	1383
C	1025	4·10	16	—	1·50	5	81·90	0·05	100	40·9	86·9	13·8	1195
D	1025	4·10	16	—	1·50	5	81·90	0·05	315	88·5	296·4	12·8	1391

FIG. 11. EXAMPLES OF TOWING PERFORMANCE

FIG. 11.

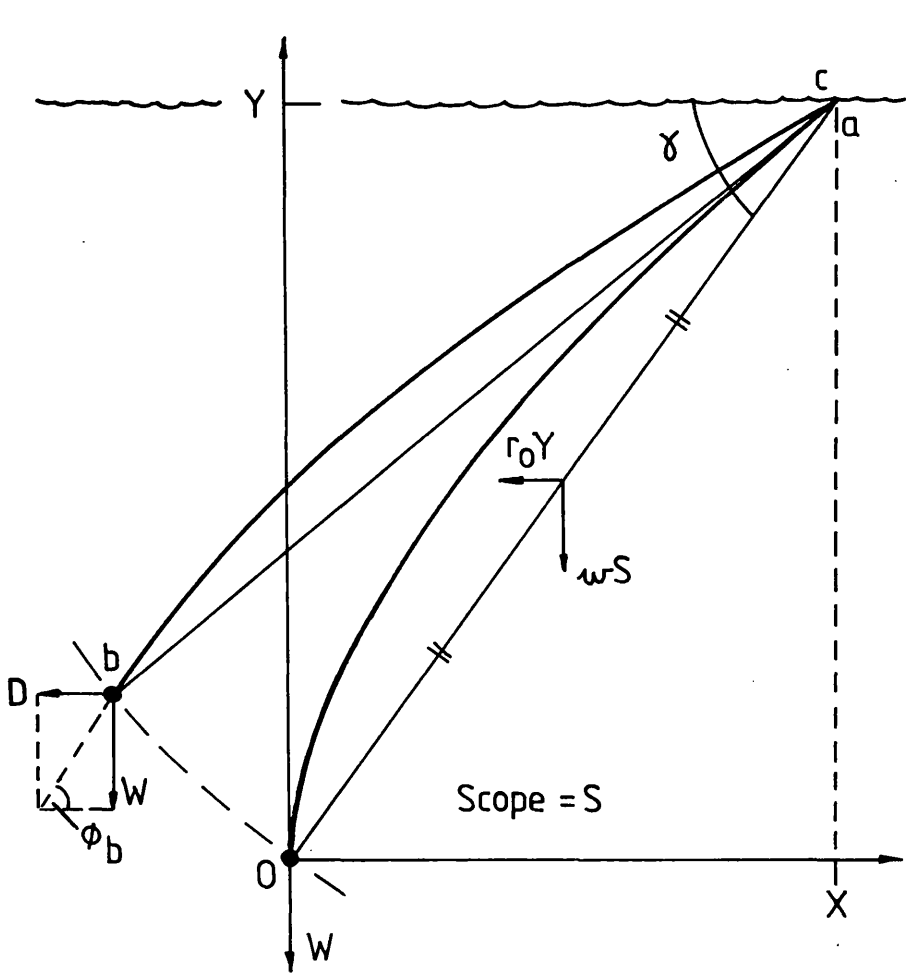

(a) Dimensional. Exaggerated Effect

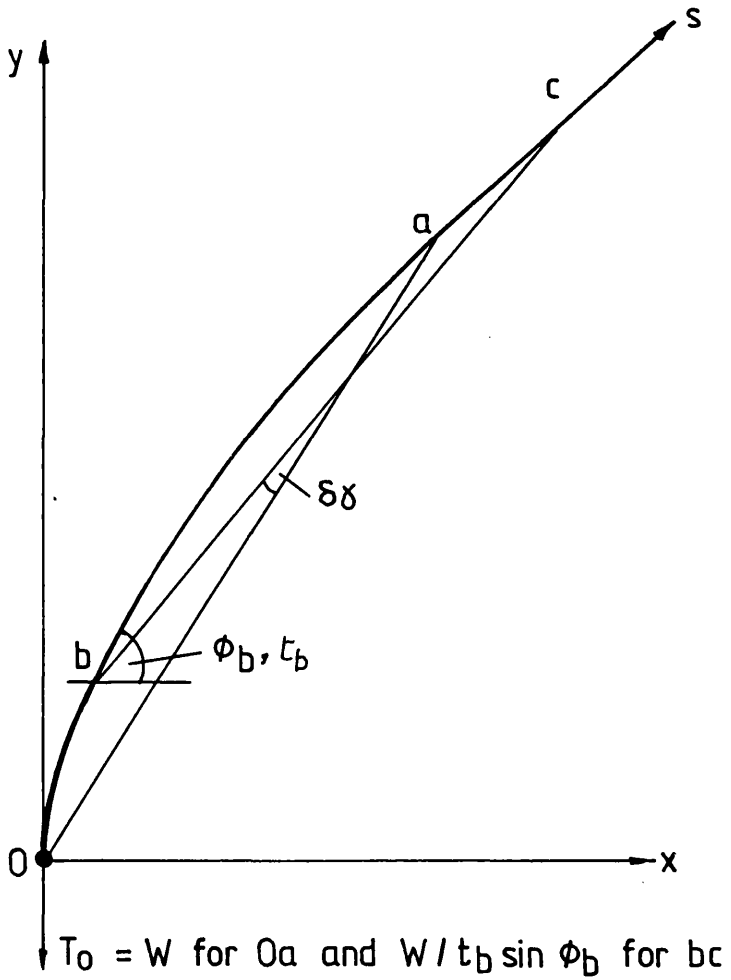

(b) Corresponding non - dimensional

FIG. 12

FIG.12. EFFECT OF FISH DRAG ON CABLE PROFILE AT CONSTANT SCOPE AND ω / r_0

BARE

w/r_o =0.0125 psi= 6.40

s	x	y	gamma	phi	t	C/S
0.0000	0.0000	0.0000	90.00	90.00	1.000	1.000
0.0250	0.0154	0.0182	49.84	27.30	1.018	0.952
0.0500	0.0338	0.0267	34.56	15.21	1.027	0.942
0.1000	0.0878	0.0366	22.63	9.08	1.037	0.951
0.1500	0.1373	0.0436	17.63	7.42	1.044	0.960
0.2000	0.1869	0.0493	14.92	6.82	1.050	0.967
0.3000	0.2863	0.0613	12.08	6.47	1.061	0.976
0.4000	0.3856	0.0725	10.65	6.41	1.072	0.981
0.5000	0.4850	0.0837	9.79	6.40	1.084	0.984
1.0000	0.9819	0.1394	8.08	6.40	1.139	0.992
2.0000	1.9757	0.2508	7.24	6.40	1.251	0.996
3.0000	2.9694	0.3623	6.96	6.40	1.362	0.997
4.0000	3.9632	0.4737	6.82	6.40	1.474	0.998

w/r_o =0.0250 psi= 9.04

s	x	y	gamma	phi	t	C/S
0.0000	0.0000	0.0000	90.00	90.00	1.000	1.000
0.0250	0.0102	0.0221	65.15	45.76	1.022	0.975
0.0500	0.0305	0.0366	50.17	27.98	1.037	0.953
0.1000	0.0771	0.0544	35.18	16.31	1.054	0.944
0.1500	0.1256	0.0666	27.92	12.48	1.067	0.948
0.2000	0.1746	0.0766	23.68	10.81	1.077	0.953
0.3000	0.2731	0.0940	19.00	9.56	1.094	0.963
0.4000	0.3718	0.1103	16.52	9.20	1.110	0.969
0.5000	0.4705	0.1262	15.01	9.09	1.126	0.974
1.0000	0.9643	0.2048	11.99	9.04	1.205	0.986
2.0000	1.9518	0.3619	10.51	9.04	1.362	0.993
3.0000	2.9394	0.5191	10.01	9.04	1.519	0.995
4.0000	3.9270	0.6762	9.77	9.04	1.676	0.996

FAIRED

w/r_o =0.0125 psi= 2.61

s	x	y	gamma	phi	t	C/S
0.0000	0.0000	0.0000	90.00	90.00	1.000	1.000
0.0250	0.0145	0.0192	52.94	33.76	1.847	0.963
0.0500	0.0367	0.0307	39.98	23.09	2.681	0.957
0.1000	0.0840	0.0468	29.13	15.71	4.069	0.961
0.1500	0.1325	0.0588	23.94	12.47	5.331	0.966
0.2000	0.1815	0.0688	20.75	10.58	6.541	0.970
0.3000	0.2801	0.0851	16.89	8.42	8.888	0.976
0.4000	0.3792	0.0986	14.57	7.20	11.186	0.980
0.5000	0.4785	0.1104	12.99	6.41	13.458	0.982
1.0000	0.9763	0.1570	9.13	4.65	24.666	0.989
2.0000	1.9738	0.2278	6.58	3.67	46.855	0.993
3.0000	2.9720	0.2884	5.54	3.33	68.959	0.995
4.0000	3.9704	0.3448	4.96	3.15	91.030	0.996

w/r_o =0.0250 psi= 5.11

s	x	y	gamma	phi	t	C/S
0.0000	0.0000	0.0000	90.00	90.00	1.000	1.000
0.0250	0.0099	0.0224	66.23	48.87	1.361	0.978
0.0500	0.0288	0.0386	53.20	34.26	1.866	0.963
0.1000	0.0729	0.0621	40.43	23.84	2.722	0.957
0.1500	0.1194	0.0803	33.92	19.40	3.464	0.959
0.2000	0.1670	0.0958	29.84	16.80	4.154	0.962
0.3000	0.2635	0.1219	24.82	13.79	5.457	0.968
0.4000	0.3610	0.1441	21.76	12.05	6.706	0.972
0.5000	0.4590	0.1640	19.66	10.91	7.926	0.975
1.0000	0.9523	0.2452	14.44	8.32	13.832	0.983
2.0000	1.9440	0.3740	10.89	6.80	25.339	0.990
3.0000	2.9375	0.4871	9.42	6.25	36.724	0.993
4.0000	3.9319	0.5934	8.58	5.97	48.061	0.994

TABLE 2. NON-DIMENSIONAL CHARACTERISTICS OF BARE AND FAIRED CABLES

TABLE 2

BARE

w/r_o =0.0500 psi=12.76

s	x	y	gamma	phi	t	C/S
0.0000	0.0000	0.0000	90.00	90.00	1.000	1.000
0.0250	0.0058	0.0241	76.43	64.01	1.024	0.991
0.0500	0.0203	0.0444	65.46	46.50	1.044	0.976
0.1000	0.0603	0.0741	50.86	29.33	1.074	0.955
0.1500	0.1055	0.0954	42.12	22.06	1.095	0.948
0.2000	0.1524	0.1125	36.43	18.39	1.112	0.947
0.3000	0.2483	0.1408	29.56	15.08	1.141	0.952
0.4000	0.3452	0.1656	25.63	13.79	1.166	0.957
0.5000	0.4425	0.1889	23.12	13.24	1.189	0.962
1.0000	0.9299	0.3004	17.90	12.77	1.300	0.977
2.0000	1.9052	0.5212	15.30	12.76	1.521	0.988
3.0000	2.8805	0.7421	14.45	12.76	1.742	0.992
4.0000	3.8558	0.9629	14.02	12.76	1.963	0.994

w/r_o =0.0750 psi=15.59

s	x	y	gamma	phi	t	C/S
0.0000	0.0000	0.0000	90.00	90.00	1.000	1.000
0.0250	0.0040	0.0246	80.77	71.99	1.025	0.996
0.0500	0.0147	0.0471	72.61	57.63	1.047	0.987
0.1000	0.0483	0.0839	60.10	39.82	1.084	0.968
0.1500	0.0893	0.1124	51.53	30.63	1.112	0.957
0.2000	0.1335	0.1357	45.47	25.46	1.136	0.952
0.3000	0.2258	0.1740	37.61	20.31	1.174	0.950
0.4000	0.3204	0.2066	32.82	18.03	1.207	0.953
0.5000	0.4158	0.2365	29.63	16.91	1.236	0.957
1.0000	0.8964	0.3745	22.67	15.67	1.374	0.971
2.0000	1.8595	0.6435	19.09	15.59	1.644	0.984
3.0000	2.8227	0.9123	17.91	15.59	1.912	0.989
4.0000	3.7859	1.1811	17.33	15.59	2.181	0.991

FAIRED

w/r_o =0.0500 psi= 9.58

s	x	y	gamma	phi	t	C/S
0.0000	0.0000	0.0000	90.00	90.00	1.000	1.000
0.0250	0.0057	0.0241	76.65	64.79	1.133	0.992
0.0500	0.0195	0.0449	66.49	49.47	1.381	0.979
0.1000	0.0570	0.0778	53.76	35.27	1.905	0.964
0.1500	0.0995	0.1041	46.28	28.92	2.378	0.960
0.2000	0.1441	0.1268	41.34	25.31	2.807	0.959
0.3000	0.2361	0.1659	35.09	21.20	3.595	0.962
0.4000	0.3301	0.2000	31.21	18.86	4.331	0.965
0.5000	0.4252	0.2309	28.51	17.33	5.037	0.968
1.0000	0.9075	0.3623	21.76	13.83	8.368	0.977
2.0000	1.8834	0.5803	17.12	11.78	14.695	0.985
3.0000	2.8638	0.7773	15.19	11.04	20.884	0.989
4.0000	3.8460	0.9653	14.09	10.67	27.015	0.991

w/r_o =0.0750 psi=13.29

s	x	y	gamma	phi	t	C/S
0.0000	0.0000	0.0000	90.00	90.00	1.000	1.000
0.0250	0.0040	0.0246	80.84	72.27	1.076	0.996
0.0500	0.0144	0.0472	73.04	59.04	1.224	0.988
0.1000	0.0461	0.0857	61.73	43.90	1.586	0.973
0.1500	0.0845	0.1176	54.30	36.25	1.945	0.966
0.2000	0.1261	0.1455	49.09	31.75	2.281	0.962
0.3000	0.2136	0.1938	42.23	26.70	2.894	0.961
0.4000	0.3041	0.2364	37.86	23.88	3.458	0.963
0.5000	0.3962	0.2753	34.79	22.05	3.995	0.965
1.0000	0.8671	0.4429	27.06	17.96	6.486	0.974
2.0000	1.8257	0.7276	21.73	15.62	11.142	0.983
3.0000	2.7909	0.9891	19.51	14.80	15.662	0.987
4.0000	3.7587	1.2406	18.27	14.38	20.126	0.990

TABLE 2. NON-DIMENSIONAL CHARACTERISTICS OF BARE AND FAIRED CABLES

BARE

w/r_o =0.1000 psi=17.96

s	x	y	gamma	phi	t	C/S
0.0000	0.0000	0.0000	90.00	90.00	1.000	1.000
0.0250	0.0030	0.0248	83.02	76.29	1.025	0.998
0.0500	0.0115	0.0482	76.63	64.56	1.048	0.992
0.1000	0.0397	0.0893	66.05	47.90	1.089	0.977
0.1500	0.0765	0.1231	58.14	37.97	1.123	0.966
0.2000	0.1176	0.1515	52.19	31.87	1.152	0.959
0.3000	0.2057	0.1987	44.00	25.28	1.199	0.953
0.4000	0.2974	0.2385	38.73	22.09	1.239	0.953
0.5000	0.3906	0.2746	35.11	20.40	1.275	0.955
1.0000	0.8637	0.4364	26.81	18.20	1.436	0.968
2.0000	1.8147	0.7458	22.34	17.97	1.746	0.981
3.0000	2.7659	1.0542	20.86	17.96	2.054	0.987
4.0000	3.7172	1.3626	20.13	17.96	2.363	0.990

w/r_o =0.1500 psi=21.90

s	x	y	gamma	phi	t	C/S
0.0000	0.0000	0.0000	90.00	90.00	1.000	1.000
0.0250	0.0020	0.0249	85.32	80.76	1.025	0.999
0.0500	0.0079	0.0492	80.91	72.39	1.049	0.996
0.1000	0.0287	0.0945	73.08	58.86	1.094	0.988
0.1500	0.0583	0.1348	66.62	49.23	1.135	0.979
0.2000	0.0932	0.1705	61.34	42.49	1.171	0.972
0.3000	0.1720	0.2319	53.43	34.21	1.232	0.962
0.4000	0.2570	0.2845	47.90	29.67	1.284	0.959
0.5000	0.3451	0.3319	43.87	27.00	1.332	0.957
1.0000	0.8012	0.5366	33.81	22.74	1.537	0.964
2.0000	1.7273	0.9138	27.88	21.95	1.914	0.977
3.0000	2.6550	1.2871	25.86	21.91	2.287	0.984
4.0000	3.5828	1.6602	24.86	21.90	2.660	0.987

FAIRED

w/r_o =0.1000 psi=16.37

s	x	y	gamma	phi	t	C/S
0.0000	0.0000	0.0000	90.00	90.00	1.000	1.000
0.0250	0.0030	0.0248	83.06	76.42	1.054	0.998
0.0500	0.0113	0.0483	76.84	65.30	1.156	0.992
0.1000	0.0383	0.0902	67.01	50.64	1.423	0.980
0.1500	0.0729	0.1263	60.00	42.33	1.708	0.972
0.2000	0.1114	0.1581	54.82	37.20	1.985	0.967
0.3000	0.1944	0.2139	47.73	31.29	2.503	0.963
0.4000	0.2814	0.2631	43.08	28.01	2.981	0.963
0.5000	0.3706	0.3084	39.77	25.92	3.432	0.964
1.0000	0.8302	0.5048	31.30	21.31	5.504	0.972
2.0000	1.7714	0.8426	25.44	18.74	9.337	0.981
3.0000	2.7211	1.1557	23.01	17.86	13.039	0.985
4.0000	3.6741	1.4585	21.65	17.43	16.690	0.988

w/r_o =0.1500 psi=21.21

s	x	y	gamma	phi	t	C/S
0.0000	0.0000	0.0000	90.00	90.00	1.000	1.000
0.0250	0.0020	0.0249	85.33	80.80	1.038	0.999
0.0500	0.0078	0.0492	80.98	72.65	1.100	0.996
0.1000	0.0281	0.0948	73.48	60.13	1.269	0.989
0.1500	0.0563	0.1360	67.51	51.74	1.465	0.981
0.2000	0.0893	0.1736	62.78	46.04	1.667	0.976
0.3000	0.1633	0.2407	55.84	39.02	2.065	0.970
0.4000	0.2434	0.3006	51.00	34.94	2.445	0.967
0.5000	0.3267	0.3558	47.44	32.31	2.807	0.966
1.0000	0.7644	0.5972	38.00	26.66	4.458	0.970
2.0000	1.6718	1.0171	31.31	23.68	7.470	0.978
3.0000	2.5915	1.4098	28.55	22.71	10.362	0.983
4.0000	3.5157	1.7917	27.00	22.24	13.209	0.986

TABLE 2. NON-DIMENSIONAL CHARACTERISTICS OF BARE AND FAIRED CABLES

BARE

w/r_o =0.2000 psi=25.18

s	x	y	gamma	phi	t	C/S
0.0000	0.0000	0.0000	90.00	90.00	1.000	1.000
0.0250	0.0015	0.0249	86.49	83.05	1.025	0.999
0.0500	0.0060	0.0495	83.13	76.61	1.050	0.998
0.1000	0.0223	0.0967	77.01	65.59	1.097	0.992
0.1500	0.0464	0.1404	71.70	57.02	1.140	0.986
0.2000	0.0761	0.1807	67.16	50.49	1.181	0.980
0.3000	0.1459	0.2522	59.95	41.69	1.252	0.971
0.4000	0.2237	0.3148	54.60	36.38	1.315	0.966
0.5000	0.3061	0.3716	50.52	33.02	1.372	0.963
1.0000	0.7427	0.6147	39.61	26.91	1.615	0.964
2.0000	1.6429	1.0501	32.58	25.34	2.050	0.975
3.0000	2.5474	1.4766	30.10	25.20	2.477	0.981
4.0000	3.4523	1.9023	28.86	25.18	2.902	0.985

w/r_o =0.2500 psi=28.02

s	x	y	gamma	phi	t	C/S
0.0000	0.0000	0.0000	90.00	90.00	1.000	1.000
0.0250	0.0012	0.0250	87.19	84.43	1.025	1.000
0.0500	0.0048	0.0497	84.49	79.22	1.050	0.999
0.1000	0.0182	0.0978	79.49	70.04	1.098	0.995
0.1500	0.0384	0.1435	75.04	62.52	1.144	0.990
0.2000	0.0638	0.1865	71.12	56.49	1.187	0.986
0.3000	0.1255	0.2651	64.66	47.81	1.265	0.978
0.4000	0.1965	0.3355	59.65	42.18	1.336	0.972
0.5000	0.2729	0.4000	55.70	38.40	1.400	0.968
1.0000	0.6888	0.6769	44.50	30.82	1.677	0.966
2.0000	1.5619	1.1644	36.70	28.40	2.164	0.974
3.0000	2.4431	1.6370	33.82	28.10	2.637	0.980
4.0000	3.3256	2.1074	32.36	28.04	3.107	0.984

FAIRED

w/r_o =0.2000 psi=24.95

s	x	y	gamma	phi	t	C/S
0.0000	0.0000	0.0000	90.00	90.00	1.000	1.000
0.0250	0.0015	0.0249	86.49	83.06	1.033	0.999
0.0500	0.0059	0.0495	83.16	76.73	1.079	0.998
0.1000	0.0220	0.0968	77.20	66.25	1.202	0.993
0.1500	0.0453	0.1410	72.18	58.49	1.349	0.987
0.2000	0.0736	0.1822	67.99	52.80	1.507	0.982
0.3000	0.1396	0.2573	61.52	45.30	1.829	0.976
0.4000	0.2129	0.3253	56.80	40.72	2.146	0.972
0.5000	0.2904	0.3883	53.21	37.69	2.454	0.970
1.0000	0.7065	0.6652	43.28	31.02	3.881	0.970
2.0000	1.5818	1.1484	35.98	27.58	6.480	0.977
3.0000	2.4732	1.6017	32.93	26.49	8.966	0.982
4.0000	3.3703	2.0434	31.23	25.99	11.409	0.985

w/r_o =0.2500 psi=27.99

s	x	y	gamma	phi	t	C/S
0.0000	0.0000	0.0000	90.00	90.00	1.000	1.000
0.0250	0.0012	0.0250	87.19	84.44	1.030	1.000
0.0500	0.0048	0.0497	84.50	79.28	1.069	0.999
0.1000	0.0180	0.0979	79.59	70.41	1.168	0.995
0.1500	0.0377	0.1438	75.31	63.43	1.286	0.991
0.2000	0.0622	0.1873	71.63	58.02	1.415	0.987
0.3000	0.1210	0.2681	65.71	50.48	1.685	0.981
0.4000	0.1881	0.3423	61.22	45.64	1.958	0.976
0.5000	0.2601	0.4116	57.71	42.34	2.227	0.974
1.0000	0.6548	0.7180	47.64	34.85	3.500	0.972
2.0000	1.4989	1.2539	39.91	30.89	5.844	0.977
3.0000	2.3633	1.7565	36.62	29.65	8.085	0.982
4.0000	3.2350	2.2466	34.78	29.09	10.283	0.985

TABLE 2. NON-DIMENSIONAL CHARACTERISTICS OF BARE AND FAIRED CABLES

BARE

w/r_o =0.3000 psi=30.55

s	x	y	gamma	phi	t	C/S
0.0000	0.0000	0.0000	90.00	90.00	1.000	1.000
0.0250	0.0010	0.0250	87.65	85.35	1.025	1.000
0.0500	0.0040	0.0498	85.40	80.98	1.050	0.999
0.1000	0.0153	0.0985	81.18	73.15	1.098	0.996
0.1500	0.0326	0.1453	77.37	66.55	1.145	0.993
0.2000	0.0547	0.1902	73.95	61.06	1.190	0.989
0.3000	0.1096	0.2736	68.17	52.79	1.274	0.983
0.4000	0.1742	0.3500	63.54	47.12	1.350	0.977
0.5000	0.2448	0.4207	59.80	43.14	1.421	0.973
1.0000	0.6394	0.7270	48.67	34.50	1.727	0.968
2.0000	1.4843	1.2617	40.37	31.23	2.262	0.974
3.0000	2.3423	1.7755	37.16	30.72	2.775	0.980
4.0000	3.2025	2.2853	35.51	30.61	3.285	0.984

w/r_o =0.3500 psi=32.84

s	x	y	gamma	phi	t	C/S
0.0000	0.0000	0.0000	90.00	90.00	1.000	1.000
0.0250	0.0009	0.0250	87.99	86.01	1.025	1.000
0.0500	0.0034	0.0498	86.05	82.25	1.050	0.999
0.1000	0.0132	0.0989	82.41	75.45	1.099	0.997
0.1500	0.0282	0.1465	79.09	69.59	1.147	0.995
0.2000	0.0478	0.1925	76.07	64.62	1.193	0.992
0.3000	0.0969	0.2795	70.87	56.86	1.280	0.986
0.4000	0.1558	0.3603	66.62	51.30	1.360	0.981
0.5000	0.2211	0.4360	63.11	47.27	1.436	0.978
1.0000	0.5946	0.7676	52.24	37.92	1.768	0.971
2.0000	1.4106	1.3454	43.64	33.90	2.345	0.975
3.0000	2.2451	1.8964	40.19	33.15	2.896	0.980
4.0000	3.0834	2.4416	38.37	32.96	3.442	0.983

FAIRED

w/r_o =0.3000 psi=30.55

s	x	y	gamma	phi	t	C/S
0.0000	0.0000	0.0000	90.00	90.00	1.000	1.000
0.0250	0.0010	0.0250	87.66	85.36	1.028	1.000
0.0500	0.0040	0.0498	85.41	81.02	1.063	0.999
0.1000	0.0152	0.0985	81.24	73.38	1.148	0.996
0.1500	0.0321	0.1455	77.54	67.13	1.248	0.993
0.2000	0.0536	0.1906	74.28	62.10	1.358	0.990
0.3000	0.1063	0.2755	68.90	54.76	1.592	0.984
0.4000	0.1677	0.3545	64.68	49.84	1.832	0.980
0.5000	0.2346	0.4288	61.32	46.38	2.072	0.977
1.0000	0.6086	0.7600	51.32	38.29	3.228	0.974
2.0000	1.4218	1.3415	43.34	33.86	5.385	0.977
3.0000	2.2600	1.8869	39.86	32.45	7.454	0.981
4.0000	3.1071	2.4183	37.89	31.81	9.486	0.984

w/r_o =0.3500 psi=32.84

s	x	y	gamma	phi	t	C/S
0.0000	0.0000	0.0000	90.00	90.00	1.000	1.000
0.0250	0.0009	0.0250	87.99	86.02	1.027	1.000
0.0500	0.0034	0.0498	86.06	82.28	1.060	0.999
0.1000	0.0131	0.0989	82.45	75.60	1.136	0.997
0.1500	0.0280	0.1466	79.20	69.99	1.224	0.995
0.2000	0.0470	0.1928	76.30	65.34	1.320	0.992
0.3000	0.0945	0.2807	71.39	58.33	1.528	0.987
0.4000	0.1508	0.3634	67.46	53.44	1.743	0.984
0.5000	0.2129	0.4417	64.26	49.92	1.960	0.981
1.0000	0.5671	0.7940	54.47	41.40	3.024	0.976
2.0000	1.3501	1.4155	46.35	36.57	5.036	0.978
3.0000	2.1624	1.9987	42.75	35.01	6.972	0.982
4.0000	2.9855	2.5667	40.69	34.29	8.876	0.984

TABLE 2. NON-DIMENSIONAL CHARACTERISTICS OF BARE AND FAIRED CABLES

BARE

w/r_o =0.4000 psi=34.93

s	x	y	gamma	phi	t	C/S
0.0000	0.0000	0.0000	90.00	90.00	1.000	1.000
0.0250	0.0008	0.0250	88.24	86.51	1.025	1.000
0.0500	0.0030	0.0499	86.54	83.21	1.050	0.999
0.1000	0.0116	0.0991	83.34	77.20	1.099	0.998
0.1500	0.0249	0.1473	80.40	71.96	1.147	0.996
0.2000	0.0423	0.1942	77.71	67.44	1.194	0.994
0.3000	0.0867	0.2837	73.01	60.20	1.284	0.989
0.4000	0.1405	0.3679	69.09	54.86	1.368	0.985
0.5000	0.2010	0.4475	65.81	50.87	1.448	0.981
1.0000	0.5541	0.8007	55.32	41.09	1.801	0.974
2.0000	1.3409	1.4175	46.59	36.42	2.418	0.976
3.0000	2.1517	2.0023	42.95	35.43	3.003	0.980
4.0000	2.9682	2.5801	41.00	35.14	3.580	0.983

w/r_o =0.4500 psi=36.87

s	x	y	gamma	phi	t	C/S
0.0000	0.0000	0.0000	90.00	90.00	1.000	1.000
0.0250	0.0007	0.0250	88.44	86.90	1.025	1.000
0.0500	0.0027	0.0499	86.93	83.96	1.050	1.000
0.1000	0.0103	0.0993	84.07	78.58	1.099	0.998
0.1500	0.0223	0.1478	81.43	73.85	1.148	0.997
0.2000	0.0379	0.1953	79.01	69.72	1.195	0.995
0.3000	0.0783	0.2867	74.73	62.99	1.287	0.991
0.4000	0.1278	0.3736	71.12	57.89	1.374	0.987
0.5000	0.1839	0.4564	68.05	54.00	1.456	0.984
1.0000	0.5175	0.8279	57.99	44.01	1.828	0.976
2.0000	1.2752	1.4801	49.25	38.81	2.480	0.977
3.0000	2.0624	2.0967	45.47	37.59	3.097	0.980
4.0000	2.8573	2.7035	43.42	37.19	3.704	0.983

FAIRED

w/r_o =0.4000 psi=34.93

s	x	y	gamma	phi	t	C/S
0.0000	0.0000	0.0000	90.00	90.00	1.000	1.000
0.0250	0.0008	0.0250	88.24	86.51	1.027	1.000
0.0500	0.0030	0.0499	86.55	83.23	1.057	0.999
0.1000	0.0115	0.0991	83.37	77.30	1.128	0.998
0.1500	0.0247	0.1473	80.48	72.24	1.208	0.996
0.2000	0.0418	0.1943	77.87	67.96	1.295	0.994
0.3000	0.0849	0.2845	73.39	61.32	1.482	0.990
0.4000	0.1367	0.3700	69.73	56.55	1.678	0.986
0.5000	0.1944	0.4516	66.71	53.03	1.877	0.983
1.0000	0.5298	0.8218	57.19	44.23	2.867	0.978
2.0000	1.2834	1.4786	49.04	39.06	4.761	0.979
3.0000	2.0704	2.0955	45.34	37.36	6.591	0.982
4.0000	2.8699	2.6963	43.21	36.57	8.393	0.984

w/r_o =0.4500 psi=36.87

s	x	y	gamma	phi	t	C/S
0.0000	0.0000	0.0000	90.00	90.00	1.000	1.000
0.0250	0.0007	0.0250	88.44	86.90	1.027	1.000
0.0500	0.0027	0.0499	86.93	83.97	1.056	1.000
0.1000	0.0103	0.0993	84.09	78.66	1.122	0.998
0.1500	0.0221	0.1479	81.49	74.05	1.196	0.997
0.2000	0.0375	0.1954	79.12	70.11	1.276	0.995
0.3000	0.0769	0.2873	75.01	63.84	1.448	0.991
0.4000	0.1247	0.3751	71.61	59.23	1.629	0.988
0.5000	0.1786	0.4593	68.76	55.76	1.814	0.986
1.0000	0.4963	0.8448	59.57	46.81	2.743	0.980
2.0000	1.2214	1.5329	51.45	41.37	4.539	0.980
3.0000	1.9837	2.1801	47.70	39.55	6.282	0.982
4.0000	2.7601	2.8103	45.52	38.68	8.000	0.985

TABLE 2. NON-DIMENSIONAL CHARACTERISTICS OF BARE AND FAIRED CABLES

TABLE 2

BARE

w/r_o =0.5000 psi=38.67

s	x	y	gamma	phi	t	C/S
0.0000	0.0000	0.0000	90.00	90.00	1.000	1.000
0.0250	0.0006	0.0250	88.59	87.21	1.025	1.000
0.0500	0.0024	0.0499	87.23	84.56	1.050	1.000
0.1000	0.0093	0.0994	84.66	79.70	1.099	0.999
0.1500	0.0201	0.1482	82.27	75.39	1.148	0.997
0.2000	0.0344	0.1962	80.06	71.60	1.196	0.996
0.3000	0.0713	0.2890	76.15	65.33	1.289	0.992
0.4000	0.1170	0.3780	72.81	60.49	1.378	0.989
0.5000	0.1691	0.4632	69.94	56.73	1.463	0.986
1.0000	0.4846	0.8504	60.33	46.69	1.850	0.979
2.0000	1.2136	1.5343	51.66	41.07	2.534	0.978
3.0000	1.9772	2.1799	47.79	39.63	3.180	0.981
4.0000	2.7506	2.8139	45.65	39.13	3.814	0.984

w/r_o =0.6000 psi=41.92

s	x	y	gamma	phi	t	C/S
0.0000	0.0000	0.0000	90.00	90.00	1.000	1.000
0.0250	0.0005	0.0250	88.83	87.67	1.025	1.000
0.0500	0.0020	0.0499	87.69	85.46	1.050	1.000
0.1000	0.0078	0.0996	85.54	81.39	1.100	0.999
0.1500	0.0169	0.1488	83.54	77.74	1.149	0.998
0.2000	0.0289	0.1973	81.67	74.49	1.197	0.997
0.3000	0.0603	0.2922	78.33	69.03	1.292	0.994
0.4000	0.0998	0.3840	75.44	64.69	1.384	0.992
0.5000	0.1453	0.4730	72.92	61.22	1.473	0.990
1.0000	0.4280	0.8848	64.19	51.39	1.885	0.983
2.0000	1.1020	1.6223	55.82	45.21	2.623	0.981
3.0000	1.8194	2.3195	51.89	43.41	3.319	0.983
4.0000	2.5506	3.0016	49.64	42.71	4.002	0.985

FAIRED

w/r_o =0.5000 psi=38.67

s	x	y	gamma	phi	t	C/S
0.0000	0.0000	0.0000	90.00	90.00	1.000	1.000
0.0250	0.0006	0.0250	88.59	87.21	1.026	1.000
0.0500	0.0024	0.0499	87.23	84.57	1.055	1.000
0.1000	0.0093	0.0994	84.67	79.75	1.118	0.999
0.1500	0.0200	0.1483	82.31	75.54	1.188	0.997
0.2000	0.0341	0.1962	80.15	71.89	1.263	0.996
0.3000	0.0702	0.2894	76.36	66.00	1.423	0.993
0.4000	0.1145	0.3790	73.19	61.57	1.592	0.990
0.5000	0.1648	0.4654	70.50	58.18	1.765	0.988
1.0000	0.4661	0.8639	61.65	49.18	2.643	0.982
2.0000	1.1636	1.5799	53.63	43.51	4.357	0.981
3.0000	1.9019	2.2543	49.85	41.58	6.027	0.983
4.0000	2.6558	2.9112	47.63	40.65	7.675	0.985

w/r_o =0.6000 psi=41.92

s	x	y	gamma	phi	t	C/S
0.0000	0.0000	0.0000	90.00	90.00	1.000	1.000
0.0250	0.0005	0.0250	88.83	87.67	1.026	1.000
0.0500	0.0020	0.0499	87.69	85.47	1.053	1.000
0.1000	0.0078	0.0996	85.55	81.42	1.112	0.999
0.1500	0.0168	0.1488	83.56	77.83	1.176	0.998
0.2000	0.0287	0.1973	81.73	74.67	1.244	0.997
0.3000	0.0597	0.2924	78.46	69.45	1.388	0.995
0.4000	0.0982	0.3846	75.68	65.40	1.540	0.992
0.5000	0.1424	0.4743	73.29	62.21	1.696	0.990
1.0000	0.4140	0.8936	65.14	53.33	2.494	0.985
2.0000	1.0599	1.6564	57.39	47.38	4.077	0.983
3.0000	1.7522	2.3779	53.61	45.27	5.631	0.985
4.0000	2.4631	3.0812	51.36	44.23	7.167	0.986

TABLE 2. NON-DIMENSIONAL CHARACTERISTICS OF BARE AND FAIRED CABLES

BARE

w/r_o =0.7000 psi=44.81

s	x	y	gamma	phi	t	C/S
0.0000	0.0000	0.0000	90.00	90.00	1.000	1.000
0.0250	0.0004	0.0250	88.99	88.00	1.025	1.000
0.0500	0.0017	0.0500	88.02	86.11	1.050	1.000
0.1000	0.0067	0.0997	86.17	82.60	1.100	0.999
0.1500	0.0145	0.1491	84.45	79.45	1.149	0.999
0.2000	0.0249	0.1980	82.84	76.62	1.198	0.998
0.3000	0.0522	0.2941	79.93	71.80	1.294	0.996
0.4000	0.0868	0.3880	77.39	67.90	1.388	0.994
0.5000	0.1271	0.4795	75.16	64.72	1.479	0.992
1.0000	0.3817	0.9091	67.22	55.33	1.909	0.986
2.0000	1.0049	1.6906	59.27	48.89	2.691	0.983
3.0000	1.6779	2.4301	55.38	46.83	3.430	0.984
4.0000	2.3684	3.1535	53.09	45.95	4.153	0.986

w/r_o =0.8000 psi=47.39

s	x	y	gamma	phi	t	C/S
0.0000	0.0000	0.0000	90.00	90.00	1.000	1.000
0.0250	0.0004	0.0250	89.12	88.25	1.025	1.000
0.0500	0.0015	0.0500	88.27	86.59	1.050	1.000
0.1000	0.0058	0.0998	86.65	83.52	1.100	0.999
0.1500	0.0127	0.1493	85.13	80.74	1.149	0.999
0.2000	0.0218	0.1985	83.72	78.24	1.198	0.998
0.3000	0.0460	0.2955	81.15	73.94	1.295	0.997
0.4000	0.0767	0.3906	78.89	70.42	1.391	0.995
0.5000	0.1127	0.4839	76.89	67.51	1.484	0.994
1.0000	0.3436	0.9269	69.66	58.64	1.927	0.988
2.0000	0.9205	1.7430	62.16	52.14	2.743	0.986
3.0000	1.5518	2.5185	58.36	49.90	3.518	0.986
4.0000	2.2034	3.2770	56.08	48.89	4.277	0.987

FAIRED

w/r_o =0.7000 psi=44.81

s	x	y	gamma	phi	t	C/S
0.0000	0.0000	0.0000	90.00	90.00	1.000	1.000
0.0250	0.0004	0.0250	88.99	88.00	1.026	1.000
0.0500	0.0017	0.0500	88.02	86.11	1.052	1.000
0.1000	0.0067	0.0997	86.18	82.62	1.109	0.999
0.1500	0.0145	0.1491	84.46	79.51	1.170	0.999
0.2000	0.0248	0.1980	82.87	76.74	1.233	0.998
0.3000	0.0518	0.2943	80.02	72.08	1.366	0.996
0.4000	0.0857	0.3883	77.55	68.38	1.506	0.994
0.5000	0.1250	0.4803	75.41	65.42	1.649	0.993
1.0000	0.3711	0.9150	67.92	56.83	2.389	0.987
2.0000	0.9698	1.7154	60.52	50.76	3.874	0.985
3.0000	1.6194	2.4756	56.81	48.52	5.339	0.986
4.0000	2.2897	3.2177	54.56	47.41	6.792	0.987

w/r_o =0.8000 psi=47.39

s	x	y	gamma	phi	t	C/S
0.0000	0.0000	0.0000	90.00	90.00	1.000	1.000
0.0250	0.0004	0.0250	89.12	88.25	1.025	1.000
0.0500	0.0015	0.0500	88.27	86.60	1.052	1.000
0.1000	0.0058	0.0998	86.65	83.53	1.107	0.999
0.1500	0.0127	0.1493	85.15	80.78	1.165	0.999
0.2000	0.0218	0.1985	83.74	78.32	1.225	0.998
0.3000	0.0457	0.2955	81.21	74.14	1.351	0.997
0.4000	0.0759	0.3908	79.00	70.76	1.483	0.995
0.5000	0.1112	0.4844	77.07	68.02	1.618	0.994
1.0000	0.3354	0.9309	70.19	59.81	2.314	0.989
2.0000	0.8915	1.7614	63.15	53.72	3.721	0.987
3.0000	1.5014	2.5538	59.55	51.41	5.118	0.987
4.0000	2.1339	3.3284	57.34	50.24	6.505	0.988

TABLE 2. NON-DIMENSIONAL CHARACTERISTICS OF BARE AND FAIRED CABLES

BARE

w/r_o =0.9000 psi=49.72

s	x	y	gamma	phi	t	C/S
0.0000	0.0000	0.0000	90.00	90.00	1.000	1.000
0.0250	0.0003	0.0250	89.22	88.45	1.025	1.000
0.0500	0.0013	0.0500	88.46	86.97	1.050	1.000
0.1000	0.0052	0.0998	87.02	84.23	1.100	1.000
0.1500	0.0113	0.1494	85.67	81.76	1.149	0.999
0.2000	0.0195	0.1988	84.41	79.51	1.199	0.999
0.3000	0.0411	0.2964	82.11	75.64	1.296	0.997
0.4000	0.0687	0.3925	80.08	72.44	1.392	0.996
0.5000	0.1011	0.4871	78.27	69.77	1.487	0.995
1.0000	0.3117	0.9401	71.65	61.43	1.940	0.990
2.0000	0.8471	1.7841	64.60	55.01	2.784	0.987
3.0000	1.4396	2.5396	60.93	52.66	3.590	0.988
4.0000	2.0546	3.3781	58.69	51.55	4.378	0.988

w/r_o =1.0000 psi=51.83

s	x	y	gamma	phi	t	C/S
0.0000	0.0000	0.0000	90.00	90.00	1.000	1.000
0.0250	0.0003	0.0250	89.30	88.60	1.025	1.000
0.0500	0.0012	0.0500	88.61	87.27	1.050	1.000
0.1000	0.0047	0.0999	87.32	84.81	1.100	1.000
0.1500	0.0102	0.1495	86.10	82.57	1.150	0.999
0.2000	0.0175	0.1990	84.96	80.54	1.199	0.999
0.3000	0.0371	0.2971	82.88	77.02	1.297	0.998
0.4000	0.0621	0.3939	81.04	74.09	1.394	0.997
0.5000	0.0916	0.4894	79.40	71.64	1.489	0.996
1.0000	0.2849	0.9501	73.31	63.81	1.950	0.992
2.0000	0.7831	1.8166	66.68	57.53	2.817	0.989
3.0000	1.3398	2.6473	63.16	55.13	3.647	0.989
4.0000	1.9207	3.4612	60.97	53.96	4.461	0.990

FAIRED

w/r_o =0.9000 psi=49.72

s	x	y	gamma	phi	t	C/S
0.0000	0.0000	0.0000	90.00	90.00	1.000	1.000
0.0250	0.0003	0.0250	89.22	88.45	1.025	1.000
0.0500	0.0013	0.0500	88.46	86.97	1.051	1.000
0.1000	0.0052	0.0998	87.02	84.24	1.106	1.000
0.1500	0.0113	0.1494	85.68	81.78	1.162	0.999
0.2000	0.0194	0.1988	84.42	79.57	1.220	0.999
0.3000	0.0409	0.2964	82.15	75.78	1.341	0.997
0.4000	0.0681	0.3926	80.16	72.69	1.466	0.996
0.5000	0.1000	0.4874	78.40	70.15	1.595	0.995
1.0000	0.3054	0.9429	72.05	62.35	2.258	0.991
2.0000	0.8232	1.7978	65.40	56.34	3.604	0.989
3.0000	1.3965	2.6171	61.92	53.98	4.945	0.989
4.0000	1.9938	3.4191	59.75	52.77	6.279	0.989

w/r_o =1.0000 psi=51.83

s	x	y	gamma	phi	t	C/S
0.0000	0.0000	0.0000	90.00	90.00	1.000	1.000
0.0250	0.0003	0.0250	89.30	88.60	1.025	1.000
0.0500	0.0012	0.0500	88.61	87.27	1.051	1.000
0.1000	0.0047	0.0999	87.32	84.81	1.105	1.000
0.1500	0.0102	0.1495	86.11	82.59	1.160	0.999
0.2000	0.0175	0.1990	84.97	80.58	1.216	0.999
0.3000	0.0369	0.2971	82.91	77.13	1.334	0.998
0.4000	0.0617	0.3940	81.10	74.28	1.454	0.997
0.5000	0.0908	0.4896	79.49	71.92	1.578	0.996
1.0000	0.2799	0.9521	73.62	64.54	2.215	0.992
2.0000	0.7633	1.8270	67.33	58.66	3.513	0.990
3.0000	1.3031	2.6688	63.97	56.29	4.809	0.990
4.0000	1.8678	3.4940	61.87	55.05	6.100	0.990

TABLE 2. NON-DIMENSIONAL CHARACTERISTICS OF BARE AND FAIRED CABLES

BARE

w/r_o =1.2500 psi=56.34

s	x	y	gamma	phi	t	C/S
0.0000	0.0000	0.0000	90.00	90.00	1.000	1.000
0.0250	0.0002	0.0250	89.44	88.88	1.025	1.000
0.0500	0.0010	0.0500	88.89	87.82	1.050	1.000
0.1000	0.0037	0.0999	87.85	85.84	1.100	1.000
0.1500	0.0082	0.1497	86.88	84.04	1.150	1.000
0.2000	0.0141	0.1994	85.96	82.41	1.199	0.999
0.3000	0.0299	0.2981	84.29	79.55	1.298	0.999
0.4000	0.0501	0.3960	82.79	77.14	1.396	0.998
0.5000	0.0741	0.4931	81.45	75.11	1.493	0.997
1.0000	0.2337	0.9666	76.41	68.41	1.967	0.994
2.0000	0.6553	1.8739	70.72	62.66	2.873	0.992
3.0000	1.1352	2.7502	67.57	60.27	3.750	0.992
4.0000	1.6413	3.6126	65.57	59.04	4.613	0.992

w/r_o =1.5000 psi=60.00

s	x	y	gamma	phi	t	C/S
0.0000	0.0000	0.0000	90.00	90.00	1.000	1.000
0.0250	0.0002	0.0250	89.53	89.07	1.025	1.000
0.0500	0.0008	0.0500	89.08	88.18	1.050	1.000
0.1000	0.0031	0.0999	88.21	86.53	1.100	1.000
0.1500	0.0068	0.1498	87.40	85.03	1.150	1.000
0.2000	0.0117	0.1996	86.63	83.66	1.200	0.999
0.3000	0.0249	0.2987	85.23	81.26	1.299	0.999
0.4000	0.0419	0.3972	83.98	79.23	1.397	0.999
0.5000	0.0621	0.4951	82.85	77.49	1.495	0.998
1.0000	0.1976	0.9762	78.56	71.69	1.976	0.996
2.0000	0.5609	1.9075	73.61	66.50	2.908	0.994
3.0000	0.9798	2.8155	70.81	64.24	3.816	0.994
4.0000	1.4248	3.7119	69.00	63.02	4.711	0.994

FAIRED

w/r_o =1.2500 psi=56.34

s	x	y	gamma	phi	t	C/S
0.0000	0.0000	0.0000	90.00	90.00	1.000	1.000
0.0250	0.0002	0.0250	89.44	88.88	1.025	1.000
0.0500	0.0010	0.0500	88.89	87.82	1.051	1.000
0.1000	0.0037	0.0999	87.85	85.84	1.103	1.000
0.1500	0.0082	0.1497	86.88	84.05	1.156	1.000
0.2000	0.0141	0.1994	85.97	82.43	1.211	0.999
0.3000	0.0297	0.2981	84.30	79.60	1.322	0.999
0.4000	0.0499	0.3961	82.82	77.25	1.435	0.998
0.5000	0.0737	0.4932	81.50	75.26	1.551	0.997
1.0000	0.2308	0.9676	76.58	68.84	2.145	0.995
2.0000	0.6427	1.8784	71.11	63.39	3.355	0.993
3.0000	1.1106	2.7621	68.10	61.08	4.570	0.992
4.0000	1.6044	3.6317	66.16	59.84	5.783	0.993

w/r_o =1.5000 psi=60.00

s	x	y	gamma	phi	t	C/S
0.0000	0.0000	0.0000	90.00	90.00	1.000	1.000
0.0250	0.0002	0.0250	89.53	89.07	1.025	1.000
0.0500	0.0008	0.0500	89.08	88.18	1.051	1.000
0.1000	0.0031	0.0999	88.21	86.53	1.102	1.000
0.1500	0.0068	0.1498	87.40	85.04	1.154	1.000
0.2000	0.0117	0.1996	86.63	83.67	1.207	0.999
0.3000	0.0249	0.2987	85.24	81.29	1.315	0.999
0.4000	0.0418	0.3972	83.99	79.29	1.425	0.999
0.5000	0.0619	0.4952	82.88	77.59	1.536	0.998
1.0000	0.1958	0.9767	78.67	71.97	2.103	0.996
2.0000	0.5526	1.9106	73.87	67.00	3.259	0.994
3.0000	0.9629	2.8225	71.16	64.81	4.420	0.994
4.0000	1.3988	3.7224	69.40	63.60	5.582	0.994

TABLE 2. NON-DIMENSIONAL CHARACTERISTICS OF BARE AND FAIRED CABLES

TABLE 2

SOME CAUSES AND EFFECTS OF TOW-OFF

ABSTRACT

The phenomenon of tow-off, or kiting, associated with faired cable systems has been studied in order to identify probable causes and demonstrate their effects. Three-dimensional cable profiles have been computed, embodying experimentally determined values of all hydrodynamic quantities. The work encompasses fish induced and fairing induced tow-off, with light and heavy fairings, and provides generalised data for estimation purposes plus examples of the variation with towing speed and scope of the tow-off angles and fish displacements to be expected of a typical towed system.

LIST OF CONTENTS

Figs. cont/d:-

Fig. 20. Variation of tow-off angle with speed and scope of fish yawed 2 deg. with neoprene fairings having α_H = 0.5 deg. at w/r_o = 1.

Fig. 21. Comparison between tow-off angles observed at sea and two theoretical simulations.

Fig. 22. The fairings tested at sea - showing possible sources of misaligned streaming.

Fig. 23. Towing tank experimental rig for measuring fairing lift force variation with speed and inclination.

Fig. 24. The results from the towing tank experiment.

Fig. 25. Towing tank experiment - data reduction.

Fig. A1. Co-ordinate system and forces on cable element.

NOMENCLATURE

A, B, C	Direction angles of cable element.
A_F	Maximum cross sectional area of fish.
a, b, c	Direction cosines of cable element.
a_o, b_o, c_o	Direction cosines of cable element at the origin.
c_g	Distance between cable centre and c.g. of fairing.
c_a	Distance between cable centre and aerodynamic centre of fairing.
$\bar{c}$	Chord length of faired cable.
D	Fish drag force = $C_D.\frac{1}{2}\rho v^2.A_F$
d	Diameter of cable.
F	Resultant external force per unit length of faired cable.
f	Non-dimensional value of F, = F/w.
G	A calibration factor (Fig. 25).
g	Gap between cable and fairing or between fairings (Fig. 12).
i, j, k	Direction cosines of F and f.
L_M	Moment arm (Fig. 25B).
L_s	Submerged length (Fig. 25B).
ℓ	Lift force per unit length of fairing.
ℓ_o	Lift force per unit length of fairing when the leading edge is normal to the flow.
ℓ_F	Length of fish.
M_F	Moment of fairing weight about cable centre.
M_H	Hydrodynamic moment of fairing about cable centre.
m	Pitching moment per unit length of fairing about cable centre.
N	Fish yawing moment about vertical axis through fish c.g.
Q	Torque due to unbalanced cable (Appendix 4).
Q, R	Constants in equation (15).
r	Drag force per unit length of faired cable.
r_o	Drag force per unit length of faired cable when the leading edge is normal to the flow.
S	Arc length (scope) measured along cable.
s	Non-dimensional arc length, = S/(W/w).
T	Cable tension.

Nomenclature cont/d:-

T_o	Cable tension at the origin.
t, t_o	Non-dimensional cable tension; = T/W, T_o/W.
t	Maximum thickness of faired cable section (Equation A(15)).
v	Towing speed.
W	Weight of fish in water.
w	Weight per unit length of cable + fairing, in water.
w_c	Weight per unit length of cable alone, in water.
w_f	Weight per unit length of fairing alone, in water.
X	Trail of fish behind cable top.
Y	Lateral displacement of fish due to tow-off.
Y_F	Fish sideforce.
Z	Depth of fish below cable top.
x, y, z	Non-dimensional coordinates, = $X/(W/w)$ etc.
α	Angle of incidence of fairing relative to local flow direction.
α_H	Trimmed incidence angle of heavy fairing mounted on horizontal cable normal to the flow.
β	Angle of yaw of fish relative to towing direction.
δ	Offset distance of cable centre from fairing axis.
λ	'Bank' angle of fairings in towing tank (Figs. 23, 24).
μ	Tow-off angle at cable top (Fig. 4).
μ_o	Tow-off angle of cable at the fish.
ϕ	Inclination angle of cable element to the horizontal when cable profile is 2-dimensional with $Y = 0$ at all X, Z.
ϕ_f	Threshold value of ϕ below which the fairing could 'flop'.
ψ	Cable critical angle.
ρ	Density of sea water (taken as 1030 kg/m^3 for applications).
θ	Angle defined in Fig. 5.

Nomenclature cont/d:-

C_D	Drag coefficient of fish, $= D/\frac{1}{2}\rho v^2.A_F$
C_ℓ	Section lift coefficient of fairing, $= \ell/\frac{1}{2}\rho v^2.\bar{c}$
C_m	Section pitching moment coefficient of fairing, $= m/\frac{1}{2}\rho v^2.\bar{c}^2$
C_{m_o}	Pitching moment coefficient caused by fairing section asymmetry.
C_N	Yawing moment coefficient of fish, $= N/\frac{1}{2}\rho v^2.A_F.\ell_F$
C_{r_o}	Section drag coefficient of cable, bare or faired.
C_{Y_F}	Sideforce coefficient of fish, $= Y_F/\frac{1}{2}\rho v^2.A_F$

1. INTRODUCTION

The use of fairings to reduce the drag of towing cables often produces the phenomenon known as tow-off, or kiting, caused by unwanted sideforces generated by the faired cable or the towed body. These forces displace the cable and body out of the vertical plane it should occupy, see Fig. 1, and in severe cases cause the cable to pull sideways on its sheave wheel, thereby jeopardising its reefing behaviour. In addition, when the ship heaves, the changes of cable tension combined with the sideforces can impart an oscillatory rolling motion to the body which adversely affects the performance of body-mounted sonar systems.

The elimination of tow-off is therefore an important requirement in the design of low drag towing systems. Of the two sources of sideforce illustrated in Fig. 1 it is the force produced by the fairings which is more adverse and more difficult to remove, although (as shown later) the presence of body sideforces can induce fairing sideforces if the fairings are negatively buoyant; the so-called 'flopping' mode described in Ref. (1).

Fairing sideforces are due to the hydrodynamic lifting properties of the fairings which behave like a wing with its span disposed vertically. Unfortunately the more the fairing profile is refined, in order to reduce its drag coefficient, the more lift it generates as a result of any streaming misalignment or built-in section asymmetry. In addition, the steeper the inclination angle of the cable to the flow resulting from the drag reduction the greater is the sideforce to be expected from a given misalignment and the greater its turning moment about the cable top.

The intransigent aspect of tow-off is the fact that unacceptably high lift forces can be generated by fairing misalignment angles of order only 1/10th degree. Such small angles defy measurement and can be the result of manufacturing errors that would normally be regarded as acceptable working tolerances. This is recognised in Ref. (2) which is a theoretical investigation of the tow-off induced by small varia-

tions in the shape of integral fairings, in which the strength member is embodied in the streamlined section. Such fairings are not the subject of the present study which is concerned with units that may be added to existing bare cables, either as clip-on fairings that trail behind the cable or as wrap-round fairings that enclose the cable, see Fig. 2.

Nevertheless Ref. (2) confirms the extreme sensitivity of tow-off to very small imperfections in fairing design. For this reason it is almost impossible to ascertain the precise cause of the tow-off behaviour exhibited by many towed systems. Furthermore, a lack of consistent records of tow-off observed at sea reduces the opportunity of confirming any theoretical work. In addition, considerable test work is needed to determine the many hydrodynamic properties required for analysis.

In the case of wrap-round fairings the presence of only slight friction between fairing and cable is sufficient to prevent perfect streaming, and to introduce hysteresis effects that further confound the diagnosis of precise causes. Wrap-round fairings are usually assembled on the cables as a series of linked units which can become compressed by the action of their weight plus the component of their drag acting tangentially to the cable; the so-called stacking loads. As a result there may be additional friction due to rubbing of adjacent fairing ends. Experiments described in Ref. (1) show that the friction torque is related to the stacking loads in a particular case.

The elimination of tow-off will be achieved by the virtual removal of friction between cable and fairing combined with further improvements to their hydrodynamic stability. Refs. (1), (3) and (4) all describe successful developments of fairings to achieve these ends. It is recommended, for example, that the minimum clearance between a cable diameter and a wrap-round fairing nose should be 7½ percent of the cable diameter. Stacking loads can be prevented from accumulating by assembling fairing units in separate lengths of 2 to 5 metres, the top unit of each length being located by a stopper clamped to the

cable so that each length hangs from a fixed position, (Ref. 1).

Tow-off still occurs in spite of these measures and the object of this study is to provide a better understanding of the phenomenon and to quantify the effects of those causes that can be successfully simulated mathematically. Hopefully this data will make it possible to recognise certain classes of tow-off behaviour by showing how the resulting tow-off displacements and cable angles may be expected to vary with speed, scope, fish weight etc.

The text presents an examination of alternative causes, descriptions of how they have been theoretically simulated and non-dimensional data about the resulting cable profiles. In addition the theory is applied to a particular body-cable system (Fig. 3 and Appendix 5) to illustrate typical variations in real units. The theoretical data has also been used to attempt to explain a consistent set of tow-off angle measurements obtained at sea, in 1976, with the same system, (Ref. 5).

The co-ordinate system defining the cable is illustrated in Fig. 4, which shows the forces that may act on the fish. The forces acting on the cable, either faired or bare, are illustrated in Fig. 5. Appendices 1 to 3 detail the methods used for calculating the cable profiles, the calculation of the hydrodynamic forces, and the non-dimensionalisation procedure. The latter is similar to that employed in Ref. 6, where cable tensions are expressed as proportions of the fish weight, and cable dimensions as proportions of the characteristic length given by the ratio of fish weight to cable weight per unit-length, the weights being the submerged values.

The less important case of tow-off due to body sideforce is considered first. The term 'fish' is used throughout in deference to accepted jargon.

2. FISH INDUCED TOW-OFF

If the fish is yawed with respect to the towing direction the resulting sideforce, Y_F, will move the fish and cable sideways (Fig. 4).

There are two possible causes of such yaw; misaligned vertical fins, caused by faulty rigging or damage, and cable torsion due to imperfectly balanced load carrying elements in the cable. The second cause can be discounted because in practice typical non-rotating cables would not generate sufficient torque to influence the fish's yaw attitude. This is established in Appendix 4 which presents an approximate method for estimating fish sideforce due to cable torsion.

The first cause, misaligned fins, would create a constant trimmed fish yaw angle, generating a sideforce increasing with the square of the towing speed. The quantities of interest are the resulting tow-off angles and the lateral displacements (Fig. 4). It is desirable to treat separately the cases with faired and bare cable and, initially, to consider the effect of fish sideforce unrelated to the fish angle of yaw. In all faired cable cases in this section it is assumed that the fairings stream perfectly.

2.1. Tow-off Angle Due to Fish Sideforce, with Faired Cable

Fig. 6(a) illustrates a typical faired cable profile. Such profiles have been computed for fish sideforce-to-weight ratios (Y_F/W) increasing from 0 to 1/2 and it is found that the shape of the cable in elevation is hardly affected, the depth reducing by only 5 percent in the most extreme case. The lateral curvature of the cable can therefore, with little error, be treated independently of the profile in elevation. As Y_F increases the projection of the cable on plane YOZ departs increasingly from the vertical and the lateral displacement of each point on the cable is found to be closely proportional to Y_F/W.

Fig. 6(b) shows the cable as viewed from astern. When the cable is faired the drag force, $r\delta S$, acting on each element is parallel to OX

so that only Y_F and the fish and cable weights are involved in the balance of forces. It is evident that

$$\tan\mu = Y_F/(W + wS) \qquad (1)$$

independent of the magnitude of the fish and cable drag forces, and hence of the towing speed. Equation (1) is verified by the computed results. Expressing S non-dimensionally as a proportion s of the system characteristic length W/w (Appendix 2) gives

$$\tan\mu = \tan\mu_o/(1 + s) \qquad (2)$$

where $\tan\mu_o = Y_F/W$ and s is the ratio of cable weight to fish weight.

Thus for a faired cable one can expect the tow-off angle to depend only on the scope, for a given fish sideforce, as shown by the heavy line in Fig. 7.

2.2. Tow-off Angle Due to Fish Sideforce, with Bare Cable

The direction of the hydrodynamic force on a bare cable is not parallel to OX but to XB (Fig. 5). It therefore opposes any lateral cable movement, and because the bare cable drag coefficient will be several times that of the faired cable the effect is large. The curvature of the cable projected onto plane YOZ is much increased so that the tow-off angle reduces more rapidly with distance S measured up the cable from the fish. The computed results show that the lateral displacement at given S is not quite linear with Y_F at shallow depression angles but the departure from linearity is not significant for $Y_F/W < 1/2$.

Computed values of $\tan\mu/(Y_F/W)$ are shown in Fig. 7 for a bare cable at a range of w/r_o values. It is seen that at very low speed (high w/r_o) there is little difference from faired, but at high speed and long scope the tow-off angle can be zero, belying the fact that the fish will in fact be laterally displaced. These results are computed for zero fish drag but the inclusion of fish drag is found to have only very small effect when the towing cable is bare; therefore these graphs may be used

to assess tow-off angles under most conditions.

2.3. Lateral Displacement Due to Fish Sideforce

Fig. 8 shows, per unit fish sideforce-to-weight ratio, the variation of lateral displacement y with scope s, these lengths being expressed non-dimensionally. Displacements are given for both bare and faired cables over a range of w/r_o. Fish drag has been ignored so that, as $s \to 0$, the value of dy/ds is constant and equal to Y_F/W.

The marked reduction of y in the bare cable case at all but the lowest speeds is evidence of the bare cable's resistance to lateral forces. At a given speed the reduction due to removing the fairing is enhanced because the corresponding w/r_o values would reduce by a factor of at least 4 due to the increased cable drag coefficient.

The y values at a given s may be altered by up to 10% when fish drag is considered. It is found, however, that y varies linearly with depth, and the constant of proportionality is practically independent of fish drag. Thus, if at given scope the depth is known, the lateral displacement can be determined with less uncertainty, as shown below.

2.4. Lateral Displacement Related to Depth

Fig. 6(b) shows a faired cable in end view with the fish at depth Z displaced Y laterally. Assuming that the resultant cable weight, wS, acts at the mid-Y point, as shown, one may take moments about an axis parallel to OX through the cable top. This yields

$$WY + \tfrac{1}{2}wSY = YZ \qquad (3)$$

giving

$$Y/Z = Y_F/(W + \tfrac{1}{2}wS) \qquad (4)$$

and therefore

$$Y/Z = (Y_F/W)/(1 + \tfrac{1}{2}s) \qquad (5)$$

showing that at a given scope the lateral displacement per unit fish side-force-to-weight ratio is proportional to the depth; the factor reducing with increasing scope. This equation is useful because it does not presuppose a particular relationship between depth and scope.

Fig. 9(a) compares the results from Equation (5) with values computed at extreme values of w/r_o representing fast and slow towing speeds. Equation (5) underestimates Y/Z because the assumption that the cable weight acts at mid-Y is evidently too crude, a factor of about 1.2 being necessary to give parity with the mean of the other two curves. The small variation with w/r_o is in contrast with the variation of y shown in Fig. 8(a). Furthermore the computed results show that Y/Z is independent of fish drag.

The corresponding values for a bare cable are shown in Fig. 9(b). The expected larger influence of decreasing w/r_o is evident. More important is the fact that if typical fish drag values are considered the Y/Z values change very little. Fig. 9(b) has been labelled accordingly.

These graphs allow the tow-off behaviour of a given system subjected to fish sideforce to be determined.

2.5. Application to a Constant Angle of Fish Yaw

The above results have been applied to a particular fish and cable (see Fig. 3 and Appendix 5) to illustrate typical effects of a constant fish yaw angle due to an unwanted asymmetry of the fish body-fin configuration. A value of 2 degrees of yaw is assumed to be realistic. The resulting tow-off angle tangents and displacements are, of course, linear with yaw angle.

Fig. 10 shows how μ and Y vary with speed for scopes of 75 to 600 m of

faired and bare cable. The faired cable tow-off angles are seen, at each scope, to vary roughly as v^2, due to the corresponding variation of Y_F. When the cable is bare the combination of the increased lateral cable curvature and the more rapid reduction of depth with speed, due to higher cable drag, produce negligible tow-off angles.

The lateral displacement is also negligible for the bare cable, but when it is faired there is a marked increase with speed and scope. A small reduction is caused when fish drag is allowed for, due to the small change of depth it incurs at each speed.With the bare cable the effect is not discernible.

It is thus seen that a modest angle of yaw of the fish can, with a faired cable produce significant lateral effects: 30 deg. of tow-off angle being sufficient to cause reefing problems. Such difficulties should not arise with bare cables.

3. FAIRING INDUCED TOW-OFF

The tow-off created by fairings that fail to stream properly is of greater magnitude than that due to fish forces because the unwanted fairing sideforces are distributed along the cable. It is characterised by a cable shape in which the tow-off angle is greatest at the top of the cable, see Fig. 1. For this reason the tow-off angle is usually a more important consideration than the accompanying lateral displacement.

The extreme sensitivity of the system to very small angles of fairing incidence α (Fig. 5) is demonstrated by Fig. 11 which shows the cable shape produced by the fairing of Fig. 3 with α assumed constant at $\frac{1}{2}$ deg. along the cable. It is seen that the tow-off angle is about 45 deg., which would be unacceptably high, particularly if the fish were towed from the side of a ship and the displacement were inwards. The loss of depth due to tow-off in this extreme case is nearly 20 percent. The unchanged value of the trail is clear evidence that cable elements are rotating about a horizontal axis through the cable top parallel to OX. The change in top tension, due to the tow-off, is of order 1 percent, which confirms that the lateral forces have little effect upon the longitudinal properties.

The assumed constancy of the fairing angle of incidence is not necessarily realistic because the value of α may vary along the cable in a manner depending on the cause of the fairing misalignment. Three contributory causes are (i) geometric asymmetry of the fairing and cable, (ii) the effect of the fairing weight and (iii) friction between fairing and cable or between adjacent fairing units. The effects of friction are not considered because there are too many unknowns to allow a realistic simulation to be made. The presence of friction exacerbates the effects of the first two causes and gives rise to inconsistent and non-repeatable towing behaviour.

It is with wrap-round fairings that the reduction of friction is more difficult. With clip-on fairings the area of rubbing surface is much

less. It must be taken as axiomatic that friction be reduced to the absolute minimum by careful design, as recognised in Ref.(1) and discussed in Section 1.

The two other causes, geometric asymmetry and fairing weight, are considered in turn.

3.1. Fairing Incidence Caused by Constructional Asymmetry

Ignoring the effect of fairing weight, in the first instance, it is clear that due to the sensitivity of the system the fairing shape must have a high degree of geometric symmetry and be free of handed surface imperfections such as recessed screw heads. These blemishes will cause the fairing to trim at a finite α that would in theory be constant along the cable whatever its inclination angle.

The precise value of the trimmed incidence would depend upon the reaction between the out-of-balance hydrodynamic pitching moment coefficient C_{m_o} created by the asymmetry and the restoring moment coefficient due to the inherent pitching stability of the fairing, which is governed by the derivative $dC_m/d\alpha$, the moments being taken about the cable centre. Thus

$$\alpha = C_{m_o}/(dC_m/d\alpha) \tag{6}$$

where

$$dC_m/d\alpha = (dC_\ell/d\alpha).(c_a/\bar{c}) \tag{7}$$

c_a being the distance between the cable centre and the aerodynamic centre.

The resulting lift force per unit length of cable will be given by

$$\ell = \alpha(dC_\ell/d\alpha).\ \tfrac{1}{2}\rho v^2.\ \bar{c} \tag{8}$$

where $dC_\ell/d\alpha$ is the section 'lift curve slope' of the cable-fairing combination.

These two hydrodynamic derivatives can vary widely according to the type of fairing section involved.

The magnitude of $dC_\ell/d\alpha$ may vary from 2π per radian for an aeronautical section to as little as 1.5 for a clip-on fairing having a large gap between cable and fairing member. In general the smaller the drag coefficient the larger is the lift curve slope. If wrap-round fairings have gaps between units the lift slope will fall but the drag coefficient increase. The same is true of gaps between clip-on fairings and their cables. Fig. 12 shows how the lift slope and drag coefficient are related for both types of fairings, the data being derived from Ref.7 and unpublished wind tunnel tests conducted by the writer. The lower level of the lift slope of clip-on fairings due to the increased effect of the larger area of the gap is undoubtedly the reason why clip-on fairings are much less prone to tow-off than wrap-round fairings, as is generally recognised. Equally relevant is the reduction of friction due to the much smaller contact area between clips and cable.

The magnitude of $dC_m/d\alpha$ may also vary widely. While it is obviously desirable to have small $dC_\ell/d\alpha$ to reduce tow-off, any such reduction must not be achieved at the expense of loss of stability. The ideal fairing would have a low lift slope and an aft aerodynamic centre. This requirement is not always easy to achieve. For aeronautical section shapes the aerodynamic centre will be 1/4 chord behind the leading edge, but when the section has a bluff nose profile and a thick trailing edge the aerodynamic centre position can depend critically upon the exact section profile. The example given in Ref. 1 shows that the fairing illustrated in Fig. 3, but without the trailing edge extension, had its aerodynamic centre only 2.3 mm aft of the cable centre, with a lift slope of 4.06. With the extension added the aerodynamic centre was 17.5 mm aft, with $dC_\ell/d\alpha$ unavoidably increased to 5.71. Without the extension these fairings produced unacceptably large tow-off.

If the fairing stability is small the trimmed incidence due to asymmetry

can become unacceptable. In such a case it is not only necessary to avoid all surface imperfections but in addition to ensure that the cable is precisely located on the fairing centreline, otherwise the fairing drag force will create an out-of-balance pitching moment, see Fig. 13. For example, a ½ mm off-centre displacement of the cable would, for the Fig. 3 fairing without its extension, cause a trimmed incidence of 0.125 deg., sufficient to create significant tow-off.

This evidence demonstrates that constructional asymmetry can cause fairings to stream with a constant angular offset along the length of the cable when they are close to having neutral buoyancy. Such cases have been analysed to reveal their tow-off characteristics.

3.2. Constant Incidence Tow-off with Neutrally Buoyant Fairings

Computed cable properties show that the sine of the angle of tow-off is to within 10 percent linear with the fairing lift/weight ratio created by the trimmed α. This is because the addition of the fairing lift forces has negligible effect on the top tension, the lateral component of which $(T\sin\mu)$ must balance the total lateral fairing force; (it being remembered that the drag forces on the cable are parallel to the direction of tow). The lateral displacement of the fish is also nearly linear with the fairing lift/weight ratio ℓ_o/w (Appendix 2). Fig. 14 shows the resulting tow-off behaviour in normalised form, from which tow-off and displacement may be derived for any towed system given the magnitudes of the fairing angle of incidence and lift and drag characteristics.

At given speed (or w/r_o) the fairing lift, being proportional to $\sin^2\phi$ (Appendix 1) will be greatest at the fish end, so that when more scope is added the additional lift will be progressively less and will also have a smaller turning moment about the cable top. Increasing the speed will increase the lift but reduce the fish depth which governs the turning moment. These conflicting effects produce the illustrated pattern which reveals that at high speeds (low w/r_o) the tow-off angle reaches a maximum value and then reduces.

The tow-off angle is seen in Fig. 14 to vary rapidly with non-dimensional scope in the range $0<s<0.5$ which covers many practical cases. It is worth noting that tow-off angles can be reduced, at a given real scope S, by increasing the weight of the fish. The magnitude of the change can be judged by the reduction of s that would result from doing so.

The corresponding lateral displacement y is seen to increase continuously with scope but at a rate that is speed dependent.

These results have been applied to the body-cable system of Fig. 3, assuming a fairing incidence of 0.2 deg; the very slight negative buoyancy of these fairings being ignored. Fig. 15 shows the characteristics that emerge. If 30 deg. is considered to be the maximum acceptable μ value it is evident that the system is unacceptable above about 7 knots at all but the lowest scope. The corresponding lateral displacements tend to peak between 5 and 7 knots with values of order 1/5th of the scope.

Overall these results confirm that very small angles of incidence will cause significant tow-off angles that can vary with speed and scope in a manner quite different from those caused by fish yaw (Fig. 10).

4. THE EFFECT OF FAIRING WEIGHT

When the weight of the fairing is considered the steady state angle of incidence must be derived by taking moments about the cable of both the fairing weight and the hydrodynamic forces. Fig. 16 illustrates unit length of fairing at incidence α with its weight in water, w_f, located a distance c_g from the cable axis OP. It may be shown that the weight moment of w_f about OP (the 'flopping' moment) is given by

$$M_F = \frac{w_f c_g}{\sin A} (\cos B \cos\alpha + \cos A \cos C \sin\alpha) \qquad (9)$$

where A, B, C are the direction angles of the cable element. The opposing hydrodynamic moment will be

$$M_H = dC_m/d\alpha . \bar{c}^2 . \tfrac{1}{2}\rho v^2 . \sin^2 A . \alpha \qquad (10)$$

The derivative $dC_m/d\alpha$ must be -ve for a stable fairing because C_m is defined as being +ve when it acts to increase α.

Writing $w_f c_g = Q$ (11)

and $dC_m/d\alpha . \bar{c}^2 . \tfrac{1}{2}\rho v^2 = R$ (12)

equations (9) and (10) become, in terms of the direction cosines a, b, c of OP

$$M_F = \frac{Q}{(1 - a^2)^{\frac{1}{2}}} \cdot (b\cos\alpha + a\sin\alpha) \qquad (13)$$

$$M_H = R(1 - a^2)\alpha \qquad (14)$$

Equilibrium, when $M_F + M_H = 0$, will occur when

$$Qb\cos\alpha + Qa\sin\alpha + R(1 - a^2)^{3/2}\alpha = 0 \qquad (15)$$

Since R is -ve it is convenient to write (15) as

$$Q_b\cos\alpha + Q_a\sin\alpha - |R|(1 - a^2)^{3/2}\alpha = 0 \quad (16)$$

A conventional non-dimensional measure of a fairing's propensity to flop is the incidence α_H it would trim at if mounted on a horizontal cable set normal to the stream, i.e. with direction cosines 0, 1, 0. Thus, from Equation (16) assuming $\cos\alpha = 1$

$$\alpha_H = Q/|R| \quad (17)$$

The magnitude of α_H will, of course, decrease as speed increases.

Equation (16) then becomes

$$\alpha_H b\cos\alpha + \alpha_H a\sin\alpha - (1 - a^2)^{3/2}\alpha = 0 \quad (18)$$

If the cable profile is assumed to be 2-dimensional and confined to the vertical plane OXZ, so that $b = 0$, one has

$$\alpha_H a\sin\alpha - (1 - a^2)^{3/2}\alpha = 0 \quad (19)$$

and writing $\sin\alpha = \alpha - \alpha^3/6$

$$-\alpha_H ac\alpha^3 + \left[\alpha_H ac - (1-a^2)^{3/2}\right]\alpha = 0 \quad (20)$$

Because X and Z are always +ve the quantities a, c are +ve; so also is α_H. Therefore if the coefficient of α in equation (20) is -ve it will yield a single stable equilibrium point at $\alpha = 0$. If the coefficient is +ve there are 2 stable equilibrium points at

$$\alpha = \pm\sqrt{6\left[1 - \frac{(1 - a^2)^{3/2}}{\alpha_H ac}\right]} \quad (21)$$

of which only the +ve value is relevant here. There is also an unstable equilibrium point at $\alpha = 0$.

Thus the fairings on a cable lying in the XZ plane would flop over from $\alpha = 0$ to the above value if

$$(1 - a^2)^{3/2} < \alpha_H ac \quad (22)$$

This inequality is only satisfied at large a, where the cable inclination angle ϕ is very shallow; it being evident that as the cable inclination approaches the horizontal the weight moment increases and

the hydrodynamic restoring moment decreases.
Writing ϕ_f as the threshold value below which flopping could occur, and noting that in the 2-dimensional case $a^2 + c^2 = 1$, the above inequality requires that

$\phi < \phi_f$ where

$$2\cos\phi_f = (\alpha_H{}^2 + 4)^{\frac{1}{2}} - \alpha_H \qquad (23)$$

The magnitude of α_H

Figure 17 shows in cross section a neoprene clip-on fairing having a specific gravity of 1.6; an example of a 'heavy' fairing.

From Equations (12) and (A15) it is seen that

$$\alpha_H = \frac{\frac{w_f}{w} \cdot \frac{c_g}{\bar{c}} \cdot C_{r_o} \cdot t}{\left|\frac{d\,C_m}{d\alpha}\right| \cdot \frac{}{\bar{c}}} \cdot \left(\frac{w}{r_o}\right) \qquad (24)$$

Substitution of the appropriate values for this fairing gives

$\alpha_H = 0.50$ deg at $w/r_o = 1$.

It may be noted that if the fairing material is homogeneous, α_H depends only upon the fairing shape and its specific gravity; not upon its size.

From Equation (23) this fairing could only flop on the part of the cable where $\phi_f < 5.3$ deg., an angle far lower than could conceivably occur at $w/r_o = 1$. Figure 18 shows the variation of ψ, the critical cable angle, as a function of w/r_o, compared to that of ϕ_f for $\alpha_H = 1^o$ and 10^o at $w/r_o = 1$. This fairing would require a specific gravity of about 13 to give $\alpha_H = 10$ deg. It is evident that when the cable is 2-dimensional such fairings can never flop, even if disturbed, because the hydrodynamic restoring moment always exceeds the weight moment.

If, however, the cable is already displaced laterally, due to fish yaw, the cable fairings will trim at some flopped angle and produce an additional sideforce on the system that would increase the tow-off.

Referring back to equation (16), and retaining the term in b, provides the fairing equilibrium condition relevant to a 3-dimensional cable profile. Writing $\cos\alpha = 1-\alpha^2/2$ and $\sin\alpha = \alpha - \alpha^3/6$ gives

$$\frac{\alpha_H ac}{6}\alpha^3 + \frac{\alpha_H b}{2}\alpha^2 + \left[(1-a^2)^{3/2} - \alpha_H ac\right]\alpha - \alpha_H b = 0 \qquad (25)$$

Since both α_H and α are of order .01 radian the terms in α^3 and α^2 may be ignored, to give

$$\alpha = \frac{\alpha_H b}{(1-a^2)^{3/2} - \alpha_H ac} \qquad (26)$$

It will be seen from Fig. 5 that the fairing lift force ℓ due to +ve α is arranged to act so that the direction cosines a, b, c remain +ve. This requires that

$$(1-a^2)^{3/2} > \alpha_H ac \qquad (27)$$

which is the opposite of the inequality required for flopping to occur in the 2-dimensional case. However, in the 3-d case this condition is always satisfied. Assuming that b = B, a constant, and writing $a^2 + B^2 + c^2 = 1$, the inequality (27) becomes

$$(B^2 + c^2)^{3/2} > \alpha_H c\sqrt{1 - (B^2 + c^2)} \qquad (28)$$

where c could vary from 0 to $\sqrt{1-B^2}$ along the cable. This inequality is found to be satisfied in all the practical cases examined.

Equation (26) can therefore be used to calculate the angle of incidence of heavy fairings on a cable that is forced to be 3-dimensional by another cause such as fish yaw. The resulting lift force to weight ratio of unit length of flopped fairing is given by equation (A24).

4.1. The Combined Effects of Flopping and Fish Yaw

A series of computations has been made of the cable shapes resulting from the combined effects of fish yaw angles β of 0, 1, 2 deg. with heavy fairings having α_H values of 0, 0.25, 0.5, 0.75 deg. It is found that in spite of large tow-off angles the cable top tension is affected little by the fish and fairing lateral forces. It is also found that the inclusion of fish drag makes negligible difference to the resulting tow-off.

In qualitative terms the revealed non-dimensional patterns of cable shape, although non-linear with α_H and β, can be exemplified by results at one value of w/r_o, as shown in Fig. 19. The cable shape as seen from astern is shown, for $s = 4$ and compared with the case when $\alpha_H = 0$, i.e. with neutrally buoyant fairings. The magnitudes of the tow-off angle are also plotted against scope. The curvature of the cable is seen to change sign as α_H increases, and it becomes almost straight at $\alpha_H = \frac{1}{2}$ deg., with a tow-off angle of about 30 deg. at all scopes. At $\alpha_H = 0.75$ the tow-off angle becomes excessive.

A conversion of these data into real units provides a practical comparison. Fig. 20 shows the effect of flopping on a towed system involving the Fig. 3 fish assuming that a neoprene fairing of specific gravity 1.6 were used in place of the fairing shown in Fig. 3. The tow-off angle is seen to increase approximately with speed squared, and there is negligible change with scope when flopping occurs.

These results may be compared with those of Figs. 10 and 15. Taken together they demonstrate that the tow-off behaviour of a given system, if friction effects are ignored, can vary considerably according to the cause. The characteristics revealed by these calculations may be helpful in diagnosing the cause of tow-off where a consistent set of measurements is available.

4.2. Fairings Having Positive Buoyancy

Lighter-than-water fairings are rare but, as pointed out by J.F. Henderson,

advantage would accrue from their use. Not only would flopping be prevented but the fairing incidence due to geometrical asymmetry would also be reduced. In cases where the static stability of a fairing is low the possession of buoyancy would much reduce its tendency to cause tow-off.

5. ANALYSIS OF SOME TOW-OFF ANGLES OBSERVED AT SEA

The towed system of Fig. 3 was taken to sea in 1976 (Ref. 5) and large tow-off angles were observed. The fish was stern launched and the tow-off angles were recorded by photographing the cable angle made with the horizon when viewed looking astern. The sea conditions were very calm.

The most noteworthy feature of the observed angles was their repeatability from one day to another, which suggested that little friction was present between cable and fairings. This was, perhaps, to be expected because a 3 mm diameter difference existed between the cable and the fairing enclosing it.

The direction of tow-off was always to port and unaffected by the angle of yaw at which the fish was lowered into the water. The cable scope was varied from 60 to 135 m, which ruled out the likelihood that the ship wake was influencing the cable profile. The speed range was up to 6½ knots.

The observed tow-off angles are shown in Fig. 21 and it is seen that the μ values increase roughly linearly with both $(\text{speed})^2$ and scope, which suggests that the sideforces are due to fairing incidence rather than fish yaw.

A first attempt to simulate the observations was based upon the assumption that the fairings were trimming at some constant angle of incidence, due to some shape asymmetry. The value of α was adjusted, using the programme, to provide a tow-off angle matching the point shown in Fig. 21 at 90 m scope. Only 0.18 deg. was needed. The μ variation at other speeds and scopes, when α = 0.18 deg., is shown. The resulting trends are not in good agreement with those observed. Scaling the value of α up or down did not improve the agreement.

The fairings have an α_H angle of only 0.225 deg. at $w/r_o = 1$ (Appendix 5), and it was confirmed that no realistic combinations of fish yaw angle with flopping could provide μ variations of the pattern observed.

The constant α curves in Fig. 21 are seen to have falling gradients above 4 kt., in contrast to the trends exhibited by the observed points, particularly at the higher scopes. This suggests that, in reality, the fairing angle of incidence must be increasing as the cable angle becomes shallower.

A significant difference between these particular fairings and the more ideal section shapes assumed in the theoretical applications is the presence of the trailing edge extensions, (Fig. 3) with 4 mm gaps between each adjacent pair. If, due to their loose fit on the cable and the asymmetric arrangement of the screwheads, the fairings 'buckle', as shown in Fig. 22, the resulting staggered arrangement of the trailing edge extensions would be conducive to deflecting the fairings to an incidence that would be greater the closer is the flow direction to being parallel to the cable. This is because the restoring moment decreases as the tangential component of $\frac{1}{2}\rho v^2$ increases.

In order to test this hypothesis a simple experiment was carried out.

5.1. Experimental Determination of Fairing Lift Force

Twelve fairings, see Fig. 23, were mounted on a 13 mm dia steel bar held in a frame freely pivoted on the overhead trolley of the School of Engineering Towing Tank. The fairings and frame were free to swing, like a pendulum, under the action of any lift forces generated by the fairings when they moved through the water. The trolley was accelerated at about 1 m/s^2 to speed plateaux variable from 1 to 3 knots in ½ knot steps. The 'bank' angle of the pendulum frame was recorded by a simple tally that marked the maximum angle. The tank length was sufficient to ensure several seconds of dwell at the maximum speeds. The angle of inclination ϕ of the fairings could be changed from 90 deg. to 45 deg. In the latter case the number of submerged fairings was reduced from 12 to 8.

The bank angle could be read to the nearest 1/4 deg. and the maximum recorded angle was 3 deg. Although this imples a resolution of no better than 8 percent of full scale deflection the consistency of the results, encompassing 3 repeats of each point is satisfactory. Fig.24 shows that the bank angle λ was approximately proportional to $(\text{speed})^2$, implying that the fairing incidence was constant, at each inclination angle.

Converting these angles into moments about the pivot axis involved the pendulum calibration curve of Fig. 25(a). Conversion of this moment into fairing lift force per metre was based upon the assumption that the resultant lift force acted through the mid-point of the submerged length L_s, see Fig. 25(b). Its moment arm was thus given by

$$L_M = h + \sin\phi(L - \tfrac{1}{2}L_s) - d\cos\phi \qquad (30)$$

The resulting lift force per unit length of fairing, ℓ, is given by

$$\ell = G\lambda/L_M L_s \qquad (31)$$

where G is the 'pendulum' calibration factor in Nm/deg.

This derived ℓ requires correcting to provide the equivalent 2-dimensional section lift force for use in the cable equation. The aspect ratio (span ÷ streamwise chord length) varied from 10.2 to 4.2 as ϕ reduced from 90 deg. to 45^{o}. An approximate correction factor has been derived from theoretical lift slope data from Ref. (8), giving correction factors varying from 1.2 at ϕ = 90 deg. to 1.55 at ϕ = 45 deg.

The measured values of fairing lift force are given in Fig. 24(b), the corrections to infinite aspect ratio being shown. The graph relates to a 3 knot towing speed. The trend is clearly one of small variation of ℓ with ϕ, implying that the fairing incidence does increase as ϕ gets less.

If the fairing lift force per unit length is assumed, on this evidence, to be independent of ϕ, and to vary with the square of the speed up to 6 knots, the resulting theoretical tow-off curves (Fig. 21) are in better agreement with the observed tow-off angles than are the constant α values. Equally important is the fact that, in the towing tank, the 'cable' deflected only to the port side, as occurred at sea. Whether or not the fairings were buckling could not be ascertained in the tank, the physical deflections of the fairings being, of course, very small.

It is concluded that these particular fairings, with their large clearances and trailing edge extensions, were behaving differently from the manner to be expected of more regular fairing shapes; the possible explanation being the occurrence of buckling (Fig. 22).

6. SUMMARY AND CONCLUSIONS

The well known tendency faired cable systems have for towing off has been demonstrated by calculations utilising experimentally determined hydodynamic properties of fairings, cables and body. These have confirmed that apparently minor imperfections in the design of cable fairings can give rise to unnacceptably large tow-off angles at the cable top.

Because such small angles involve no added drag to the fairings the trail of the fish is unaffected by tow-off; the latter causing each element of cable to rotate about a fore-and aft axis through the cable top.

Two alternative causes of tow-off have been studied: fish-induced and fairing-induced. The former, caused by a constant trimmed fish yaw angle, with neutrally buoyant fairings, has been shown to be the less serious and, in conjunction with an unfaired cable, to have little effect. The likelihood of fish-induced tow-off caused by the torque from an unbalanced cable has been found to be negligible.

It has also been shown that when the fairings are heavier than water fish-induced tow-off is greatly amplified because the fairing weight inclines the fairings to the local flow direction.

Normalised data has been provided for the estimation of tow-off angles and fish displacements due to these causes, given the knowledge of the many hydrodynamic properties required. This has been possible because it was found that, at a given scope and towing speed, the magnitudes of the resulting displacement were approximately linear with the fish sideforce, or the fairing lift force occurring at the bottom of the cable where its inclination is nominally vertical.

The normalised data has been applied to a given towed system to

demonstrate in real units the magnitudes to be expected in practice. It was found that if fish yaw was the primary cause the cable top tow-off angle reduced with scope increase at constant speed, but that the contrary was true if fairing incidence was the sole cause. The combined effect of fish yaw with a heavy fairing could produce either variation.

Measurements at sea of the tow-off angles generated by the towed system have been used to test the theory, but none of the above standard causes could explain the observed variations with speed and scope. Towing tank experiments using a sample of the fairings showed that they behaved differently, the measured lift force per metre length being almost independent of the cable inclination. This revised lifting law produced much improved agreement with the sea trial results, although the proposed explanation for such fairing behaviour has involved an element of conjecture.

Finally, it is hoped that this study will lead to a better understanding of the quantitative aspects of the tow-off phenomenon and contribute to the design of trouble-free fairings. The work has reinforced the view that the ideal fairing will have a low lift curve slope, high static stability, a minimum of rubbing contact area with the cable and be free of all sources of section asymmetry and surface irregularity.

7. ACKNOWLEDGEMENT

This work is part of a research programme financed by the Science and Engineering Research Council, the Department of Industry and the University of Bath. Their support is gratefully acknowledged.

The author is much indebted to many colleagues, in particular to Dr. J.F. Henderson for advice concerning many hydrodynamic matters, and to Mr. D.A. Chapman for valuable help with the computation. The practical assistance of Mr. D.W. Tallin, who constructed the apparatus, is recorded with thanks, together with the advice received from Mr. C.J. Price of Standard Telephones and Cables Ltd., relating to unbalanced cable torque.

8. REFERENCES

1. J.F. Henderson — Some Towing Problems with Faired Cables. Ocean Engineering, Vol. 5, No. 2, April 1978.

2. H.T. Wang — Numerical studies of the kiting of faired towlines. ASME Symposium on Ocean Engineering Mechanics, Houston, pp. 61-76, 1975.

3. N.E. Hale — Performance Investigation of Improved 'Flexnose' and 'Rigstream' Cable Fairings with an Emphasis on Anti-Kiting. Report No. 4-116-F1. December 1979 Fathom Oceanology Limited, Port Credit, Ontario, Canada.

4. N.E. Hale & R. Kemsley — AN/SQS-504 Cable Fairing. Modification Study Phase 1. Report No. 4-134-R1. Feb. 1982 Fathom Oceanology Limited, Port Credit, Ontario, Canada.

5. P.J. Wingham & N.R. Keshavan — Predicting the Equilibrium Depth of a Body Towed by a Faired Cable. Ocean Engineering, Vol. 5, No. 1, February 1979.

6. P.J. Wingham — Comparative steady state deep towing performance of bare and faired cable systems. Ocean Engineering, Vol. 10, No. 1, 1983.

7. S.G.G. Dalton & C.R. Hiett — Force and Restoring Moment Measurements on Fairings for Underwater Towing Cables. School of Engineering Report No.335, University of Bath, June 1976.

8. B.W. McCormick — Aerodynamics, Aeronautics and Flight Mechanics, p. 286, John Wiley & Sons, Inc. 1979.

9. D.S. Weaver — Unmanned submersible umbilical drag and analysis - a review with recommendations for future research. BHRA TRC1203, December 1979. Cranfield, England.

10. P.T. Gibson, H.A. Cross, W.J. Kaufman, W.E. Gallant — Analysis of wire rope torque. Wire and Wire Products for November 1970.

11. J.F. Henderson — Wind tunnel tests on a ½ scale model of the Mk. 3 Sonar Fish. School of Engineering Report No.560, University of Bath, September 1981.

APPENDIX 1

DERIVATION OF CABLE SHAPES IN THREE DIMENSIONS

A1.1. The Cable Equations

Fig. A1 shows the coordinate system of a fully flexible inextensible cable in equilibrium under an external loading represented by a force per unit cable length, F, having direction cosines i, j, k; these variables being known functions of S, the cable length measured from the origin.

If an element δS is under tension, T, the differences between the direction cosines at its ends required to balance the component of F normal to the cable are given by:

$$a_2 - a_1 = (F\delta S/T_1)\left[-i(1 - a_1^2) + j a_1 b_1 + k a_1 c_1\right] \qquad A(1)$$

$$b_2 - b_1 = (F\delta S/T_1)\left[i a_1 b_1 - j(1 - b_1^2) + k b_1 c_1\right] \qquad A(2)$$

$$c_2 - c_1 = (F\delta S/T_1)\left[i a_1 c_1 + j b_1 c_1 - k(1 - c_1^2)\right] \qquad A(3)$$

where a_1, b_1, c_1 are the direction cosines at the lower end.

The change in tension along the element is given by

$$T_2 - T_1 = -F\delta S(i a_1 + j b_1 + k c_1) \qquad A(4)$$

Assuming that the element is smoothly curved the coordinates of the upper end in terms of those at the lower end are given by

$$S_2 - S_1 = \delta S \qquad A(5)$$

$$X_2 - X_1 = \tfrac{1}{2}(a_1 + a_2)\delta S \qquad A(6)$$

$$Y_2 - Y_1 = \tfrac{1}{2}(b_1 + b_2)\delta S \qquad A(7)$$

$$Z_2 - Z_1 = \tfrac{1}{2}(c_1 + c_2)\delta S \qquad A(8)$$

If the tension and direction cosines are known at the origin, and the vector F is specified at all S, these equations allow a step-by-step numerical integration up the cable.

A1.2. Conditions at the Origin

These are governed by the forces acting on the towed body. Writing W, D_F as the fish weight and drag respectively, and Y_F as the sideforce produced if the fish is yawed with respect to the direction of motion, the tension T_o at the origin will have magnitude

$$T_o = \left(D_F^2 + Y_F^2 + W^2\right)^{\frac{1}{2}} \qquad A(9)$$

because the 3 forces are orthogonal (Fig. 4).

The direction cosines of the cable at the origin will thus be:

$$a_o = D_F/T_o, \quad b_o = Y_F/T_o, \quad c_o = W/T_o \qquad A(10)$$

The fish drag force is given by

$$D_F = C_D . \tfrac{1}{2}\rho v^2 . A_F \qquad A(11)$$

where C_D is the drag coefficient based upon the body maximum cross sectional area A_F.

The fish sideforce Y_F is given by

$$Y_F = (dC_{Y_F}/d\beta) . \beta . \tfrac{1}{2}\rho v^2 . A_F \qquad A(12)$$

where $dC_{Y_F}/d\beta$ is the sideforce coefficient derivative for the fish. Its magnitude depends much on the vertical fin area and is not easily estimated; wind tunnel measurements are a better source. The value, per radian, for the fish shown in Fig. 3 is 5.85.

A1.3. The External Loading, F, on the Cable

The force per unit length, F, will be compounded of the weight and drag forces plus any lift forces generated by the fairings. The term 'lift force' is retained although its line of action is effectively sideways. These three forces are shown in Fig. 5 which represents unit length of cable AB with or without a fairing. The relative flow is along the X axis towards O. If the fairing element is neutrally buoyant and streams perfectly it will lie in the plane OXP; otherwise it will generate a lift force, ℓ, proportional to α, its angle of incidence.

The magnitudes and direction of these forces are described in turn.

The drag force on a bare cable

The drag force per unit cable length when the cable is normal to the flow direction is given by

$$r_o = C_{r_o} . \tfrac{1}{2}\rho v^2 . d \qquad A(13)$$

where d is the cable diameter if unfaired. For bare cables $1.2 < C_{r_o} < 1.7$, depending upon the strumming condition. A value of 1.5 is often used as a typical average value. In the 3-dimensional case, when the cable angle to the flow is θ (Fig. 5), the drag force r lies in the plane OXP and acts perpendicular to the cable element with magnitude given by $r = r_o \sin^2\theta$. In reality there is a very small component of drag acting tangentially to the cable but this is usually ignored, see Ref.(9). In terms of the cable element direction cosines a, b, c

$$r = r_o(1 - a^2) \qquad A(14)$$

and has direction cosines $-(1-a^2)^{\frac{1}{2}}$, $ab/(1-a^2)^{\frac{1}{2}}$, $ac/(1-a^2)^{\frac{1}{2}}$.

The drag force on a faired cable

The normal flow drag force per unit length is given by A(15)

$$r_o = C_{r_o} . \tfrac{1}{2}\rho v^2 . t$$

where t is the fairing maximum thickness. C_{r_o} may vary between 0.1 and 0.4, depending upon the fairing section shape, see Ref.(6). At other cable inclinations to the flow the drag r is assumed to follow the empirical rule proposed in Ref.(6). Accordingly r lies in the plane OXP (Fig. 5) and remains parallel to OX. Its magnitude, expressed as a fraction of r_o is given by

$$r/r_o = \sin\theta \quad \text{for} \quad 30 \text{ deg} < \theta < 90 \text{ deg.} \qquad A(16)$$

$$r/r_o = 0.273 + 0.827\theta^2 \quad \text{for} \quad 0 \leq \theta < 30 \text{ deg.} \qquad A(17)$$

where θ is angle XOP in Fig. 5, given by arcos(a). The direction cosines of r are therefore -1, 0, 0. The wind tunnel tests on faired sections reported in Ref.(1) establish quite firmly that if the fairing angle of incidence lies between ± 1 deg., as may be expected, the value of r_o does not change, i.e. the vortex or lift-dependent drag is negligible for such small α.

The fairing lift force

The normal-flow lift force per unit length of faired cable will be given by

$$\ell_o = (dC_\ell/d\alpha).\alpha.\tfrac{1}{2}\rho v^2 \bar{c} \qquad A(18)$$

where $dC_\ell/d\alpha$ is the section 'lift curve slope', α the angle of incidence and $\bar{c}$ the fairing chord length. The use of chord length in place of thickness is the convention used in defining C_ℓ.
In the 3-dimensional situation (Fig. 5) the lift force will act normal to plane OXP and therefore have direction cosines 0, $-c/(1-a^2)^{\frac{1}{2}}$, $b/(1-a^2)^{\frac{1}{2}}$. Its magnitude will be given by

$$\ell = \ell_o.\sin^2\theta = \ell_o(1-a^2) \qquad A(19)$$

because the lift is proportional to the component of $\tfrac{1}{2}\rho v^2$ normal to the leading edge OP.

The weight force

The weight in water of unit length of cable, with or without fairing, is denoted by w, which acts vertically and therefore has direction cosines 0, 0, - 1.

APPENDIX 2

NON-DIMENSIONALISATION OF CABLE CHARACTERISTICS

A2.1. Conversion of Cable Equations

This has been done in accordance with the normalising technique adopted in Ref.(6). All forces are expressed as proportions of the fish weight W, and all forces per unit length as proportions of cable weight per unit length w. Cable lengths are then ratios of the characteristic length W/w and tension are ratios of the fish weight. Writing $s = S/(W/w)$, $f = F/w$, $t_1 = T_1/W$, equations A1 to A4 become

$$a_2 - a_1 = (f\delta s/t_1)\left[-i(1 - a_1^2) + ja_1b_1 + ka_1c_1\right] \qquad A(20)$$

$$b_2 - b_1 = (f\delta s/t_1)\left[ia_1b_1 - j(1-b_1^2) + kb_1c_1\right] \qquad A(21)$$

$$c_2 - c_1 = (f\delta s/t_1)\left[ia_1c_1 + jb_1c_1 - k(1-c_1^2)\right] \qquad A(22)$$

$$t_2 - t_1 = - f\delta s(ia_1 + jb_1 + kc_1) \qquad A(23)$$

Writing $x = X/(W/w)$, etc., Equations A(5) to A(8) are the same but with capital letters replaced by lower case.

At the origin, where $x = y = z = s = 0$, the value of t_1 is given by $t_1 = t_o = 1/c_o$ (from Equation A(10)).

It should be noted that the non-dimensional form, s, of the real scope S is the ratio of the cable weight to the fish weight at that scope.

A2.2. Conversion of Hydrodynamic Forces

It is standard practise to integrate the above equations at constant values of w/r_o, the weight to drag ratio of the cable; the values being successively decreased to represent increasing values of $\frac{1}{2}\rho v^2$, v being the towing speed. Since the water forces on fish and cable are themselves proportional to $\frac{1}{2}\rho v^2$ the force ratios required for the non-dimensional equations are best expressed as coefficients of $(w/r_o)^{-1}$, using equation A(15) as a basis, so that

$$\ell_o/w = \frac{\alpha(dC_\ell/d\alpha)\bar{c}}{C_{r_o} \cdot t} \Big/ (w/r_o) \quad \text{from equation A(18)} \qquad A(24)$$

$$D_F/W = \frac{C_D A_F}{C_{r_o} \cdot t} \left(\frac{w}{W}\right) \Big/ (w/r_o) \quad \text{from equation A(11)} \qquad A(25)$$

$$Y_F/W = \frac{\beta(dCy_F/d\beta)A_F}{C_{r_o} \cdot t} \left(\frac{w}{W}\right) \Big/ (w/r_o) \quad \text{from equation A(12)} \qquad A(26)$$

The numerical values of these ratios when $w/r_o = 1$ are useful constants in the computation procedure.

APPENDIX 3

THE COMPUTATION

The numerical integration of equations A(20) to A(23) has been carried out at selected values of w/r_o between 0 and 1.50, to give cable angles and x, y, z co-ordinates of cable lengths varying from s = 0 to 4.0, working from the origin at the fish.
The step size was varied during the integration; 800 steps between s = 0 and 1, 400 between s = 1 and 2, 200 for s = 1 to 3 and 100 for s = 3 to 4. This ensured that accuracy was not lost where the curvature was greatest.
Each step was computed twice; first using the direction cosine values a_1, b_1, c_1 occurring at the beginning of the step and secondly with the average values, $(a_1 + a_2)/2$ etc.

The direction cosines at the end of each step were normalised to eliminate the accumulation of rounding errors.

A single programme was developed which allowed cable shapes to be computed for all the tow-off causes investigated, giving the user the choice of bare or faired cables., with or without the presence of the fish drag force and/or fish yaw angle. In addition the angle of incidence of the fairing could be held constant or allowed to adopt the value resulting from 'flopping' (Section 4).

APPENDIX 4

THE ESTIMATION OF FISH YAW ANGLE AND SIDEFORCE DUE TO UNBALANCED CABLE TORQUE

When the spirally wound load bearing elements of a cable are imperfectly balanced a torque is produced at the cable end if the latter is not allowed to rotate. In the case of wire ropes the torque is proportional to the tension (Ref. (10)). This is assumed to be true for a towing cable in spite of the expected non-linearities due to internal friction and the fact that the cable weight contributes significantly to the tension. This simplification makes it possible to derive a valid approximation for assessing the effect of cable torque on tow-off.

Assuming, in addition, that the torque applied to the fish is zero at launch, when the cable tension equals the fish weight, the torque generated during towing may be related to the additional tension created as the scope and speed increase. Thus if, under tow, the top tension is T and the bottom tension W (ignoring fish drag) the torque Q may be assumed proportional to the average tension less the initial tension, i.e.

$$Q = k\left(\frac{T+W}{2} - W\right) = \tfrac{1}{2}k(T-W) \qquad A(27)$$

where the constant k is a property of the cable.
Writing $t = T/W$ (Appendix 2) gives

$$Q = \tfrac{1}{2}kW(t-1) \qquad A(28)$$

From Ref. (6) it is seen that the variation of cable tension under tow is given, for a bare cable, by

$$t-1 = z \qquad A(29)$$

where z is the non-dimensional depth, $= Z/(W/w)$.

For a faired cable t varies with both depth and speed. Using the data from Ref. (6) it is found that an approximation to within 15% is given by

$$t-1 = z/(w/r_o) \qquad A(30)$$

for $0 < z < 1$, which reflects the tension increase with speed that cable fairings create.

Thus $Q = \frac{1}{2}kWz$ for a bare cable A(31)

and $Q = \frac{1}{2}kWz/(w/r_o)$ for a faired cable A(32)

This torque will yaw the fish to the angle β at which the restoring moment due to its vertical fins balances Q, and the sideforce Y_F due to the yaw will be proportional to Q. They are related by

$$Y_F = \frac{Q}{\ell_F} \Big/ \frac{dC_N}{dCy_F} \qquad A(33)$$

where dC_N/dC_{Y_F} is the ratio of the fish yawing moment derivative $dC_N/d\beta$ to the sideforce derivative $dC_{Y_F}/d\beta$; ℓ_F being the fish length.

Thus the fish sideforce-to-weight ratio is given by, for a bare cable

$$Y_F/W = \frac{kz}{2\ell_F(dC_N/dC_{Y_F})} \qquad A(44)$$

and for a faired cable

$$Y_F/W = \frac{kz}{2\ell_F(dC_N/dC_{Y_F})} \Big/ (w/r_o) \qquad A(45)$$

A value of k typical of an 18 mm dia. 2-layer armour cable having a 15 ton breaking strength is about 3×10^{-5} Nm per N. Such low value precludes the possibility of unbalanced cable torque being responsible for tow-off problems, even when allowances are made for fishes having short lengths and poor directional stability. This may be confirmed by applying equations (44) and (45) to the functions given in Fig. 7.

APPENDIX 5

THE PHYSICAL AND HYDRODYNAMIC PROPERTIES OF THE TOWED SYSTEM USED FOR APPLICATIONS OF THE THEORY

Hydrodynamic data from Refs. (1), (6) and (7).
See Fig. 3 for configuration.

TOWED BODY (FISH)

Weight in water, W	1076 N
Max. cross section area, A_F	0.1633 m^2
Length, ℓ_F	1.828 m
Drag coefficient, C_D	0.290
$dC_{Y_F}/d\beta$ per radian	-5.85
$dC_N/d\beta$ per radian	2.00

CABLE AND FAIRING

Weight per unit length in water, w	3.60 N/m
Max. thickness, t	0.020 m
Chord length, $\bar{c}$	0.110 m
Section drag coefficient, C_{r_o}	0.219
$dC_\ell/d\alpha$ per radian	5.71
$dC_m/d\alpha$ per radian	-0.767
α_H at unit w/r_o (see equation 24)	0.225 deg
Distance of aero.centre aft of cable centre, C_a	0.0175 m
Distance of fairing c.g. aft of cable centre, C_g	0.030 m
Weight per unit length of fairing alone, w_f	1.00 N/m

CABLE

Weight per unit length in water, w_c	2.60 N/m
Diameter	0.013 m
Drag coefficient assumed, C_{r_o}	1.50

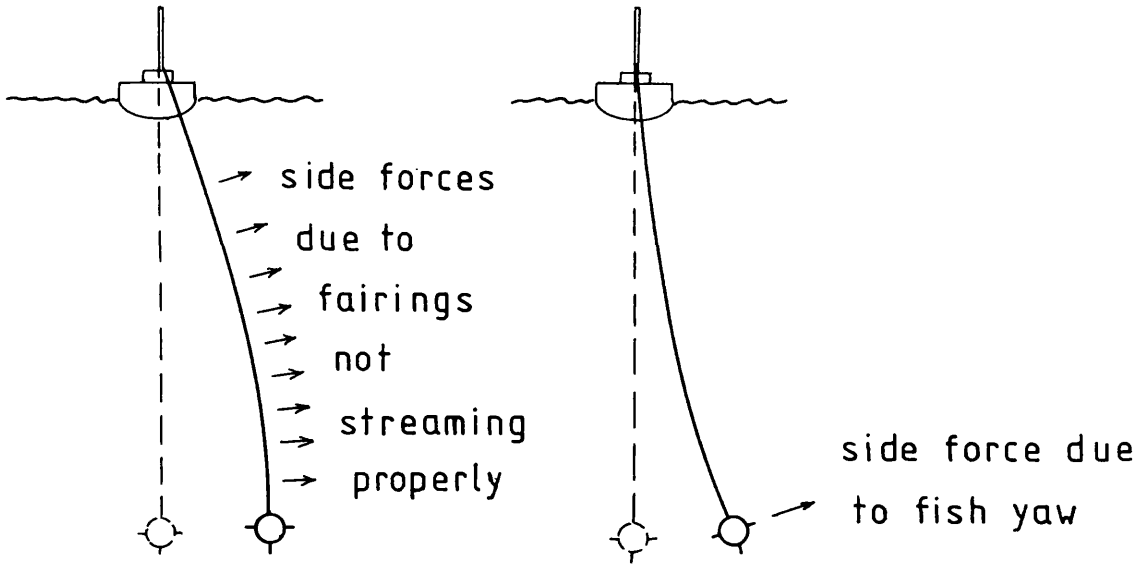

FIG.1. TWO CAUSES OF TOW-OFF.

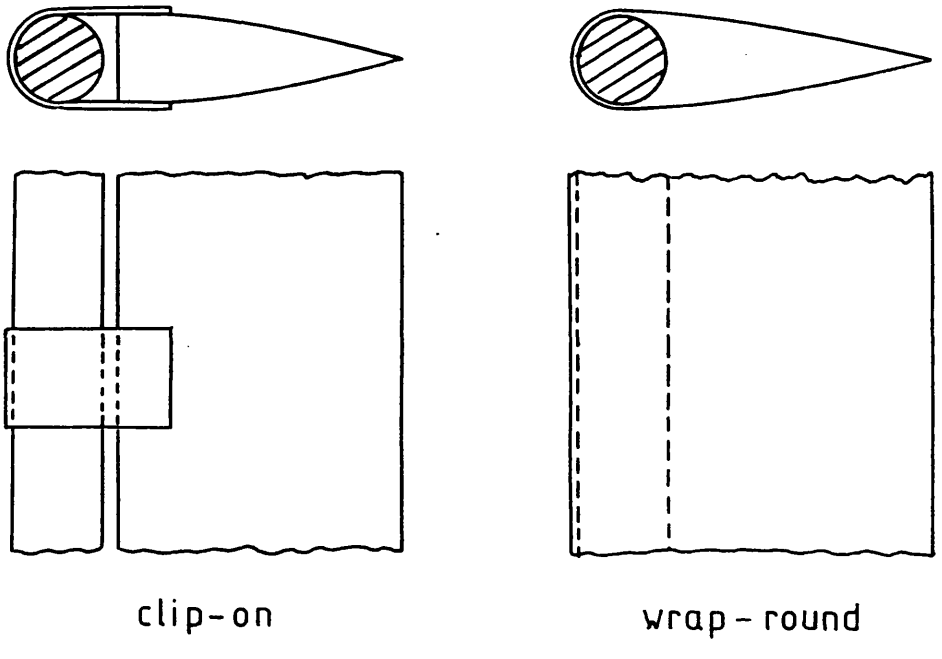

FIG.2. SWIVELLING FAIRINGS.

FIG. 3.

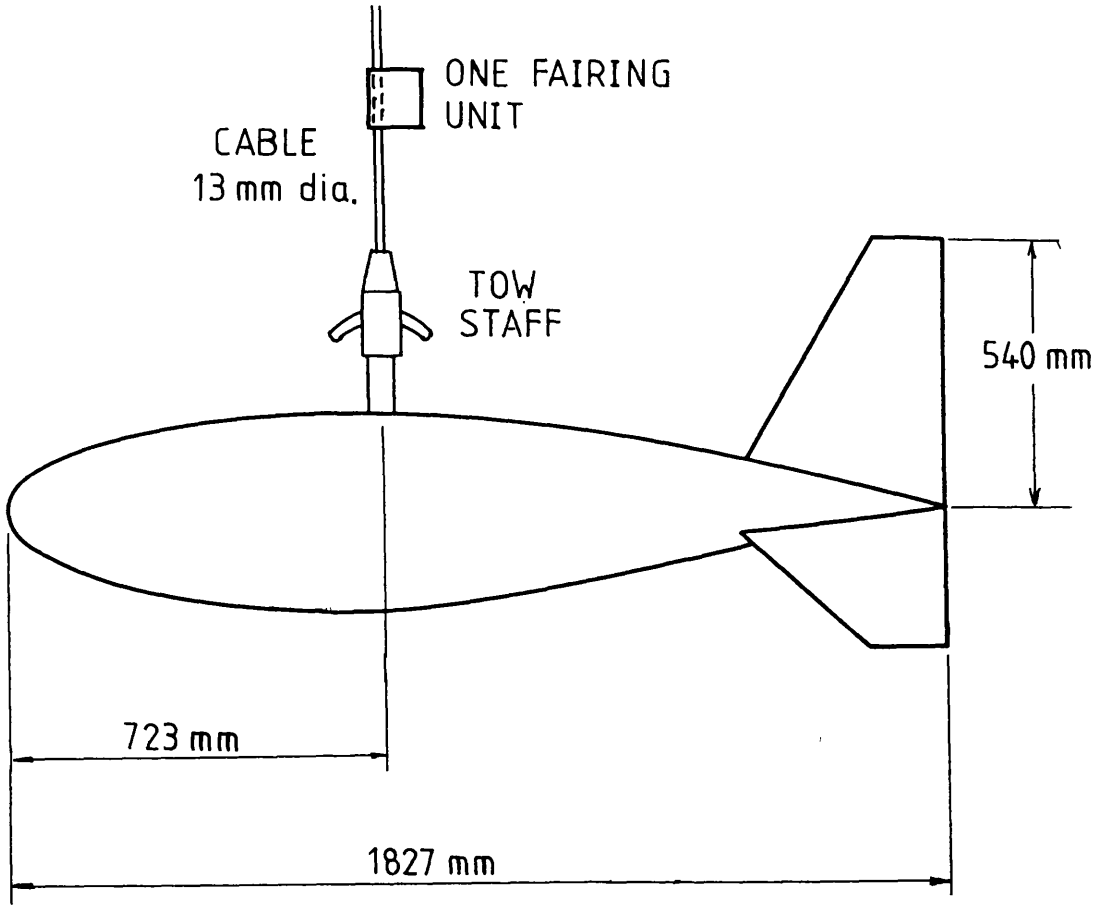

MAX. DIA. = 456 mm

WEIGHT = 1076 N

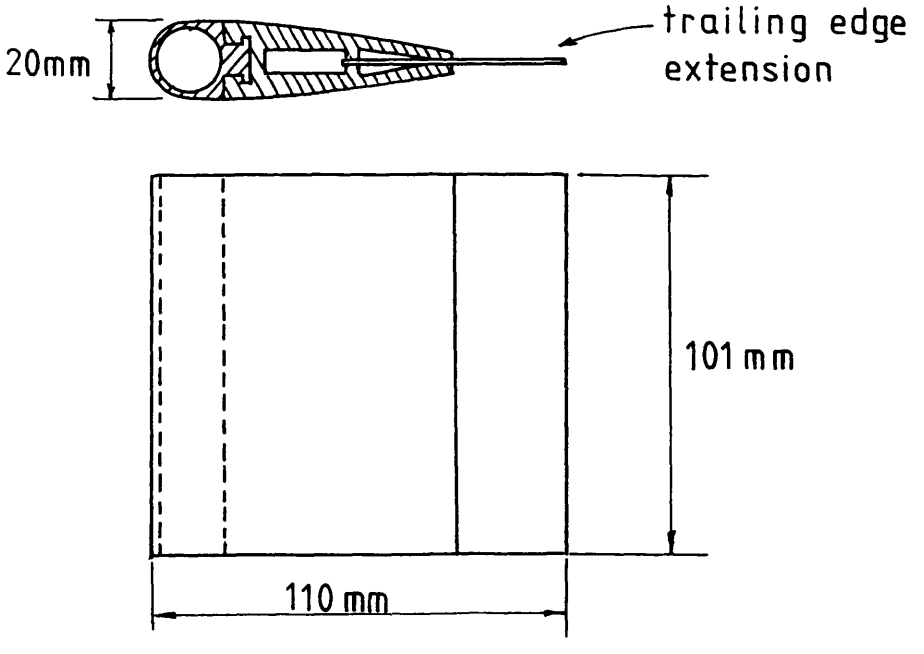

FIG. 3. DIMENSIONS OF FISH, CABLE AND FAIRING USED FOR APPLIED CALCULATIONS.

FIG. 4.

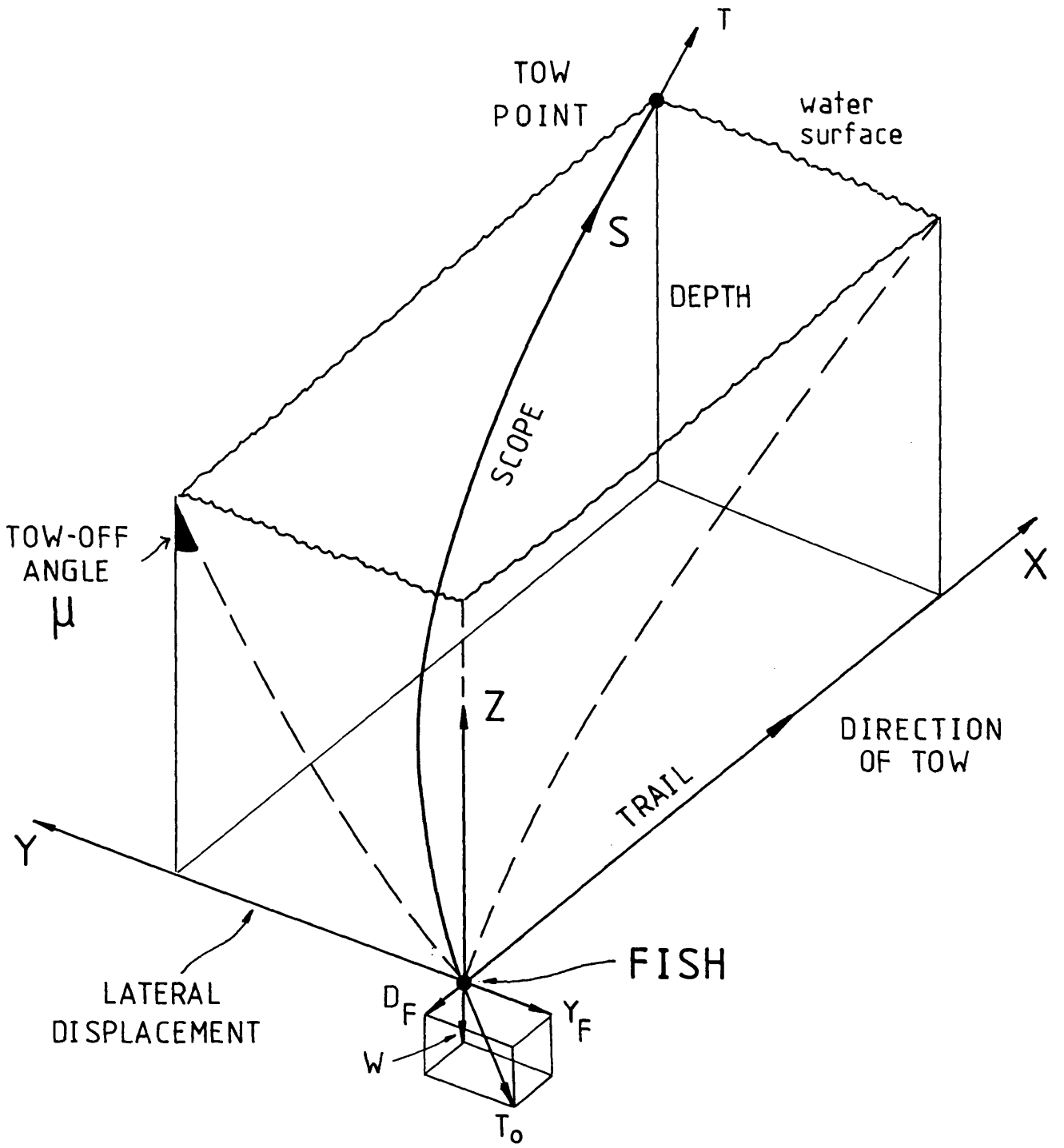

FIG. 4. DEFINITION OF CABLE SHAPE AND AXIS SYSTEM – SHOWING FISH WEIGHT, DRAG AND SIDEFORCE.

FIG. 5.

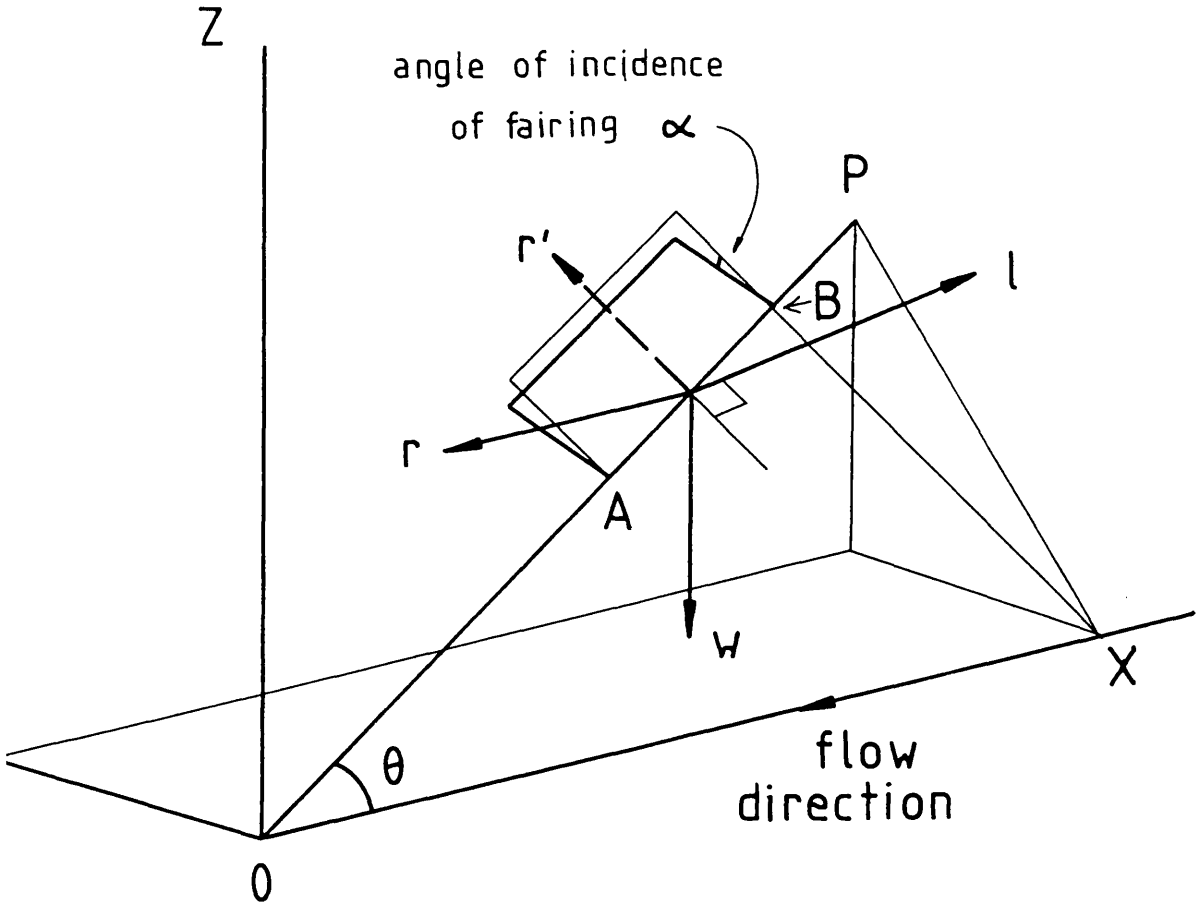

faired
- l lift force, normal to plane OXP.
- r drag force, parallel OX.
- w weight, vertical.

bare
- r' drag force, parallel XB.
- w weight, vertical.

FIG. 5. FORCES ACTING ON FAIRED OR BARE CABLE ELEMENT AB.

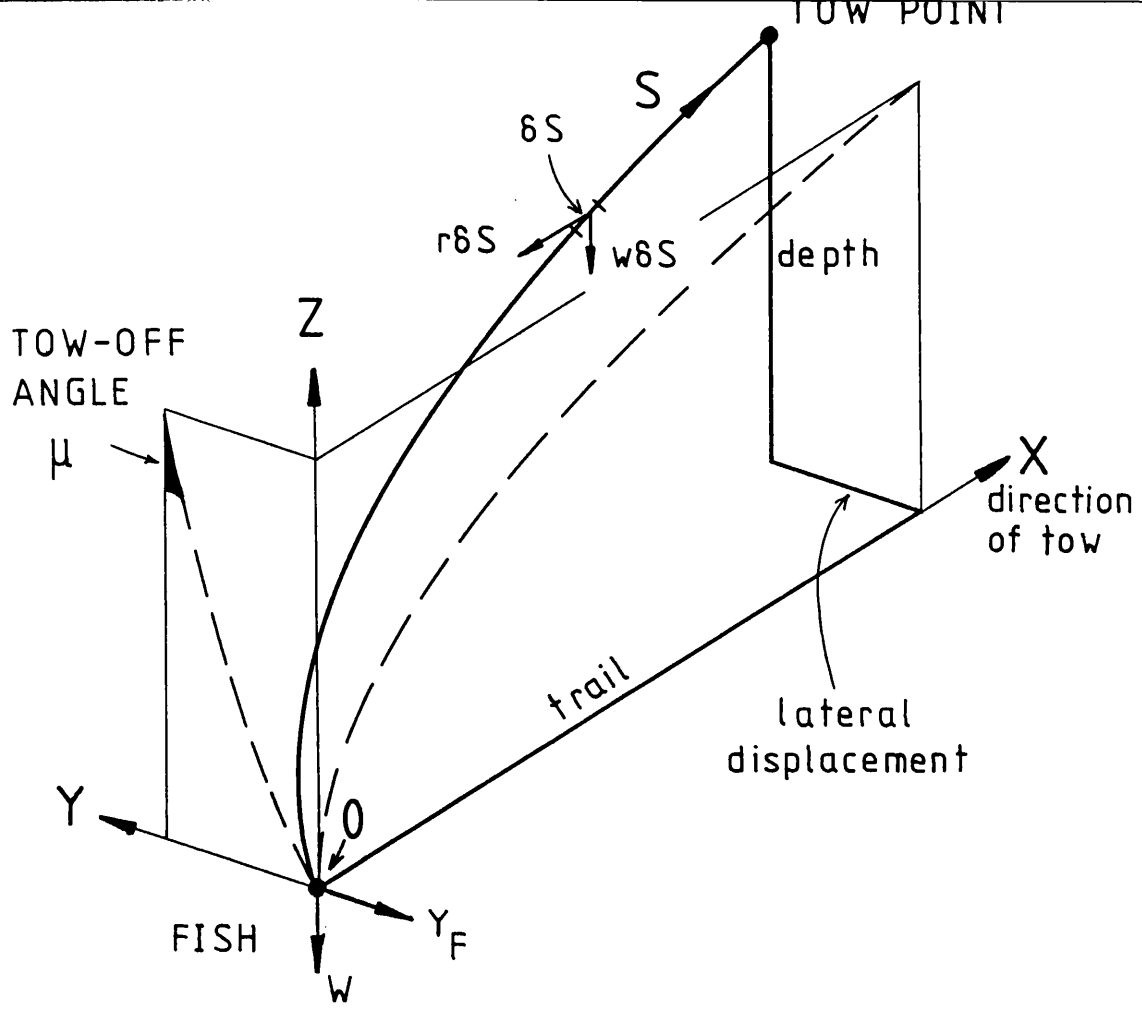

(a) SHAPE OF CABLE.

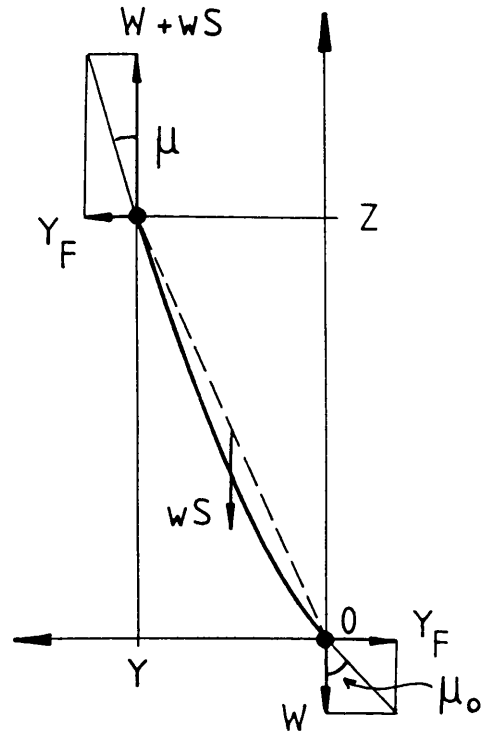

$$\tan \mu = Y_F / (W + wS)$$

(b) LATERAL EQUILIBRIUM.

FIG.6. TOW-OFF CAUSED BY FISH SIDEFORCE — WITH FAIRED CABLE.

FIG.6.

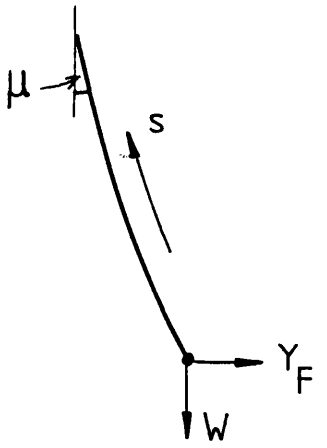

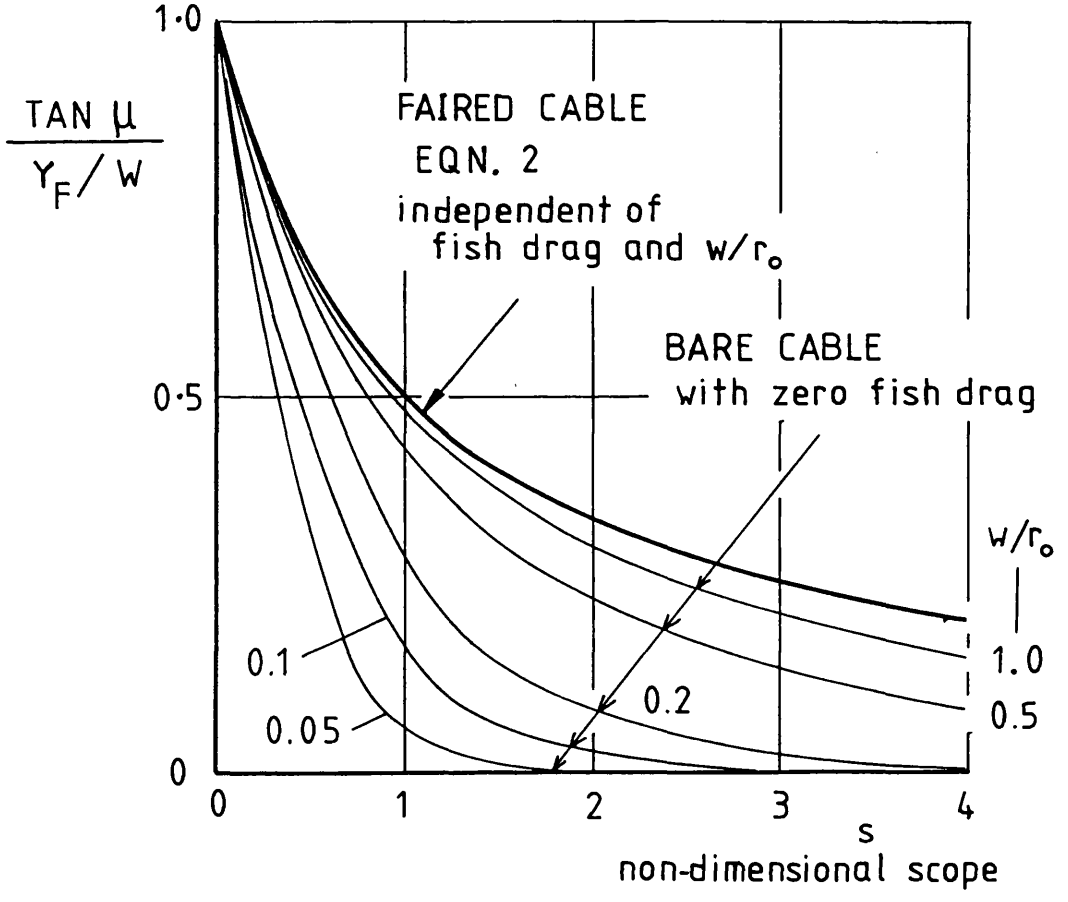

s = cable weight ÷ fish weight

FIG.7. TOW-OFF ANGLE DUE TO FISH SIDEFORCE.

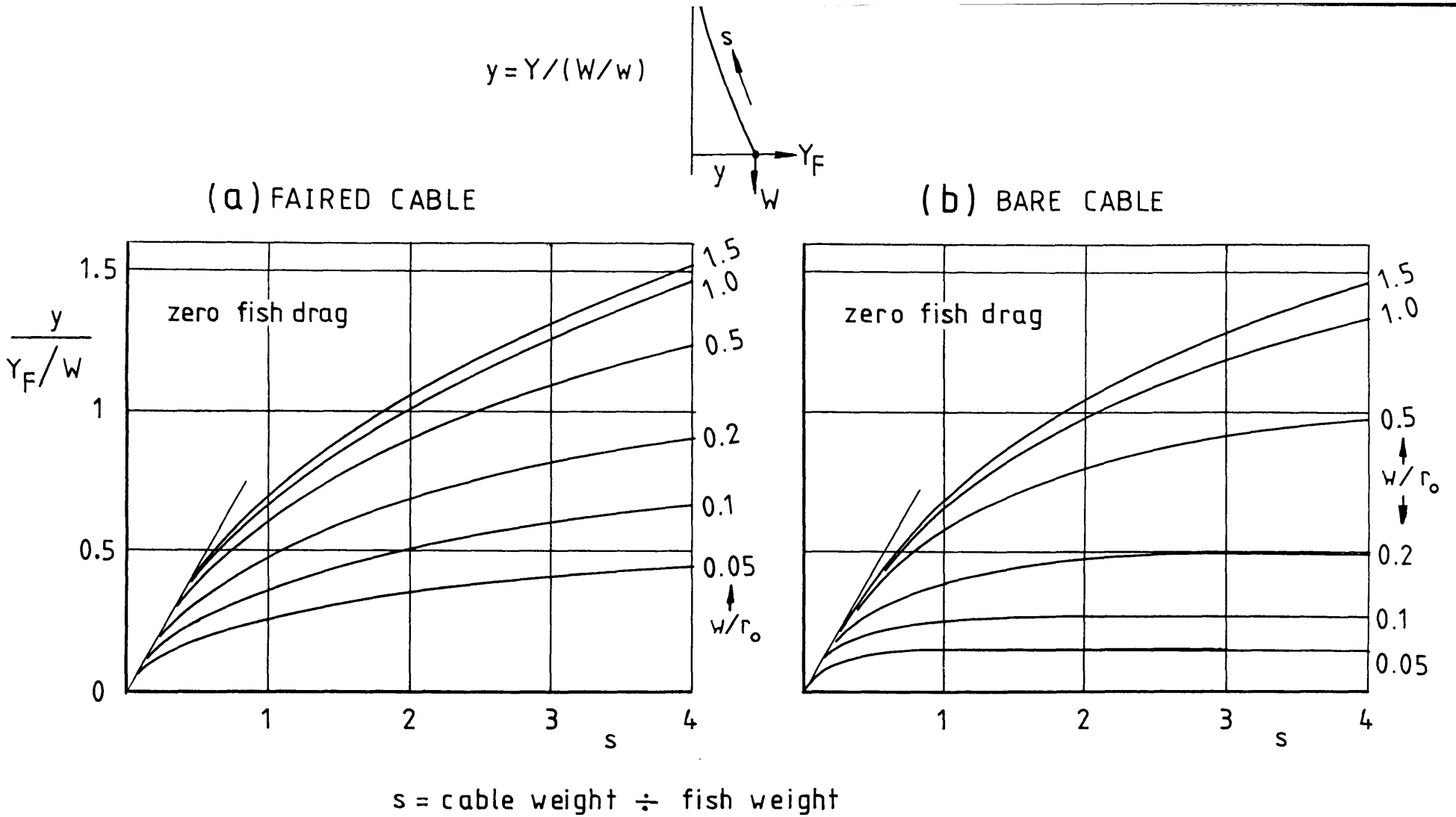

FIG. 8. LATERAL DISPLACEMENT DUE TO FISH SIDEFORCE

FIG. 8.

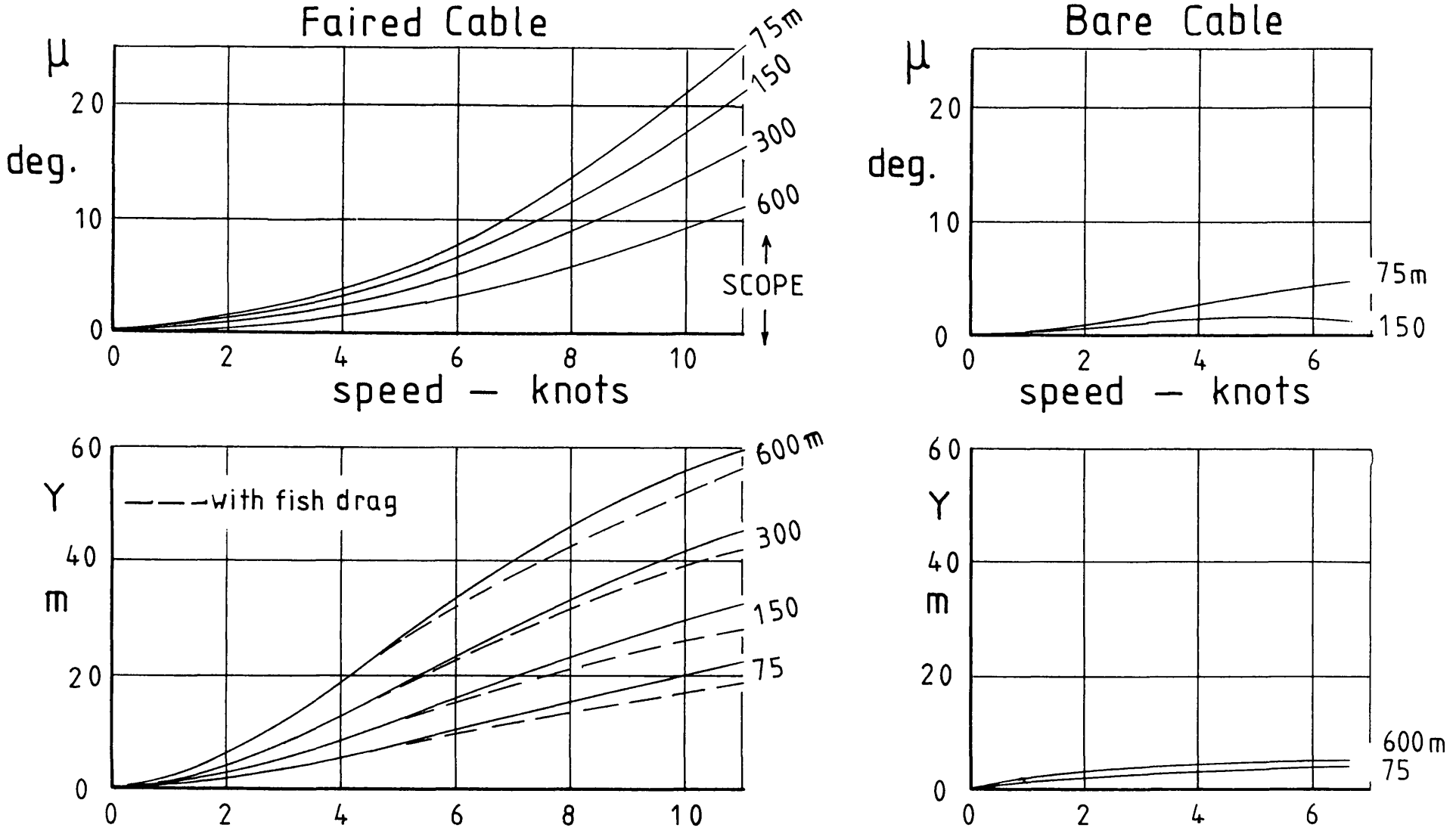

FIG.10. VARIATION WITH SPEED AND SCOPE OF TOW-OFF ANGLE AND LATERAL DISPLACEMENT DUE TO FISH YAWED TWO DEGREES.

FIG.10.

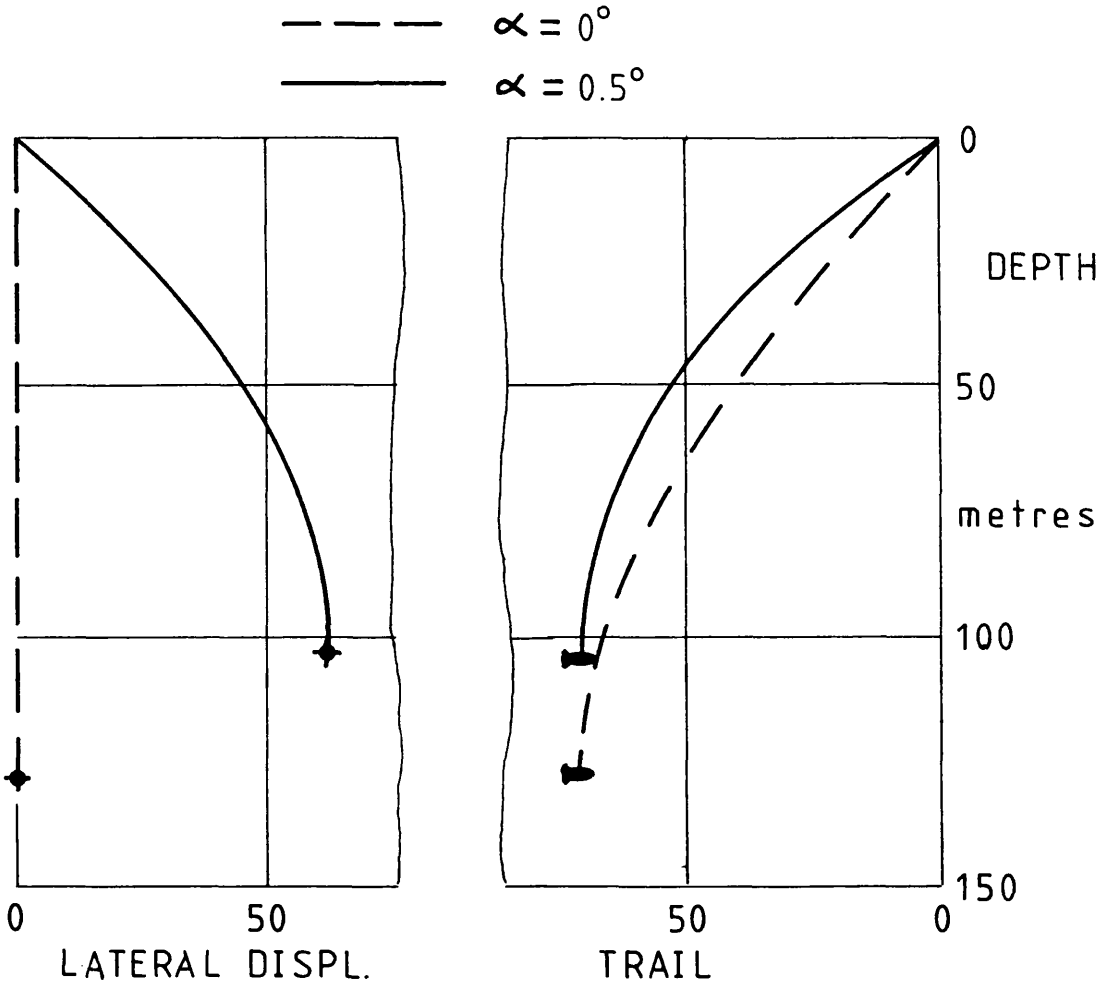

FIG.11. EXAMPLE OF TOW-OFF DUE TO ONLY HALF A DEGREE OF FAIRING INCIDENCE.
SCOPE = 150 m. SPEED = 4.5 kt.
FISH WEIGHT = HALF CABLE WEIGHT.

FIG.12.

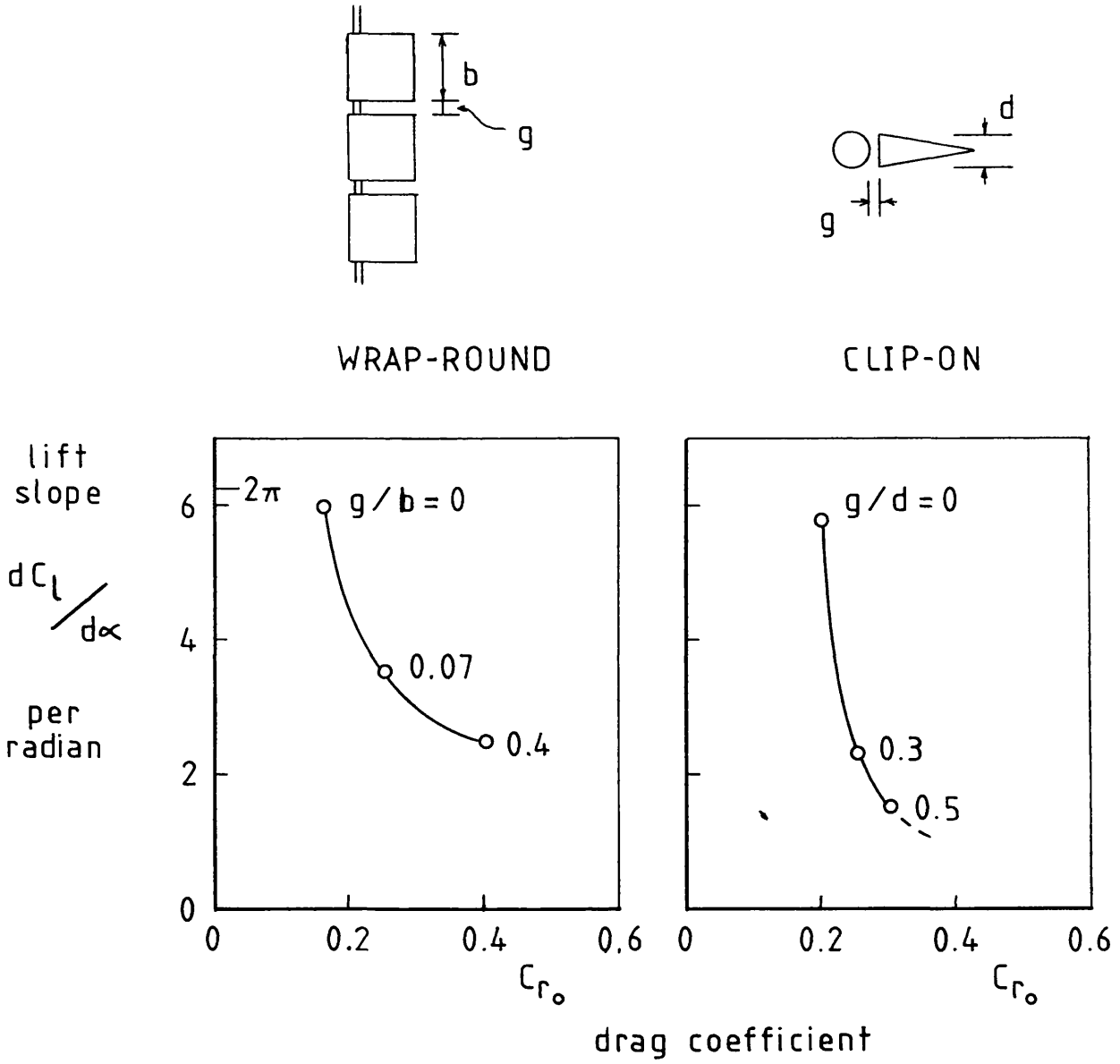

FIG.12. TYPICAL EFFECTS OF GAPS ON THE LIFT CURVE SLOPE AND DRAG COEFFT. OF CABLE FAIRINGS.

FIG.13.

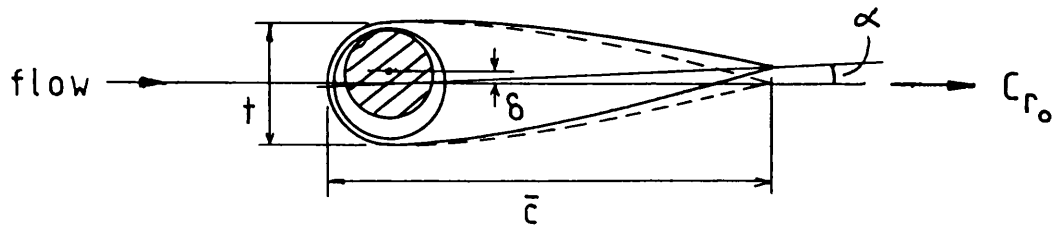

$$\alpha = \frac{C_{r_o} \cdot t \cdot \delta}{\frac{dC_m}{d\alpha} \cdot \bar{c}^2}$$

FIG.13. FAIRING INCIDENCE DUE TO OFFSET CABLE.

FIG.14.

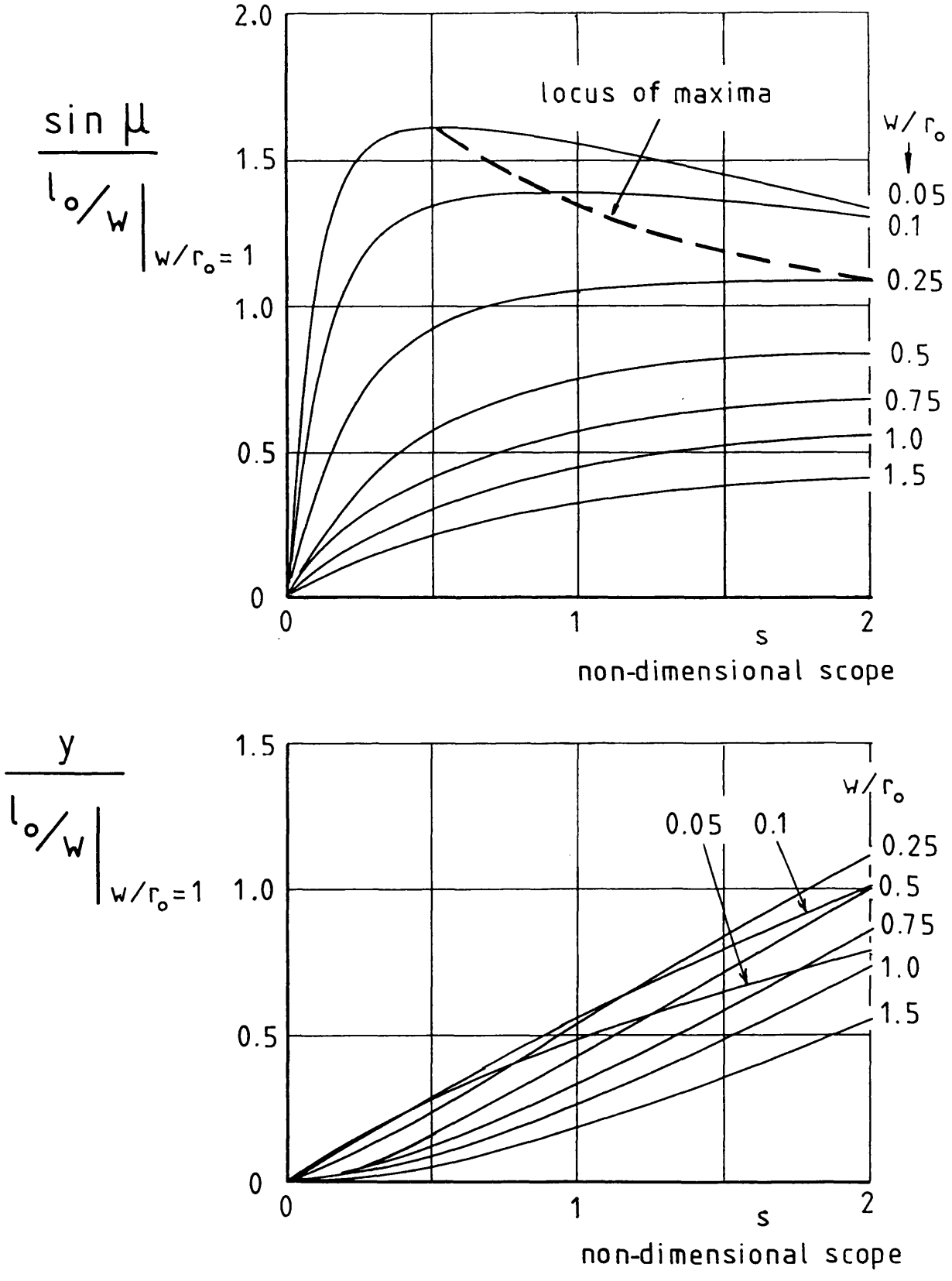

FIG.14. NORMALISED TOW-OFF CHARACTERISTICS DUE TO A CONSTANT FAIRING ANGLE OF INCIDENCE

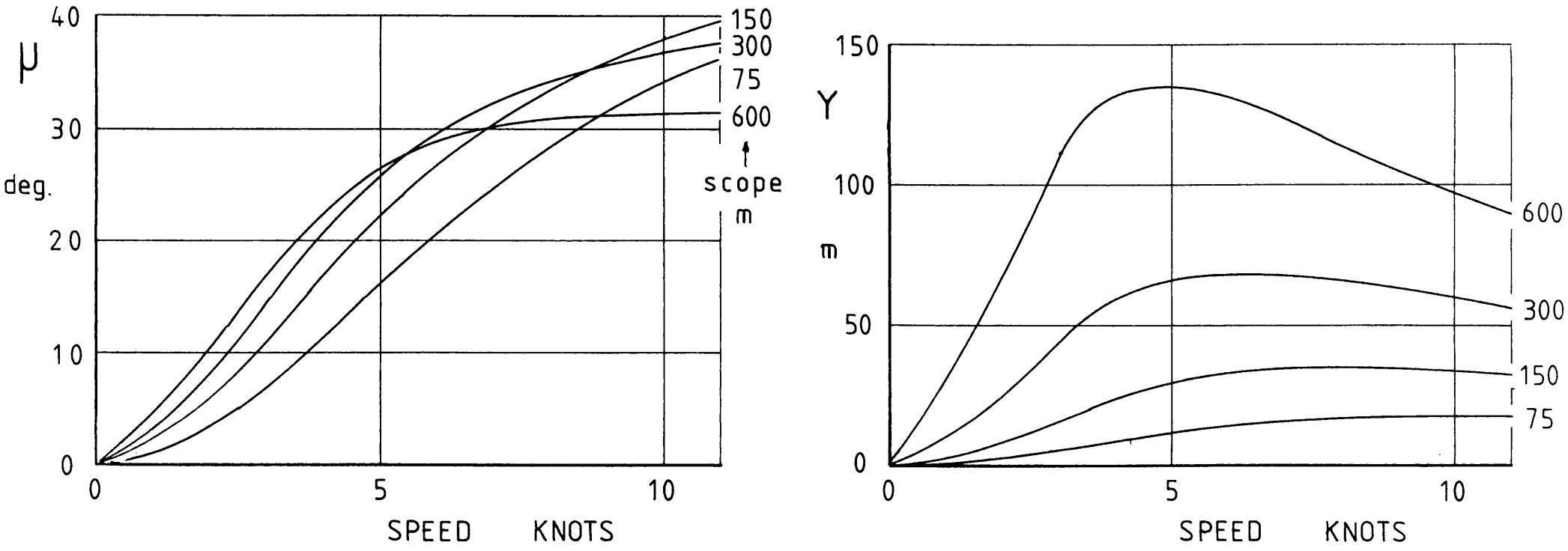

FIG.15. VARIATION WITH SPEED AND SCOPE OF TOW-OFF ANGLE AND FISH DISPLACEMENT DUE TO 0.2 deg. FAIRING INCIDENCE.

FIG.15.

FIG.16.

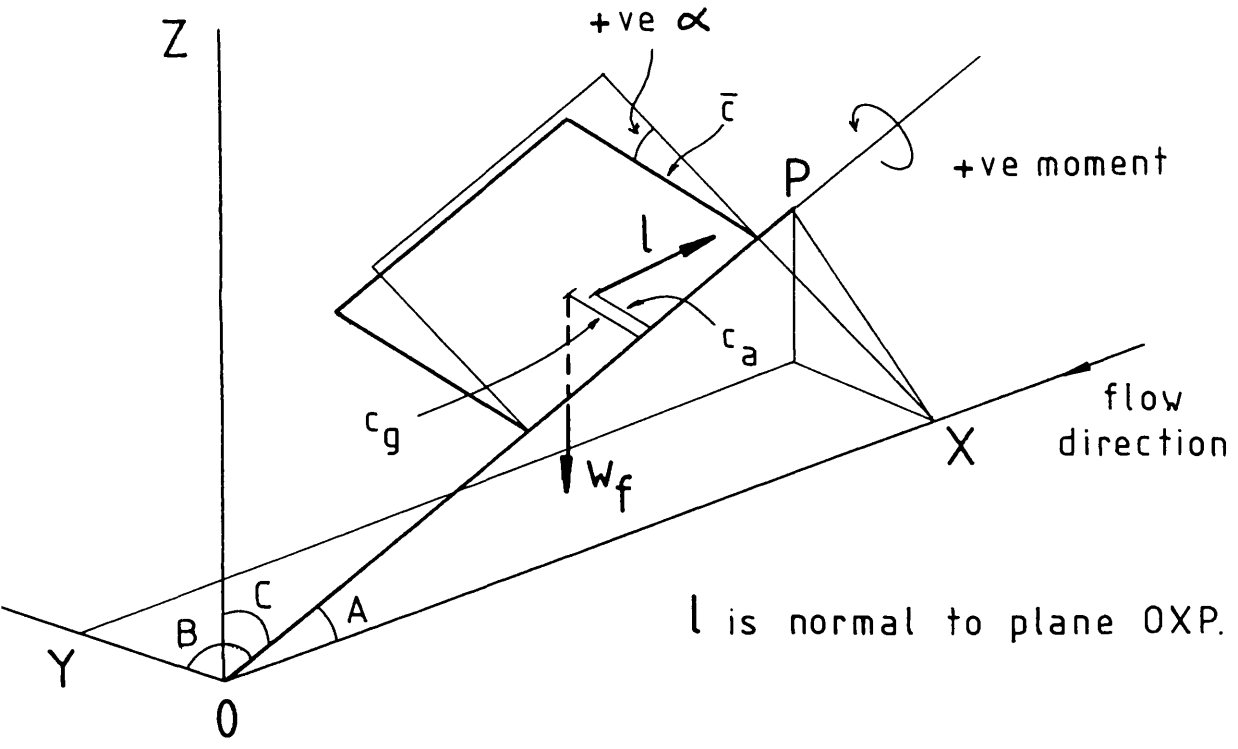

Weight moment $M_W = \frac{w_f . c_g}{\sin A}(\cos B \cos\alpha + \cos A \cos C \sin\alpha)$

Hydrodynamic moment $M_H = -l.c_a = -\frac{dC_l}{d\alpha} . \alpha . \frac{1}{2}\rho v^2 . \bar{c} . c_a . \sin^2 A$

FIG.16. MOMENTS ABOUT A CABLE OF THE WEIGHT AND LIFT FORCES ON A FAIRING.

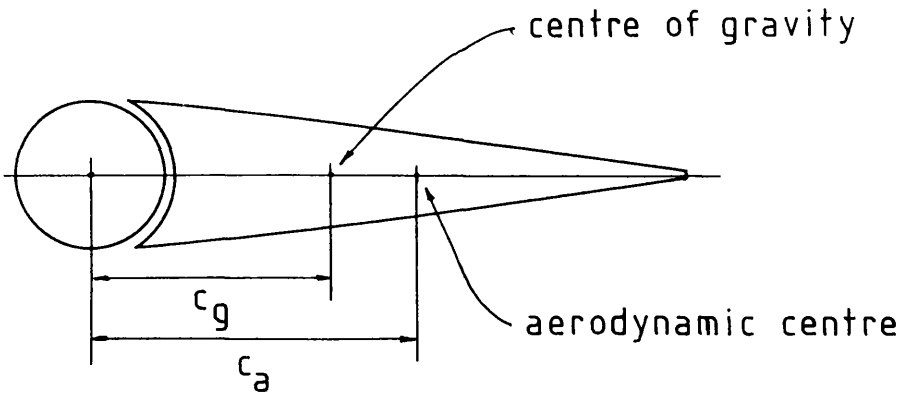

SPECIFIC GRAVITY = 1.6

FIG.17. SECTION OF TYPICAL NEOPRENE CLIP-ON FAIRING.

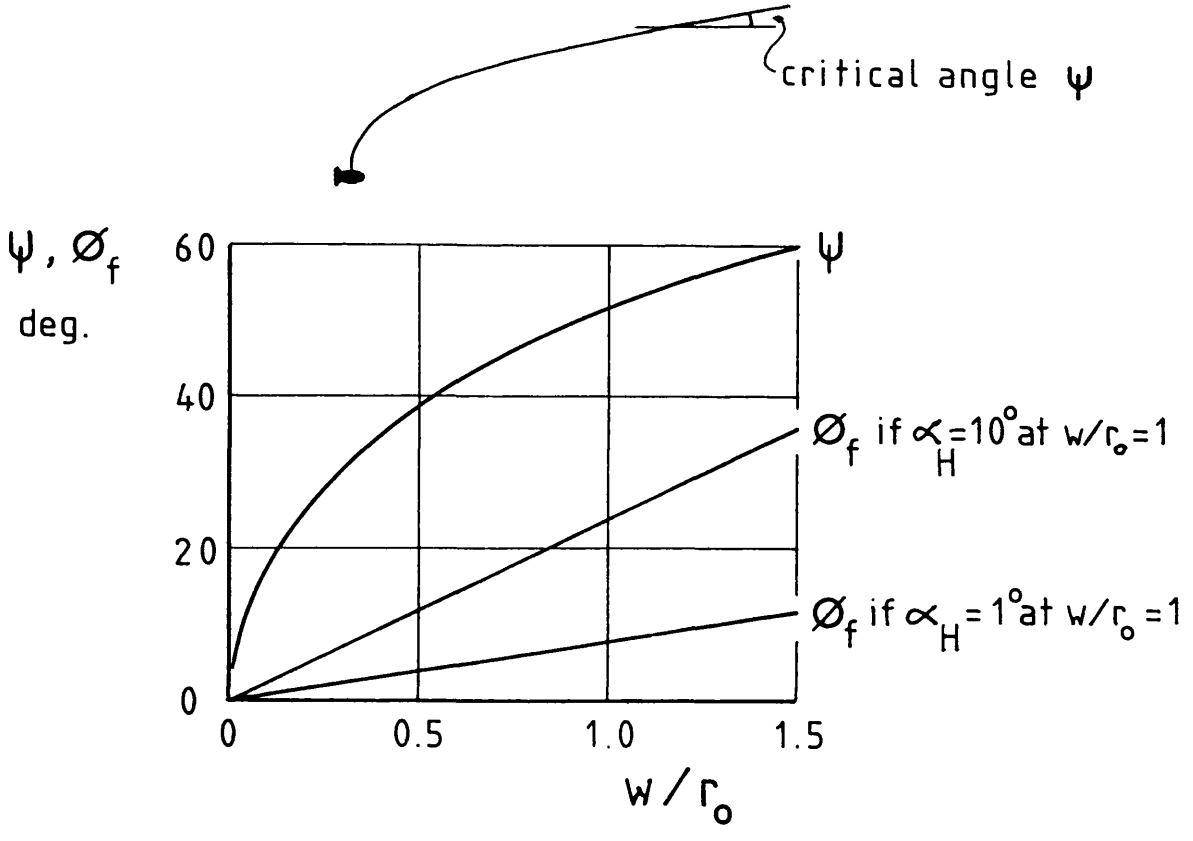

FIG.18. SHOWING THAT A HEAVY FAIRING WILL NOT FLOP IF CABLE PROFILE IS TWO-DIMENSIONAL.

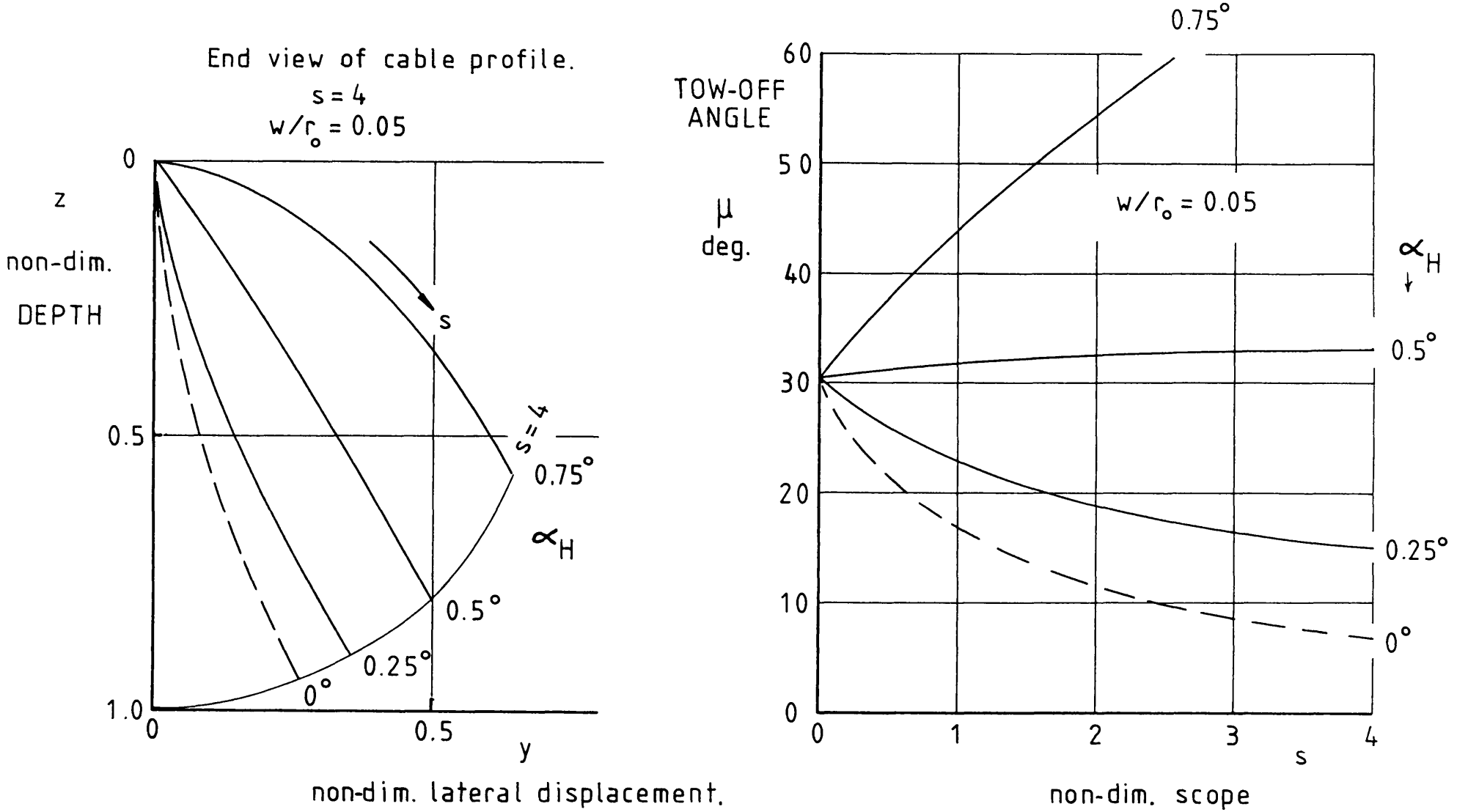

FIG.19. TOW-OFF CHARACTERISTICS OF A HEAVY FAIRING COMBINED WITH 2 deg. OF FISH YAW : AT $w/r_o = 0.05$.

FIG.19.

FIG. 20.

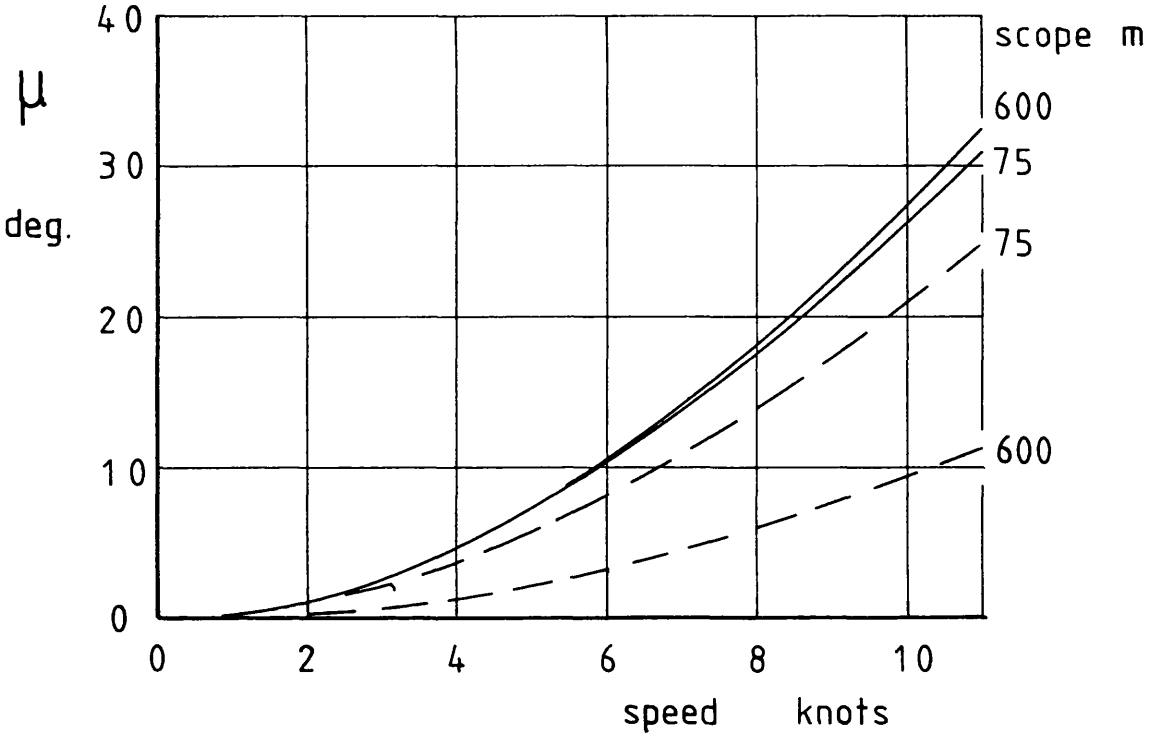

FIG. 20. VARIATION OF TOW-OFF ANGLE WITH SPEED AND SCOPE OF FISH YAWED 2 deg. WITH NEOPRENE FAIRINGS HAVING $\alpha_H = 0.5$ deg. at $w/r_o = 1$.

FIG. 21.

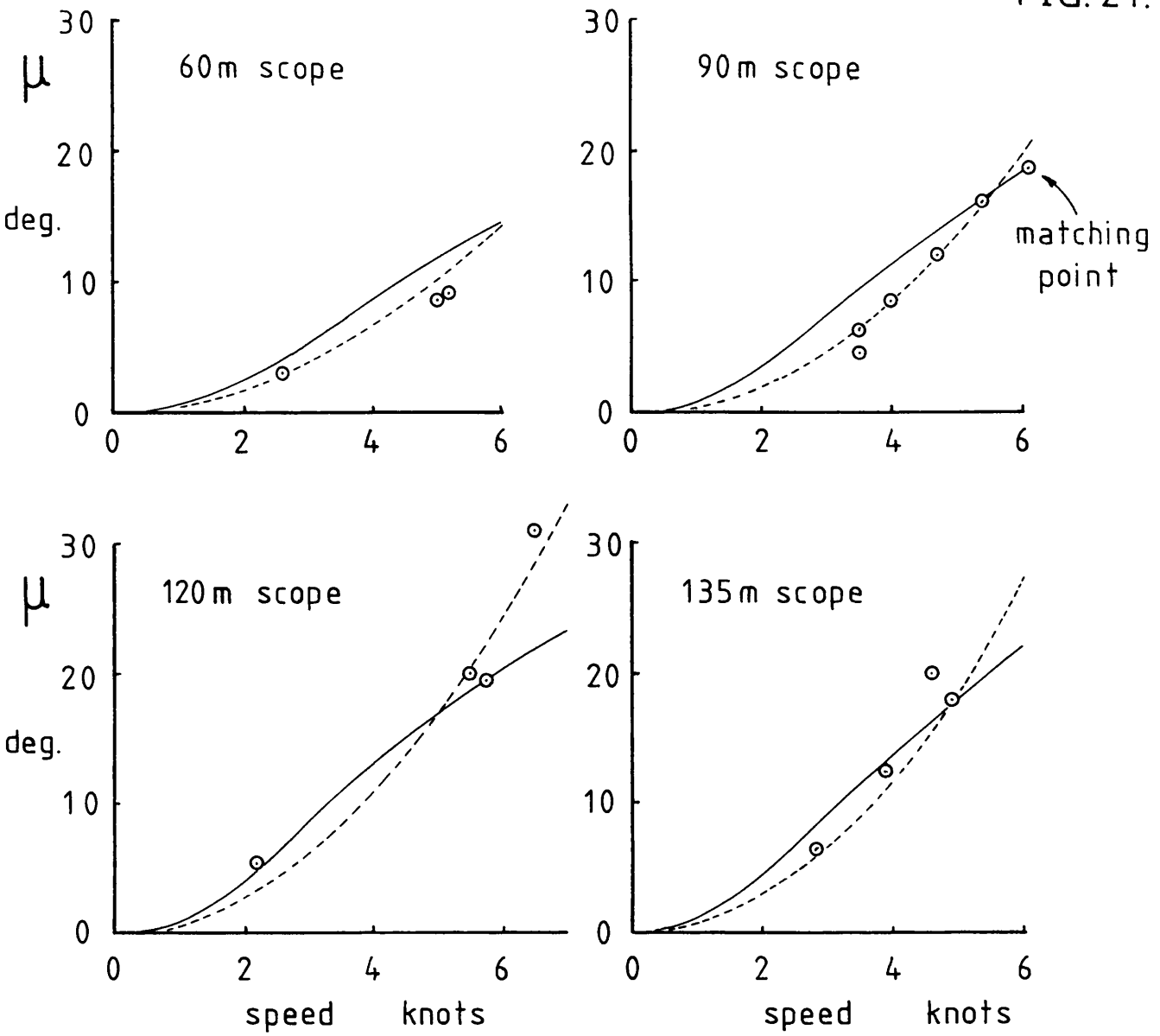

⊙ observed at sea

——— theoretical, assuming constant ∝ of 0.18 deg.

------- theoretical, using tank test result (Fig. 24.)

FIG. 21. COMPARISON BETWEEN TOW-OFF ANGLES OBSERVED AT SEA AND TWO THEORETICAL SIMULATIONS.

FIG. 22.

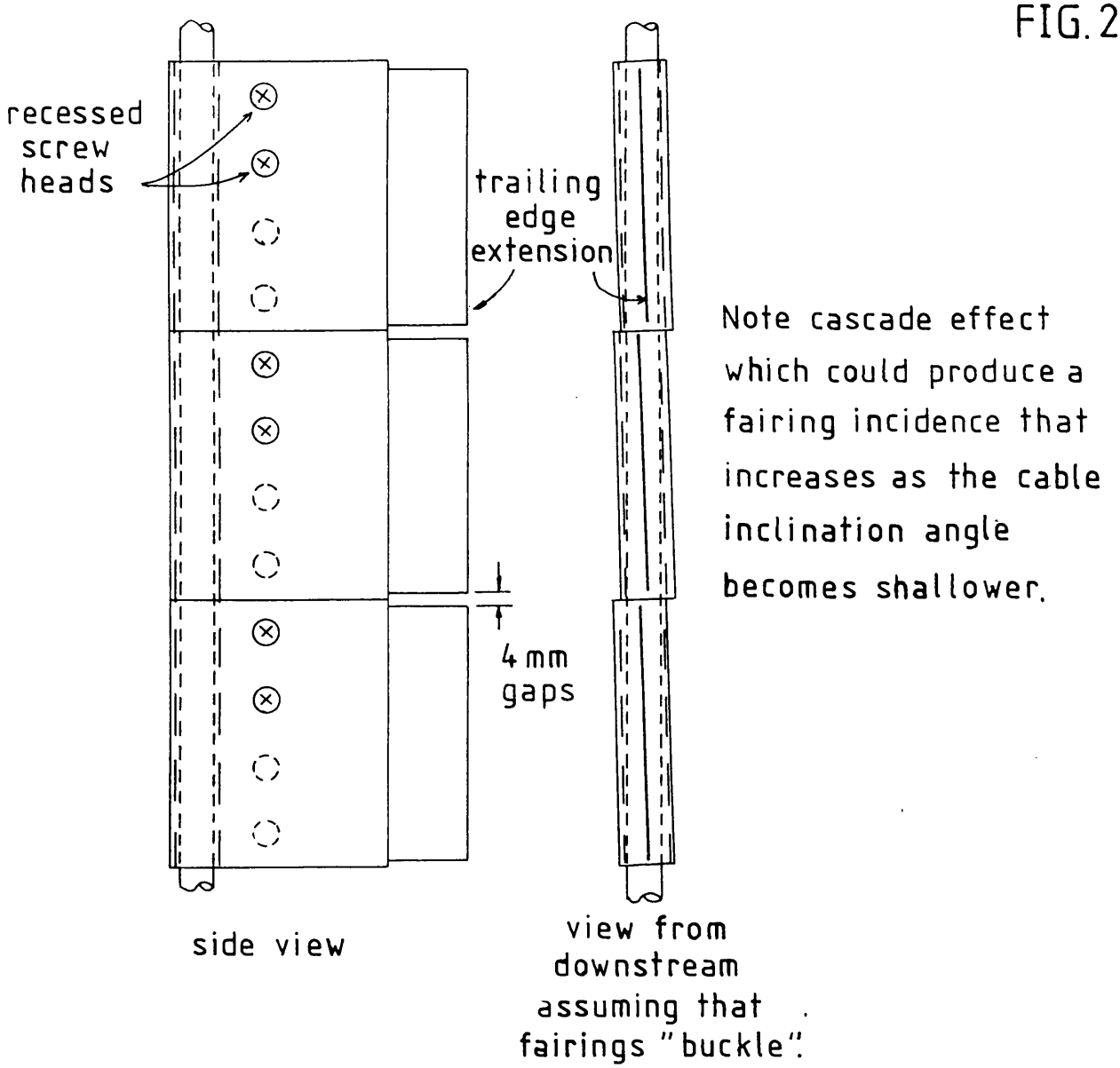

FIG. 22. THE FAIRINGS TESTED AT SEA — SHOWING POSSIBLE SOURCES OF MISALIGNED STREAMING.

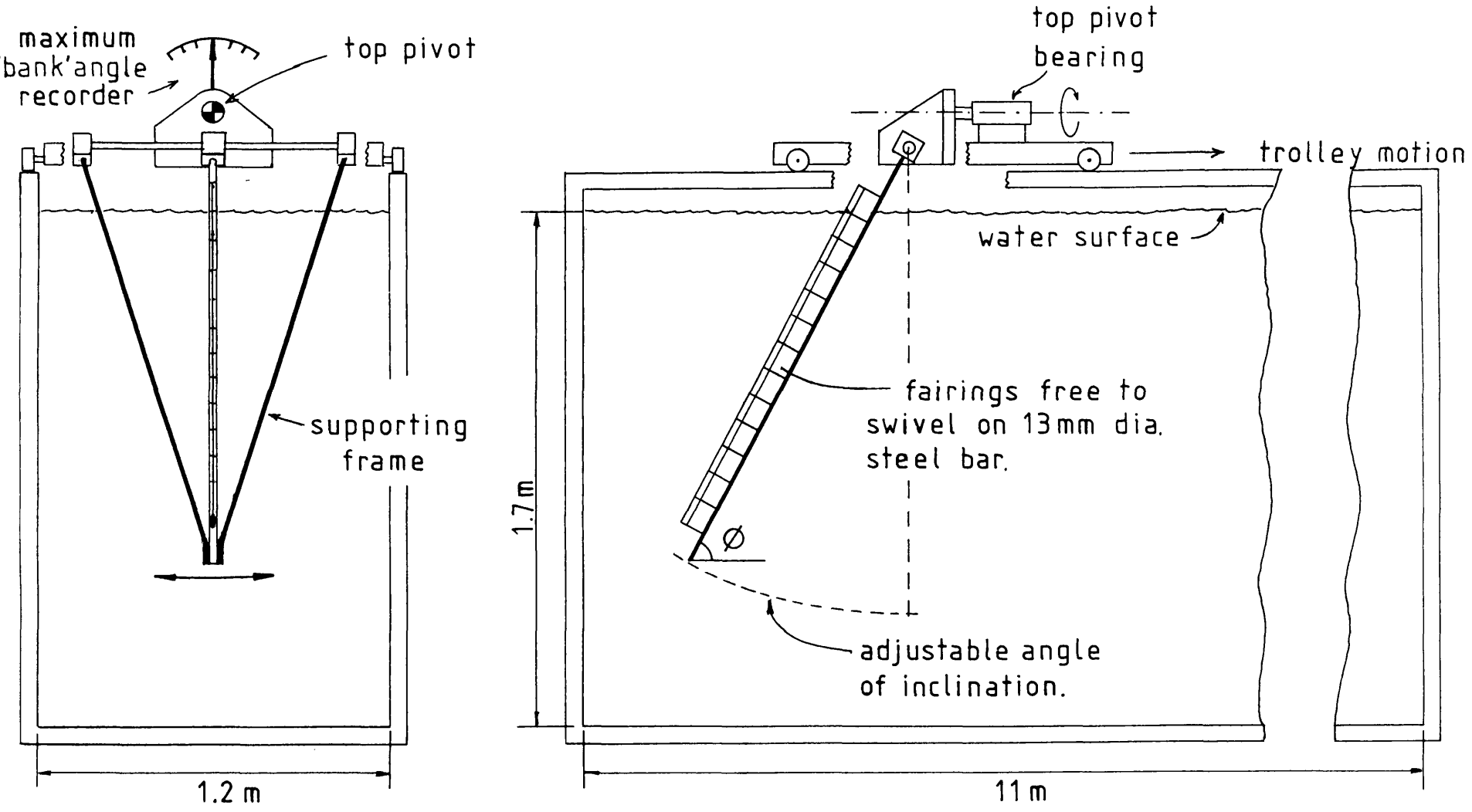

FIG.23. TOWING TANK EXPERIMENTAL RIG FOR MEASURING FAIRING LIFT FORCE VARIATION WITH SPEED AND INCLINATION.

FIG.23.

FIG. 24.

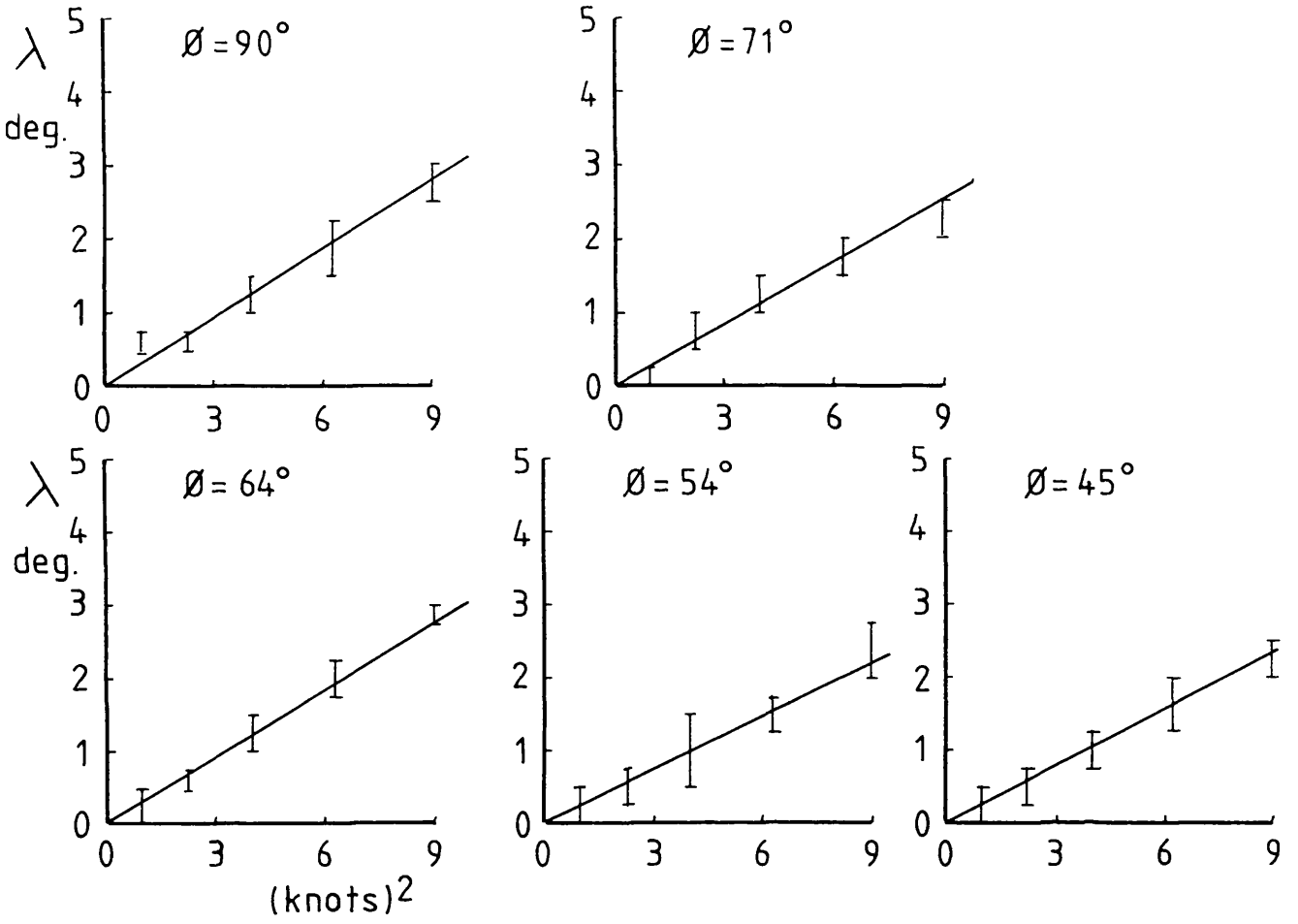

(A) VARIATION OF OBSERVED "BANK" ANGLE WITH (SPEED)^2.

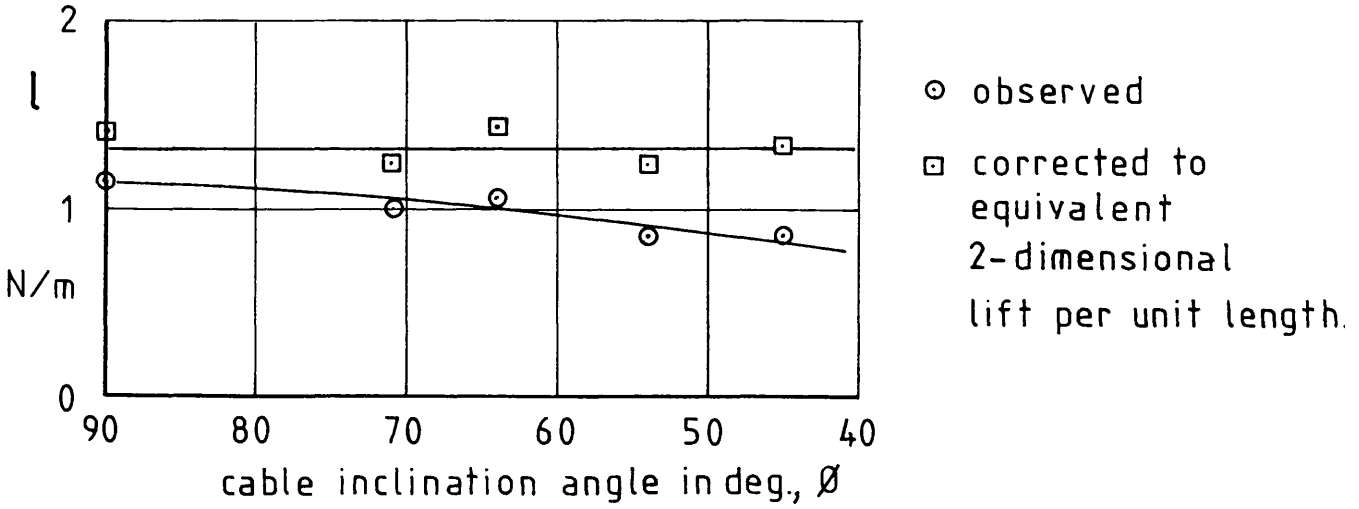

(B) DERIVED LIFT FORCE PER UNIT LENGTH RELATED TO CABLE INCLINATION —— AT 3 KNOTS.

FIG. 24. THE RESULTS FROM THE TOWING TANK EXPERIMENT.

FIG. 25.

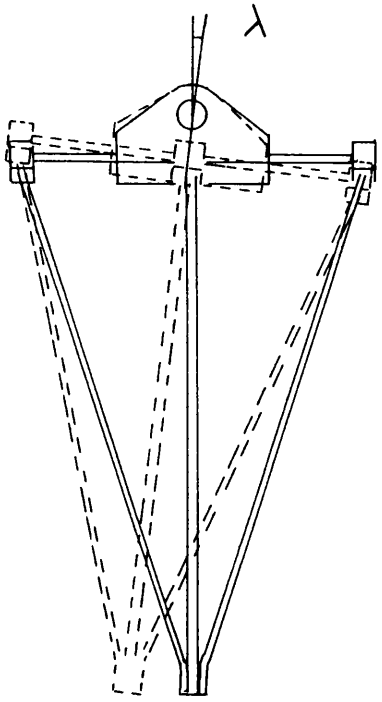

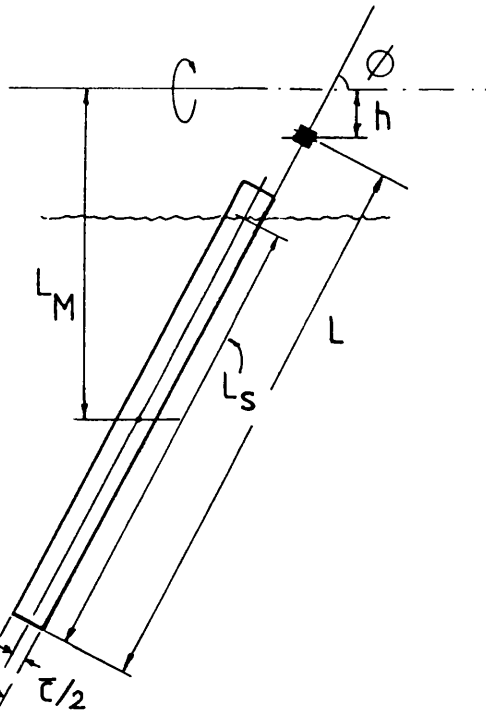

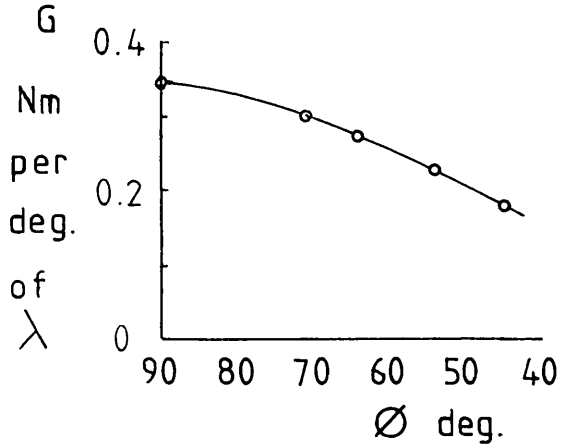

Moment arm of lift force about top pivot bearing

$= h + (L - L_s/2)\sin\emptyset$

Aspect Ratio

$= (L_s/\bar{c}).\sin^2\emptyset$

(A) CALIBRATION OF MOMENT DUE TO BANK ANGLE.

(B) RIG GEOMETRY

FIG. 25. TOWING TANK EXPERIMENT – DATA REDUCTION.

FIG. A1.

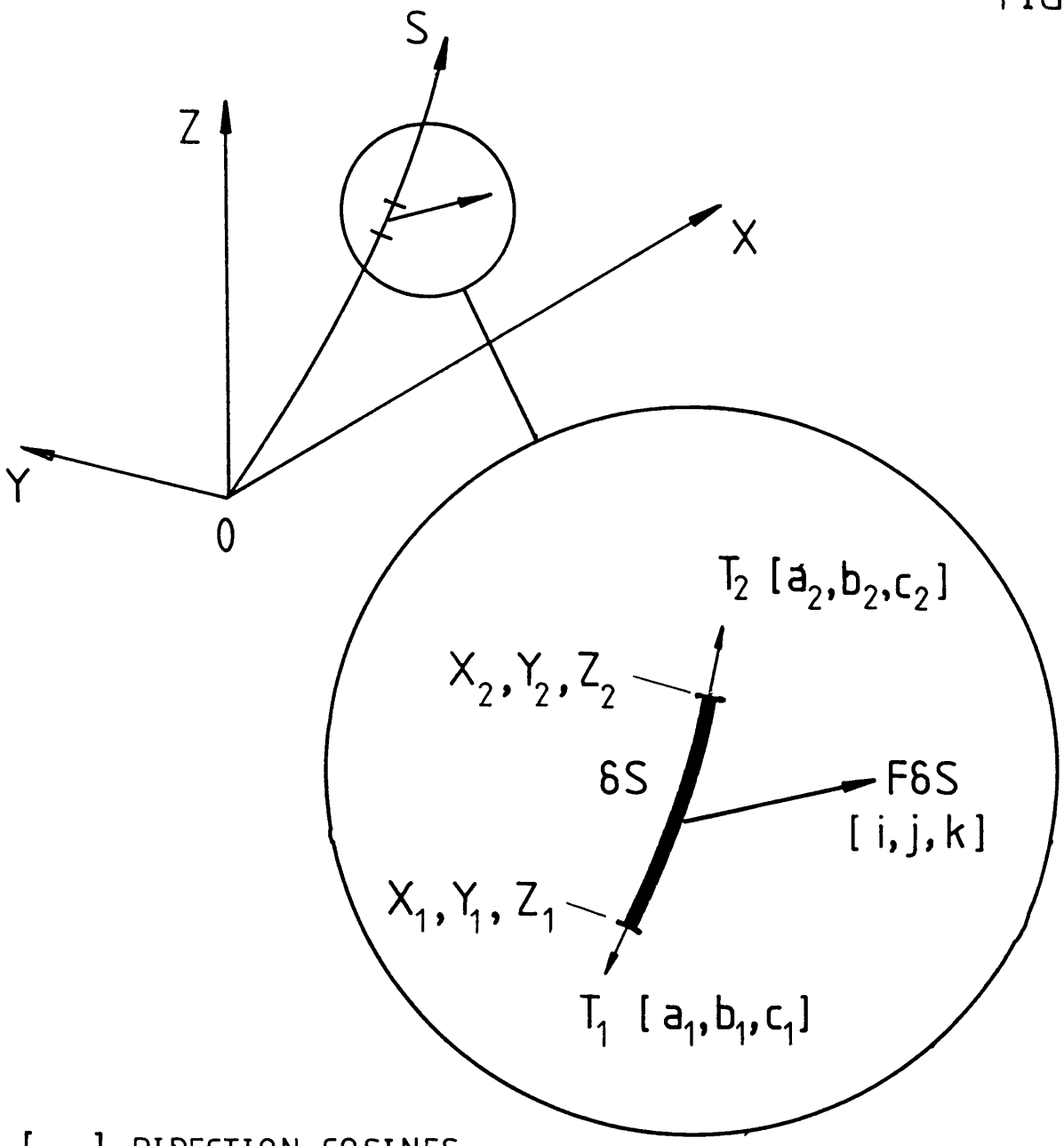

[ ] DIRECTION COSINES

FIG.A1. COORDINATE SYSTEM AND FORCES ON CABLE ELEMENT.